Cellular and Molecular Life Sciences (2021) 78:7873–7898
https://doi.org/10.1007/s00018-021-03993-6

ORIGINAL ARTICLE

Role of Akt isoforms in neuronal insulin signaling and resistance

Medha Sharma[1] · Chinmoy Sankar Dey[1]

Received: 28 April 2021 / Revised: 13 October 2021 / Accepted: 14 October 2021 / Published online: 1 November 2021

Abstract

The aim of the present study was to determine the role of Akt isoforms in insulin signaling and resistance in neuronal cells. By silencing Akt isoforms individually and in pairs, in Neuro-2a and HT22 cells we observed that, in insulin-sensitive condition, Akt isoforms differentially reduced activation of AS160 and glucose uptake with Akt2 playing the major role. Under insulin-resistant condition, phosphorylation of all isoforms and glucose uptake were severely affected. Over-expression of individual isoforms in insulin-sensitive and resistant cells differentially reversed AS160 phosphorylation with concomitant reversal in glucose uptake indicating a compensatory role of Akt isoforms in controlling neuronal insulin signaling. Post-insulin stimulation Akt2 translocated to the membrane the most followed by Akt3 and Akt1, decreasing glucose uptake in the similar order in insulin-sensitive cells. None of the Akt isoforms translocated in insulin-resistant cells or high-fat-diet mediated diabetic mice brain cells. Based on our data, insulin-dependent differential translocation of Akt isoforms to the plasma membrane turns out to be the key factor in determining Akt isoform specificity. Thus, isoforms play parallel with predominant role by Akt2, and compensatory yet novel role by Akt1 and Akt3 to regulate neuronal insulin signaling, glucose uptake, and insulin-resistance.

Keywords Akt1 · Akt2 · Akt3 · AS160 · Neuronal insulin signaling · Neuronal insulin resistance

Introduction

Neuronal insulin signaling is the primary pathway that regulates glucose homeostasis in the brain, with PI3K-Akt signaling pathway playing a principal role. Akt acts as a central node in neuronal insulin signaling and regulates cell proliferation and survival, cytoskeletal and vesicle trafficking, cellular metabolism, and glucose transport [1–3]. Any hindrance in this pathway paves the way for insulin-resistance like phenotype [3, 4]. We have observed hyperinsulinemia mediated insulin-resistance in neuronal cells in vitro, regulating a number of kinases and phosphatases [5, 6]. Frequently this has been linked to diseases like Alzheimer (Type-III diabetes) as observed by other laboratories and our [7, 8], including other diseases, like Huntington's disease [9], spinocerebellar ataxia type 1 [10], schizophrenia [11], Parkinson's disease [12], etc.

Akt is a serine/threonine kinase that belongs to AGC family. Akt comprises of three isoforms, Akt1, Akt2, and Akt3. They have been extensively studied in all insulin-responsive tissues, like skeletal muscles [13], adipocytes [14], and hepatocytes [15]. Akt1 expression varies across tissues, Akt2 is highly expressed in insulin-responsive tissues and Akt3 is expressed in brain and testis [16]. All three isoforms show high sequence similarity and common domain structure, with an N-terminal PH domain, a central kinase domain, and a C-terminal regulatory domain [1]. Akt1 plays a predominant role in cellular growth [17, 18], Akt2 plays a role in glucose homeostasis [19, 20], and Akt3 plays a role in neuronal development [21]. Studies have established that different isoforms have some overlapping yet diverse functions which can be attributed to differential expression [22], differential subcellular localization [23], regulatory partners [24], and different upstream stimulus [25].

In recent years there have been controversy regarding how the three Akt isoforms regulate glucose metabolism [26]. These studies have been conducted in vitro/in vivo, in normal and obese/diabetic condition, with single and/or double knockout or over-expressed samples. Akt2 has emerged as the predominant isoform regulating glucose

✉ Chinmoy Sankar Dey
csdey@bioschool.iitd.ac.in

[1] Kusuma School of Biological Sciences, Indian Institute of Technology-Delhi, Hauz Khas, New Delhi 110016, India

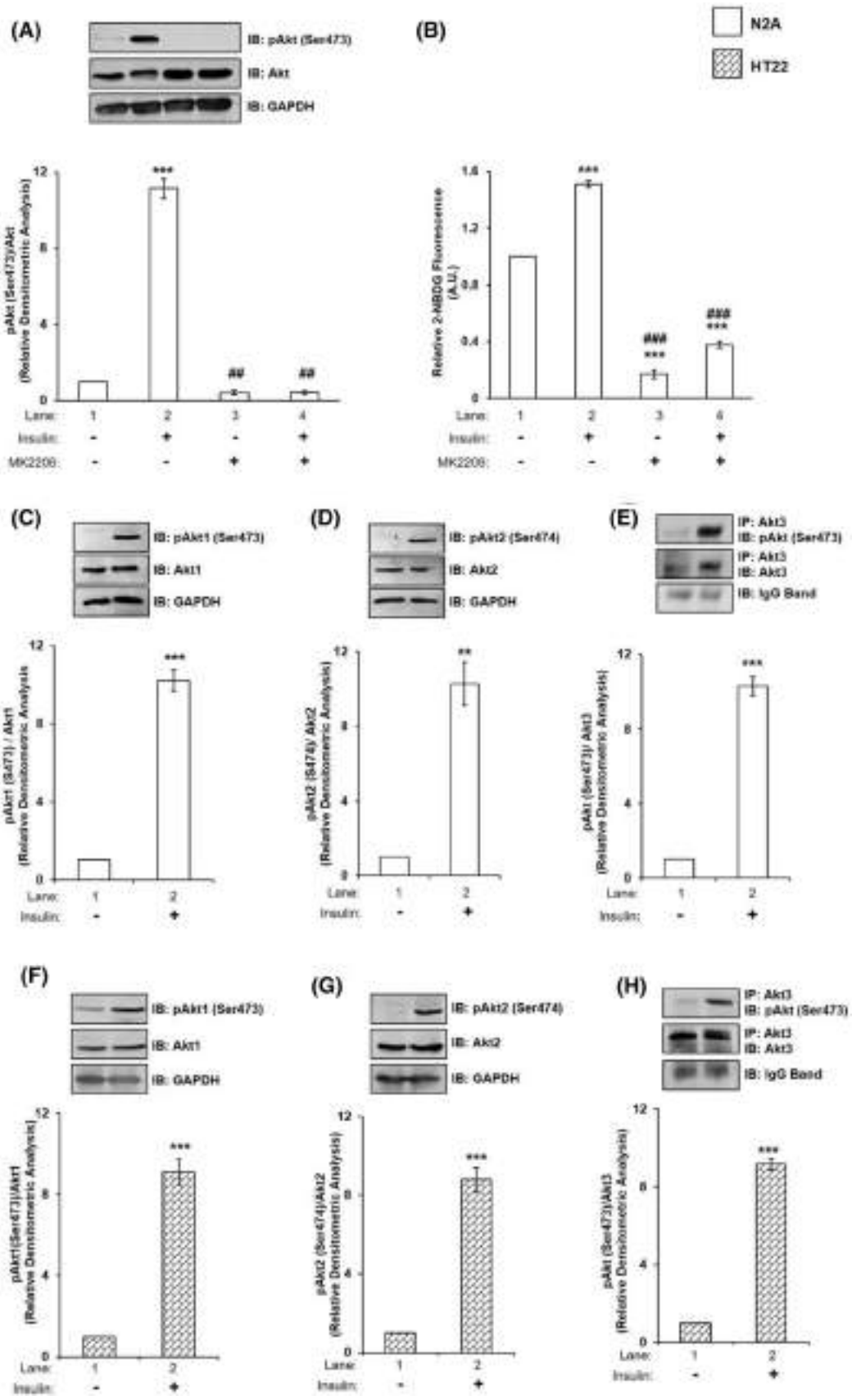
(A)
IB: pAkt (Ser473)
IB: Akt
IB: GAPDH
pAkt (Ser473)/Akt (Relative Densitometric Analysis)
Lane: 1 2 3 4
Insulin: - + - +
MK2206: - - + +
(B)
N2A
HT22
Relative 2-NBDG Fluorescence (A.U.)
(C)
IB: pAkt1 (Ser473)
IB: Akt1
IB: GAPDH
pAkt (S473) / Akt1 (Relative Densitometric Analysis)
(D)
IB: pAkt2 (Ser474)
IB: Akt2
IB: GAPDH
pAkt2 (S474) Akt2 (Relative Densitometric Analysis)
(E)
IP: Akt3
IB: pAkt (Ser473)
IP: Akt3
IB: Akt3
IB: IgG Band
pAkt (Ser473)/ Akt3 (Relative Densitometric Analysis)
(F)
IB: pAkt1 (Ser473)
IB: Akt1
IB: GAPDH
pAkt1(Ser473)/Akt1 (Relative Densitometric Analysis)
(G)
IB: pAkt2 (Ser474)
IB: Akt2
IB: GAPDH
pAkt2 (Ser474)/Akt2 (Relative Densitometric Analysis)
(H)
IP: Akt3
IB: pAkt (Ser473)
IP: Akt3
IB: Akt3
IB: IgG Band
pAkt (Ser473)/Akt3 (Relative Densitometric Analysis)

◂**Fig. 1** Effect of Akt inhibition on neuronal insulin signaling and glucose uptake; and effect of insulin on Akt and its isoforms. **A** N2A cells were differentiated in 2% DMSO for 3 days and stimulated with or without 30 µM MK2206 and/or 100 nM insulin for 30 min as indicated. Cells were lysed and subjected to western blotting, followed by probing with relevant primary antibodies. Bar represents relative change in pAkt (Ser-473) probed with anti-Akt antibody. **B** Differentiated N2A cells were serum starved for 2 h, followed by 100 nM insulin for 30 min. Uptake of 2-NBDG was then measured. Bar represents relative change in uptake of 2-NBDG. **C**–**E** N2A cells were differentiated in 2% DMSO for 3 days and stimulated with or without 100 nM insulin for 30 min. Cells were lysed and subjected to western blotting, followed by probing with relevant primary antibodies. **C** Bar represents relative change in pAkt1 (Ser-473) probed with anti-Akt1 antibody. **D** Bar represents relative change in pAkt2 (Ser-474) probed with anti-Akt2 antibody. **E** Post-insulin stimulation, lysates were subjected to immunoprecipitation using anti-Akt3 antibody. Bar represents relative change in pAkt (Ser-473) probed with anti-Akt3 antibody. **F**–**H** HT22 cells were differentiated in neurobasal media containing 2 mmol/L glutamine and 1×N2 supplement for 48 h and stimulated with or without 100 nM insulin for 30 min. Cells were lysed and subjected to western blotting, followed by probing with relevant primary antibodies. **F** Bar represents relative change in pAkt1 (Ser-473) probed with anti-Akt1 antibody. **G** Bar represents relative change in pAkt2 (Ser-474) probed with anti-Akt2 antibody. **H** Post-insulin stimulation, lysates were subjected to immunoprecipitation using anti-Akt3 antibody. Bar represents relative change in pAkt (Ser-473) probed with anti-Akt3 antibody. GAPDH has been used as a loading control (**A**, **C**, **D**, **F**, **G**). IgG band was used as loading control (E, H). Experiments were executed three times and a representative result is shown. Data expressed are mean ± SE. $^{***}P < 0.001$, $^{**}P < 0.01$ compared to lane 1, $^{\#\#\#}P < 0.001$, $^{\#\#}P < 0.01$ compared to lane 2. *IP* Immunoprecipitation; *IB* Immunoblot; *A.U* Arbitrary Units

metabolism in all metabolic tissues [19, 20, 27–29]. Majority of the reports say that Akt1 does not play any role in this regulation [13, 17, 18, 30]. However, there are others that report role of Akt1 in regulating insulin signaling and glucose transport [31] with some even supporting redundancy of Akt1 and Akt2 [14, 32, 33]. Akt3 is the least studied of the isoforms when it comes to glucose metabolism. Majority of the studies on Akt3 negate its role in regulating glucose metabolism [28].

All these studies confined to peripheral insulin-sensitive tissues indicate the role of Akt isoforms in insulin signaling is still ambiguous and could be tissue specific. There is hardly any information on Akt isoforms in regulating neuronal insulin signaling and resistance. All three Akt isoforms are expressed in the brain [16, 34]. Activation of Akt isoforms post-insulin stimulation in brain has also been studied [35]. However, majority of currently available studies focuses on the role of individual isoform in neuronal development, neuronal maturation and outgrowth, polarization and axon branching, synapse formation, and neuronal survival [36, 37]. Thus, no information is yet available to clarify the isoform specific role of Akt in neuron in insulin signaling and resistance and the underlying mechanisms that determine their functional specificity.

In our current study, we utilized neuronal cells like Neuro-2a and HT22, their insulin-resistant versions, generated in our laboratory [6, 8, 38, 39] and insulin-resistant diabetic mice whole brain tissues to study Akt isoform interplay. We elucidated this by isoform specific silencing [single (silencing of one isoform at a time) and double (silencing of two isoforms at a time)] as well as isoform specific over-expression, and elucidated how Akt isoforms regulate AS160 and ultimately glucose uptake in insulin-sensitive and resistant condition.

For clear understanding of the experimental objectives, a flowchart of the experimental design is depicted in Fig. S1.

Results

Effect of inhibition of Akt on neuronal insulin signaling and glucose uptake

To determine whether functional Akt protein exists in N2A cells, we inhibited Akt activity by MK2206, a well-known inhibitor of Akt activation [34], with or without insulin stimulation and determined its activation by assaying Akt phosphorylation and glucose uptake. To execute that, differentiated N2A cells were treated with or without 30 µM MK2206 for 30 min [34] and then stimulated with or without 100 nM insulin for 30 min. Cell lysates were western immunoblotted and probed with pan-anti-Akt antibody. No change was observed in the expression of Akt under all the conditions tested (Fig. 1A). However, the activation of Akt, as determined by phosphorylation at Ser-473, was decreased by 96.13% (Fig. 1A, lane 2 vs lane 4) due to MK2206 treatment. Inhibition of Akt activation led to a decrease in neuronal glucose uptake by 75.05% (Fig. 1B, lane 2 vs lane 4). Data indicate the presence of functional Akt in differentiated N2A cells participating in insulin signaling and glucose uptake.

Effect of insulin on the expression and activation of Akt1, Akt2, and Akt3 in neuronal cells

Next, we sought out to determine whether all the isoforms of Akt exists in N2A cells and, if so, do they undergo activation by specific phosphorylations due to insulin stimulation. To test that lysates of differentiated N2A cells, with or without insulin stimulation, were subjected to western immunoblotting probed with isoform specific and phospho-isoform specific antibodies. Due to unavailability of a specific phospho-Akt3 antibody to measure phosphorylation levels of Akt3, Akt3 protein was immunoprecipitated using anti-Akt3 antibody, and probed with anti-phospho-Akt antibody. Anti-IgG conformational antibody was used to mask remaining IgG band. No change was observed

in the expression of Akt1, Akt2 (GAPDH was used as a loading control) or Akt3 (because of the reasons, as mentioned above, IgG band was used as a loading control) (Fig. 1C–E). However, the activation of Akt1, Akt2 or Akt3 as determined by their phosphorylations at Ser-473, Ser-474, and Ser-472, respectively, was increased by ten-fold as a function of insulin stimulation (Fig. 1C–E, lane 1 vs lane 2). To determine whether the above mentioned effects were N2A cell specific we tested the effect of insulin stimulation on individual Akt isoforms in differentiated HT22 cells, a hippocampal neuronal cell line [39, 40]. Ten fold increase in phosphorylation of individual isoforms were obtained as a function of insulin stimulation (Fig. 1 F–H). Data show that all Akt isoforms are expressed in N2A and HT22 cells and activated similarly as a function of insulin stimulation.

Effect of silencing of one isoform, on expression and phosphorylation of the others

To determine the effect of silencing of one isoform on the expression and activation of the others, individual isoform was silenced at the optimized dose, and its effect on expression and activation were tested on the other isoforms, with or without insulin stimulation, probing with isoform specific antibodies. Silencing was optimized and found to be 200 nM for Akt1, 100 nM for Akt2, and 150 nM for Akt3 required to obtain optimal silencing (Fig. S2, S3 and S4). Akt1 silencing (Akt^{-1}) led to a decrease in phosphorylation and expression of Akt1 by 53.11% and 77.19%, respectively, (Fig. 2A, lane 2 vs lane 4; Fig. S2B, lane 1 vs lane 4, respectively); however, it did not affect expression or phosphorylation of Akt2 (Fig. 2B) and Akt3 (Fig. 2C). Similarly, Akt2 silencing (Akt^{-2}) led to a decrease in phosphorylation and expression of Akt2 by 40.71% and 57.99%, respectively, (Fig. 2E, lane 2 vs lane 4; Fig. S3B, lane 1 vs lane 4, respectively) without affecting expression or phosphorylation of Akt1 (Fig. 2D) or Akt3 (Fig. 2F). Akt3 silencing (Akt^{-3}) led to a decrease in phosphorylation and expression of Akt3 by 57.70% and 80.42%, respectively, (Fig. 2I, lane 2 vs lane 4; Fig. S4B, lane 1 vs lane 4, respectively) without affecting expression or phosphorylation of Akt1 (Fig. 2G) or Akt2 (Fig. 2H). Thus, data show that silencing of one isoform does not affect the others. These data also validate specificity of anti-Akt isoform specific antibodies. Similarly, to determine the effect of silencing of two isoforms at a time on the other, two isoforms were silenced in pairs (e.g., Akt^{-2-3} where Akt2 and Akt3 were silenced, Akt^{-1-3} where Akt1 and Akt3 were silenced and Akt^{-1-2} where Akt1 and Akt2 were silenced) and its effect on expression were tested on the other isoform. As expected, silencing of two isoforms in pairs did not affect the expression of the third isoform (Fig. S5).

Effect of silencing of Akt isoforms, on expression and activation of AS160 (Akt Substrate of 160 kDa) (Ser-588 and Thr-642) and glucose uptake

Ser-588 and Thr-642 are two phosphorylation sites on AS160 those have been reported to be regulated by Akt and are indications of AS160 activation. Postsingle or double silencing, differentiated N2A cells with or without insulin stimulation (100 nM, 30 min), were subjected to western immunoblotting probed with anti-AS160 antibody and anti-phospho AS160 Ser-588 or anti-phospho AS160 Thr-642 antibodies. There was no change in expression of AS160 under all the conditions tested (Fig. 3, A–H). However, post-single silencing, activation of AS160 as determined by phosphorylation at Ser-588, was down-regulated by insulin stimulation post-Akt^{-1} by 15.75% (Fig. 3A, lane 2 vs lane 4), Akt^{-2} by 24.45% (Fig. 3B, lane 2 vs lane 4), and Akt^{-3} by 26.98% (Fig. 3C, lane 2 vs lane 4) silencing as compared to scrambled siRNA transfected cells. Similarly, post-double silencing, activation of AS160 was down-regulated by insulin stimulation post-Akt^{-2-3} by 32.74% (Fig. 3D, lane 2 vs lane 4), Akt^{-1-3} by 26.60% (Fig. 3D, lane 2 vs lane 6) and Akt^{-1-2} by 27.57% (Fig. 3D, lane 2 vs lane 8) silencing as compared to scrambled siRNA transfected cells with insulin stimulation. Correspondingly, the activation of AS160 as determined by phosphorylation at Thr-642 was down-regulated by insulin stimulation post-Akt^{-1} by 15.20% (Fig. 3E, lane 2 vs lane 4), Akt^{-2} by 63.41% (Fig. 3F, lane 2 vs lane 4) and Akt^{-3} by 50.47% (Fig. 3G, lane 2 vs lane 4) silencing as compared with scrambled siRNA transfected cells. Similarly, post-double silencing, activation of AS160 was down-regulated by insulin stimulation post-Akt^{-2-3} by 55% (Fig. 3H, lane 2 vs lane 4), Akt^{-1-3} by 43.09% (Fig. 3H, lane 2 vs lane 6), and Akt^{-1-2} by 50.35% (Fig. 3H, lane 2 vs lane 8) silencing as compared with scrambled siRNA transfected cells by insulin stimulation. The AS160 threonine phosphorylation was more severely affected as compared to corresponding serine. Previous studies have reported Thr-642 phosphorylation as being more important for AS160 function as compared to its Ser-588 [41, 42]. Thus, silencing the isoforms demonstrates that all three isoforms down-regulate AS160 activation at both Ser-588 and Thr-642, without any effect on its expression. Highest down-regulation was caused by Akt2, followed by Akt3 and then Akt1. When one isoform is absent other isoforms differentially regulate AS160 phosphorylation. However, when two isoforms are absent AS160 phosphorylation is regulated in a kind of a compensatory manner. Data strongly suggest that Akt isoforms does participate in insulin signaling in N2A cells via AS160.

Having observed this we sought out to determine how does those activations reflect on neuronal glucose uptake. Therefore, single or double silenced differentiated N2A cells were stimulated with or without insulin and subjected to

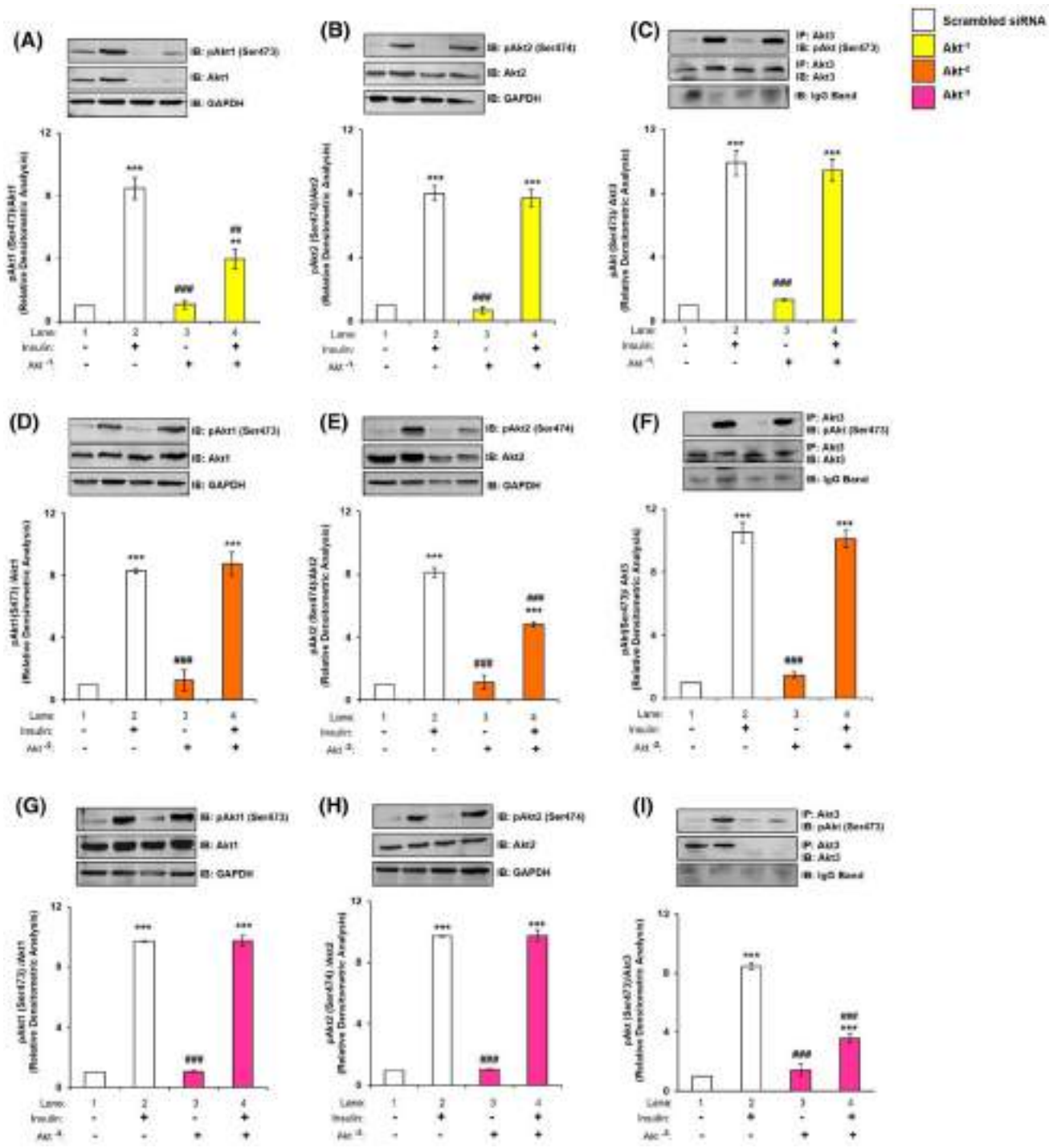

Fig. 2 Effect of silencing of one isoform, on expression and phosphorylation of other isoform in N2A cells. Three days post-proliferation, N2A cells were transfected with Akt1, Akt2 or Akt3 specific siRNA and then differentiated in 2% DMSO for 3 days. Cells were stimulated with or without 100 nM insulin for 30 min prior to cell lysis. Lysate was subjected to western blotting, followed by probing with relevant primary antibodies. **A**, **D**, **G** Bar represents relative change in pAkt1 (Ser-473) when probed with anti-Akt1 antibody. **B**, **E**, **H** Bar represents relative change in pAkt2 (Ser-474) when probed with anti-Akt2 antibody. **C**, **F**, **I** Bar represents relative change in pAkt (Ser-473) when probed with anti-Akt3 antibody. GAPDH has been used as a loading control (**A**, **B**, **D**, **E**, **G**, **H**). IgG band was used as loading control (**C**, **F**, **I**). Experiments were executed three times and a representative result is shown. Data expressed are mean ± SE. $^{***}P < 0.001$, $^{**}P < 0.01$ as compared to lane 1; $^{\#\#\#}P < 0.001$, $^{\#\#}P < 0.01$ as compared to lane 2. *IP* Immunoprecipitation; *IB* Immunoblot

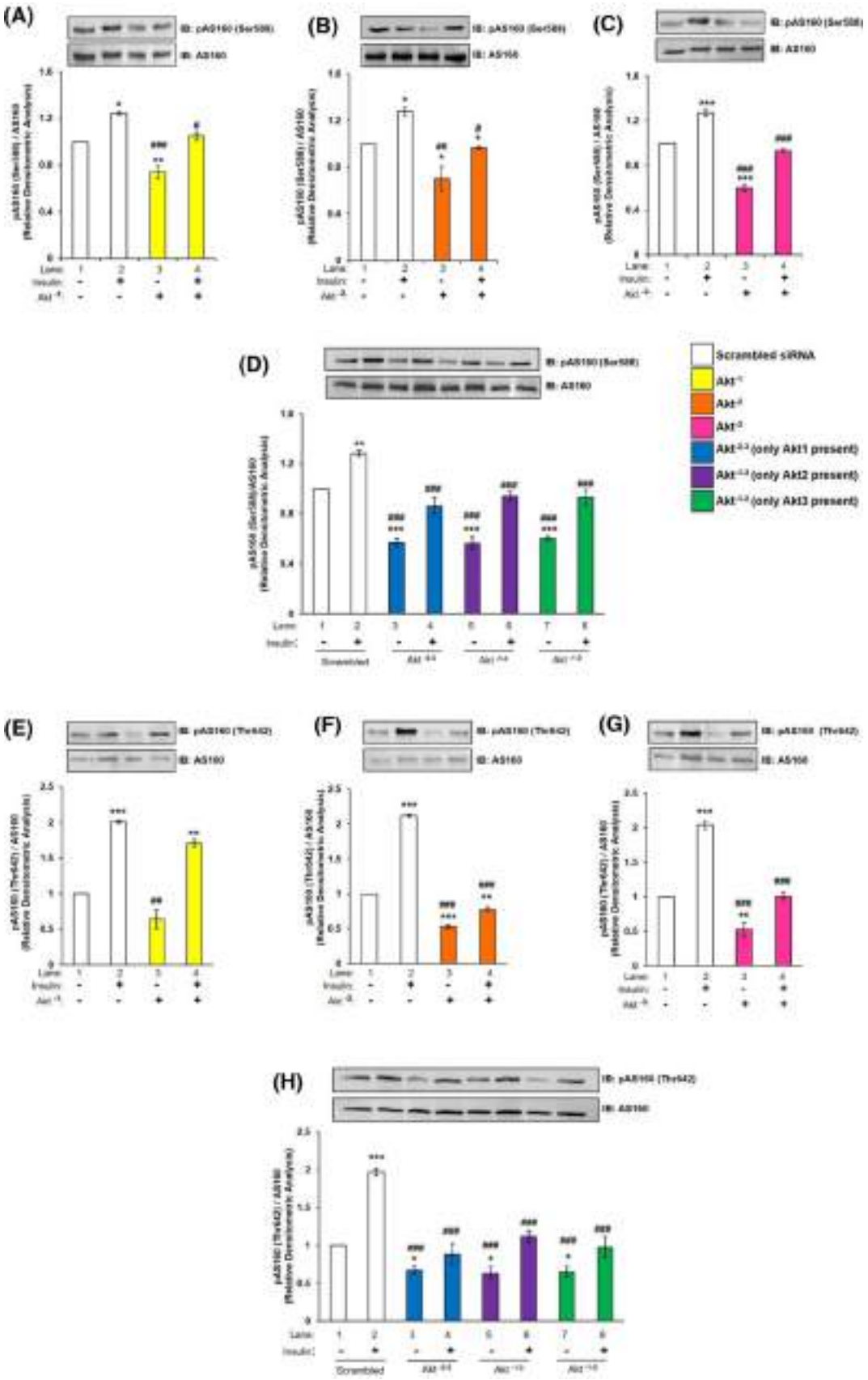
(A)
(B)
(C)
(D)
(E)
(F)
(G)
(H)
Scrambled siRNA
Akt1-/-
Akt2-/-
Akt3-/-
Akt1-/- (only Akt1 present)
Akt2-/- (only Akt2 present)
Akt3-/- (only Akt3 present)

◂**Fig. 3** Effect of Akt isoform silencing on AS160 in N2A cells. Three days post-proliferation, N2A cells were transfected with single (Akt^{-1}, Akt^{-2}, and Akt^{-3}) or double (Akt^{-2-3}, Akt^{-1-3} or Akt^{-1-2}) specific siRNA and then differentiated in 2% DMSO for 3 days. Cells were stimulated with or without 100 nM insulin for 30 min prior to cell lysis. Lysate was subjected to western blotting, followed by probing with relevant primary antibodies. (**A**–**D**) Bar represents relative change in pAS160 (Ser-588) when probed with anti-AS160 antibody. (**E**–**H**) Bar represents relative change in pAS160 (Thr-642) when probed with anti-AS160 antibody. Experiments were executed three times and a representative result is shown. Data expressed are mean ± SE. $^{***}P < 0.001$, $^{**}P < 0.01$, $^{*}P < 0.05$ as compared to lane 1; $^{\#\#\#}P < 0.001$, $^{\#\#}P < 0.01$, $^{\#}P < 0.05$ as compared to lane 2. *IB* Immunoblot

glucose uptake assay. As shown in Fig. 4 A and B, all three isoforms, irrespective of single or double silencing, contributed in glucose uptake in N2A cells. Under single silenced condition, Akt^{-1}, Akt^{-2} or Akt^{-3} silencing caused a decrease of 35.98% (Fig. 4A, lane 2 vs lane 4), 53.64% (Fig. 4A, lane 2 vs lane 6), and 48.53% (Fig. 4A, lane 2 vs lane 8), respectively, in insulin stimulated 2-NBDG uptake when compared to their respective scrambled siRNA transfected cells. Under double silenced condition, it was observed that Akt^{-2-3} silenced cells showed a maximum decrease of 76.73% in insulin stimulated 2-NBDG uptake as compared to scrambled siRNA transfected cells (Fig. 4B, lane 2 vs lane 4). Similarly, Akt^{-1-2} and Akt^{-1-3} silenced cells also caused 61.13% (Fig. 4B, lane 2 vs lane 8) and 54.19% (Fig. 4B, lane 2 vs lane 6) decrease, respectively, in insulin stimulated 2-NBDG uptake as compared with scrambled siRNA transfected cells. Thus, data demonstrate that Akt2 contributes most to the glucose uptake, followed by Akt3 and then Akt1, suggesting that there is an isoform specific regulation of the degree of glucose uptake in N2A cells. A summary of outcome of silencing is presented in Table S1.

In HT22 cells, it was found that Akt^{-1-3} silenced cells caused a decreased of 55.85% in insulin stimulated 2-NBDG uptake as compared to scrambled siRNA transfected cells (Fig. 4C, lane 2 vs lane 6). Similarly, Akt^{-2-3} and Akt^{-1-2} silenced cells also showed 76.73% and 65.91% decrease, respectively, in insulin stimulated 2-NBDG uptake as compared to scrambled siRNA transfected cells (Fig. 4C, lane 2 vs lane 4; and lane 2 vs lane 8, respectively). Therefore, data strongly indicated that in neuronal cells all Akt isoforms contribute in regulating neuronal glucose uptake and Akt2 contributes to the maximum, followed by Akt3 and Akt1.

Effect of insulin on subcellular translocation of Akt1, Akt2, Akt3, and AS160 in neuronal system

Recent reports in adipocytes and skeletal muscle cells demonstrate that, insulin stimulated subcellular translocation and membrane localization of Akt isoforms [23, 43] and AS160 [43] determines Akt isoform specific signaling. One of the first things that the translocated Akt isoform at the membrane does is that it interacts with AS160 to undertake the function of glucose uptake [24, 44, 45]. In neuronal system, there is no study of insulin-dependent translocation of Akt isoforms to plasma membrane. To address this, differentiated N2A cells stimulated with or without insulin (100 nM, 30 min) were lysed and fractionated into cytoplasmic and membrane fractions. Expression of Caveolin-1 is considered as a plasma membrane marker [46]. Thus, expression of Caveolin-1 was tested to establish purity of membrane fractions. Expression of Caveolin-1 was only observed in membrane fraction as compared to cytoplasm (Fig.S6, lane 1 vs lane 2). However, in all membrane translocation experiments GAPDH was used as a loading control, to perform densitometric analysis, as it is present in both "cytoplasm" and "membrane", as compared to only membrane-specific markers (which cannot be used for densitometry analysis of "cytoplasm" fractions) [47]. Our data show that in cytoplasmic fraction, post-insulin stimulation expression of Akt1 was down-regulated by 12.77% (Fig. 5A, Panel 1 and 4, lane 1 vs lane 2), Akt2 by 13.02% (Fig. 5A, Panel 2 and 4, lane 1 vs lane 2), and Akt3 by 12.53% (Fig. 5A, Panel 3 and 4, lane 1 vs lane 2). In contrast to that, post-insulin stimulation in the membrane fraction, Akt1 translocated and accumulated on the plasma membrane by 59.64% (Fig. 5A, Panel 1 and 4, lane 3 vs lane 4), Akt2 by 230.18% (Fig. 5A, Panel 2 and 4, lane 3 vs lane 4), and Akt3 by 152.51% (Fig. 5A, Panel 3 and 4, lane 3 vs lane 4). Data show that as a function of insulin stimulation all Akt isoforms translocated to the plasma membrane, with Akt2 translocating the most, followed by Akt3 and Akt1 as compared to respective cytoplasmic expression without insulin. In HT22 cells, in cytoplasmic fractions, insulin stimulation down-regulated Akt1 expression by 12% (Fig. 5B, Panel 1 and 4, lane 1 vs lane 2), Akt2 by 12.44% (Fig. 5B, Panel 2 and 4, lane 1 vs lane 2), and Akt3 by 11.05% (Fig. 5B, Panel 3 and 4, lane 1 vs lane 2). Post-insulin stimulation, in the membrane fraction, Akt1 translocated and accumulated on the plasma membrane by 48.16% (Fig. 5B, Panel 1 and 4, lane 3 vs lane 4), Akt2 by 137% (Fig. 5B, Panel 2 and 4, lane 3 vs lane 4), and Akt3 by 80.29% (Fig. 5B, Panel 3 and 4, lane 3 vs lane 4). The trend of this membrane translocation correlates with the trend as observed in glucose uptake (Fig. 4 A, B). Data show that all isoforms translocate to the plasma membrane post-insulin stimulation to different extents. Akt2 comes out as the predominant isoform on the plasma membrane, followed by Akt3 and Akt1 in both the cell lines tested. Therefore, data prove that it is the abundance of a specific Akt isoform in the membrane due to translocation from cytoplasm as a function of insulin stimulation that regulate glucose uptake.

As did earlier, we tested the compartmentalised Akt isoform interaction(s) with AS160 in the cytoplasm and plasma membrane fractions. Phosphorylation of AS160

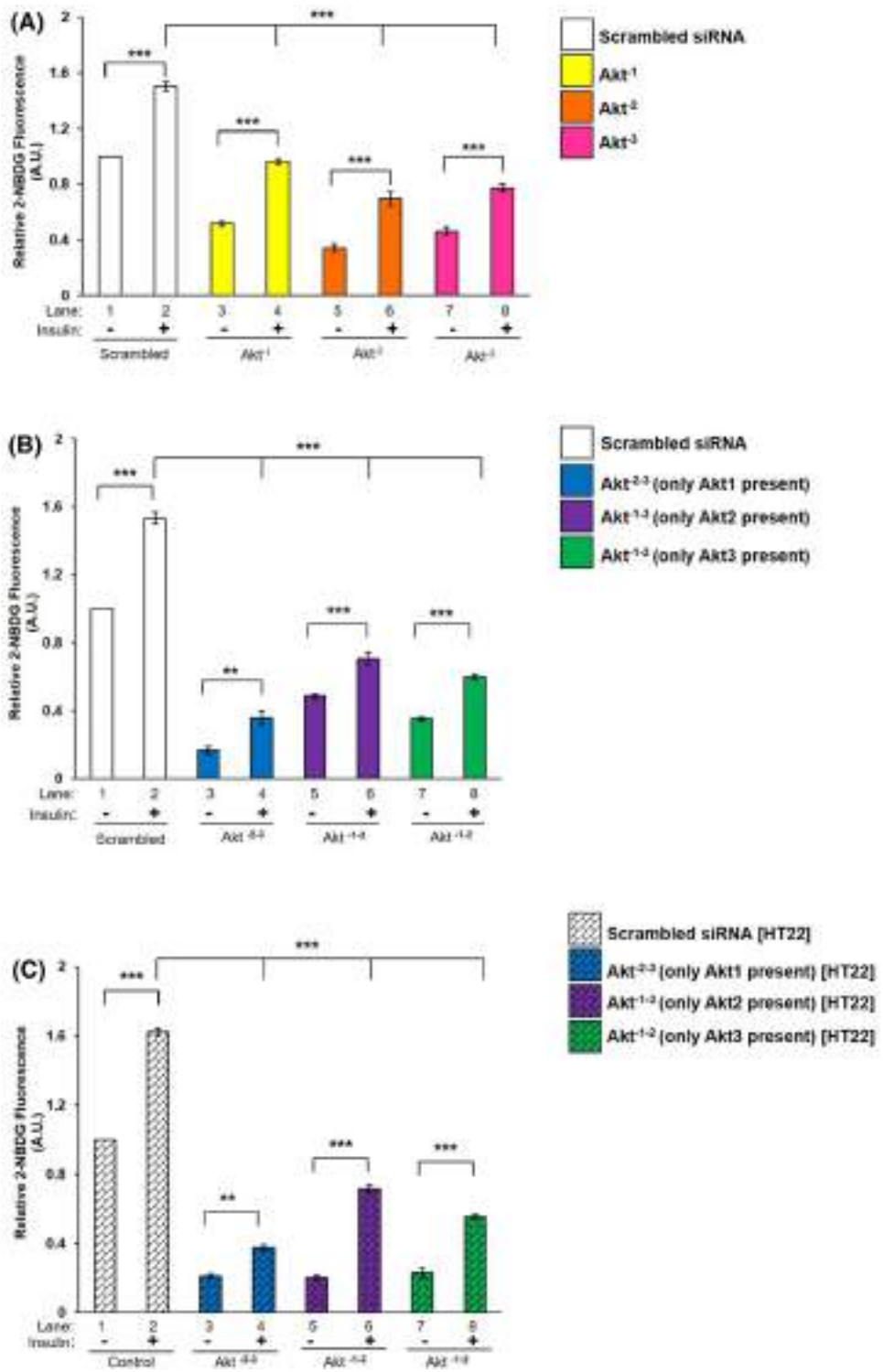

Fig. 4 Effect of Akt isoform silencing on glucose uptake. Three days post-proliferation, cells were transfected with **(A)** Single (Akt^{-1}, Akt^{-2} or Akt^{-3}) (N2A) **(B)** Double (Akt^{-2-3}, Akt^{-1-3}, Akt^{-1-2}) (N2A) **(C)** Double (Akt^{-2-3}, Akt^{-1-3}, Akt^{-1-2}) (HT22) specific siRNA and then differentiated for 3 days. Differentiated cells were serum starved for 2 h, followed by 100 nM insulin for 30 min. Uptake of 2-NBDG was then measured. Bar represents relative change in uptake of 2-NBDG. Experiments were executed three times and a representative result is shown. Data expressed are mean ± SE. $^{***}P < 0.001$, $^{**}P < 0.01$ as indicated

at Thr-642 showed increase post-insulin stimulation in cytoplasmic fraction by 71.71% (Fig. 5C, Panel 1 and 2, lane 1 vs lane 2) and membrane fraction by 437.31% (Fig. 5C, Panel 1 and 2, lane 3 vs lane 4) as compared to their respective controls without insulin. Expression of AS160 increased in cytoplasm post-insulin stimulation by 17.06% (Fig. 5C, Panel 2 and 3, lane 1 vs lane 2). However, there was a sharp decrease by 67.46% in membrane bound AS160 post-insulin stimulation as compared to samples without stimulation (Fig. 5C, Panel 2 and 3, lane 3 vs lane 4). In HT22 cells, phosphorylation of AS160 at Thr-642 showed similar increase in cytoplasm by 78.17%

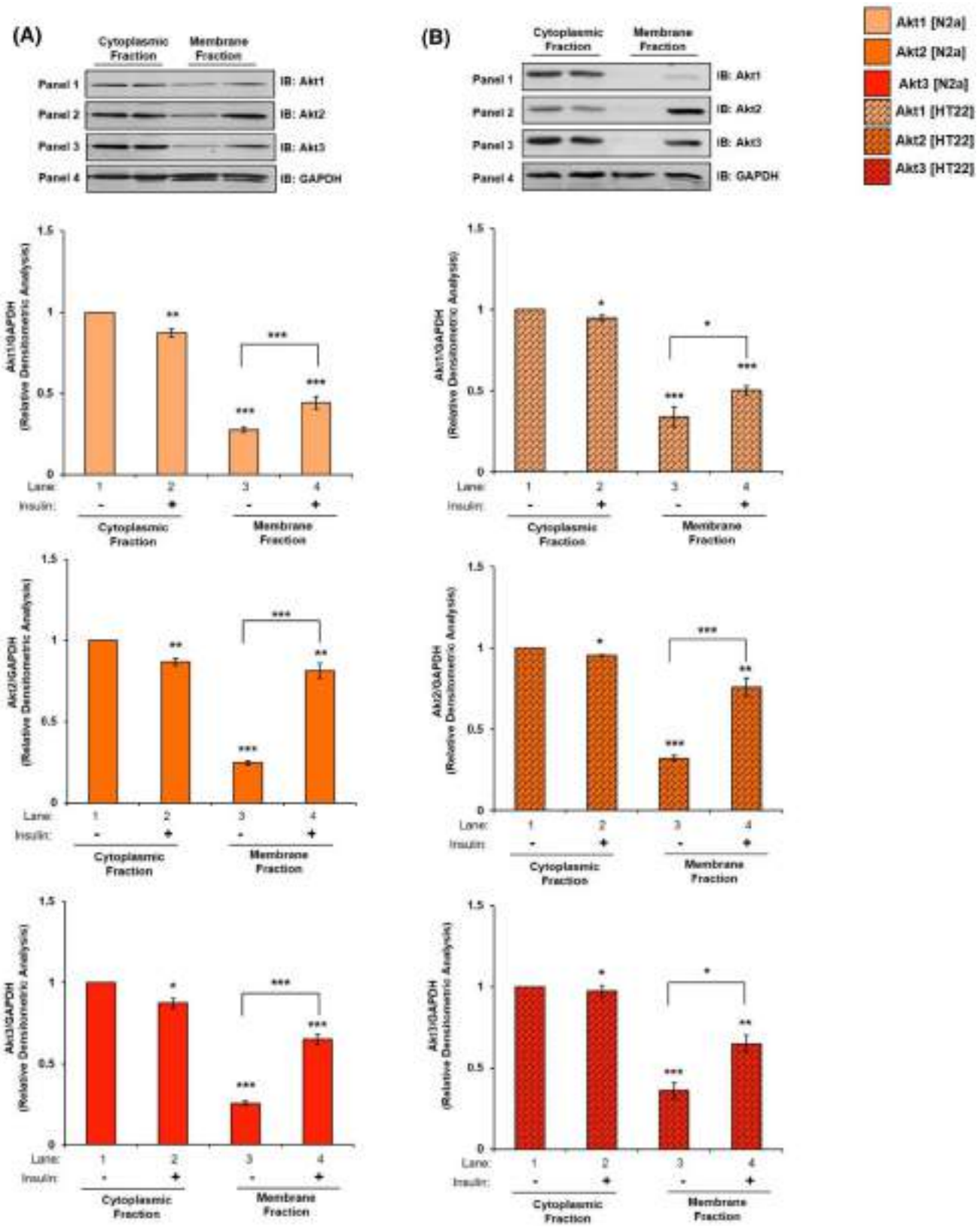
(A)
Cytoplasmic Fraction
Membrane Fraction
Panel 1
IB: Akt1
Panel 2
IB: Akt2
Panel 3
IB: Akt3
Panel 4
IB: GAPDH
(B)
Cytoplasmic Fraction
Membrane Fraction
Panel 1
IB: Akt1
Panel 2
IB: Akt2
Panel 3
IB: Akt3
Panel 4
IB: GAPDH
Akt1 [N2a]
Akt2 [N2a]
Akt3 [N2a]
Akt1 [HT22]
Akt2 [HT22]
Akt3 [HT22]
Akt1/GAPDH (Relative Densitometric Analysis)
Akt2/GAPDH (Relative Densitometric Analysis)
Akt3/GAPDH (Relative Densitometric Analysis)
Lane:
Insulin:
Cytoplasmic Fraction
Membrane Fraction

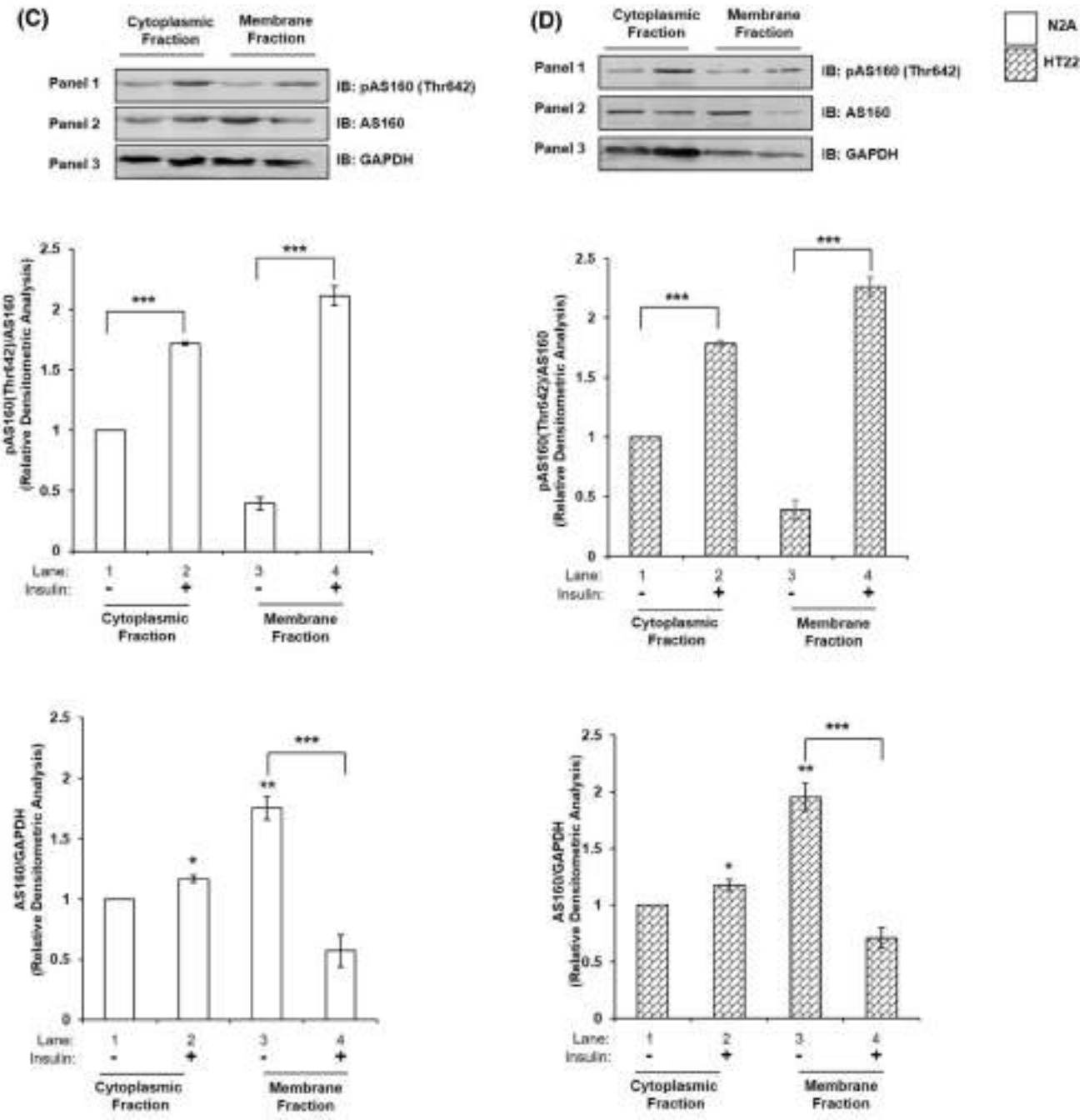

Fig. 5 Mechanism underlying Akt isoform specificity in neuronal cells. **A** N2A cells were differentiated in 2% DMSO for 3 days. Three days post-differentiation, membrane and cytosol fraction were isolated and subjected to western blotting, followed by probing with relevant primary antibodies. Bar represents relative change in Akt1, Akt2 or Akt3 when probed with anti-Akt isoform specific antibody. **B** HT22 cells were differentiated in neurobasal media containing 2 mmol/L glutamine and 1×N2 supplement for 48 h. Three days post-differentiation, membrane and cytosol fraction were isolated and subjected to western blotting, followed by probing with relevant primary antibodies. Bar represents relative change in Akt1, Akt2 or Akt3 when probed with anti-Akt isoform specific antibody. **C**, **D** Bar represents relative change in AS160 when probed with anti-AS160 antibody (N2A/HT22 as indicated). Bar represents relative change in pAS160 (Thr-642) when probed with anti-AS160 antibody (N2A/HT22 as indicated). GAPDH has been used as a loading control. Experiments were executed three times and a representative result is shown. Data expressed are mean ± SE. ***$P < 0.001$, **$P < 0.01$, *$P < 0.05$ compared to lane 1 or as indicated. *IB* Immunoblot

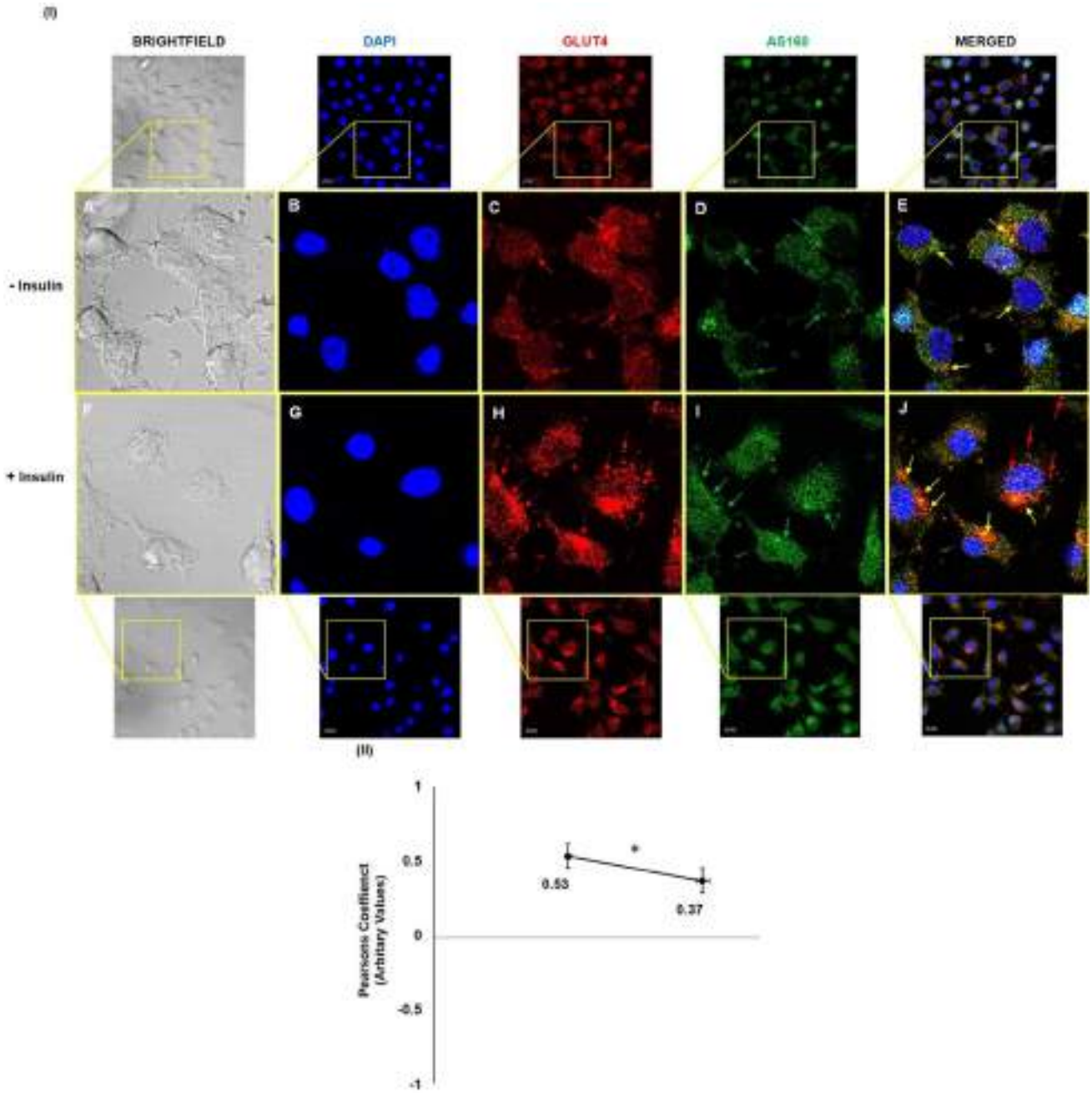

Fig. 6 Effect of insulin on subcellular translocation of GLUT4 and AS160. **I** Three days post-proliferation, N2A cells differentiated in 2% DMSO for 3 days. Cells were stimulated with or without 100 nM insulin for 30 min followed by fixation and permeabilization and probed with anti-GLUT4 and anti-AS160 antibody. Cells were subjected to immunofluorescence microscopy using anti-goat Alexa 555 and anti-rabbit CFL 488 secondary antibodies, respectively. Bar corresponds to 10 µm. Images were captured from different fields and a representative image of 3 images is presented. Red arrow indicates GLUT4, green arrow indicates AS160 and yellow arrow indicates co-localized GLUT4 and AS160. **II** Graphical representation of co-localization by Pearson's coefficient (*$P < 0.05$)

(Fig. 5D, Panel 1 and 2, lane 1 vs lane 2) and membrane fraction by 479.96% (Fig. 5D, Panel 1 and 2, lane 3 vs lane 4) as compared to their respective controls without insulin. Expression of AS160 increased in cytoplasm, post-insulin stimulation by 17.67% (Fig. 5D, Panel 2 and 3, lane 1 vs lane 2). As in N2A, there was a sharp decrease in membrane bound AS160 post-insulin stimulation as compared to control by 63.57% (Fig. 5D, Panel 2 and 3, lane 3 vs lane 4). Thus, data show the regulation of AS160 by phosphorylation at Thr-642 by activated Akt in neuronal cells.

To further investigate this insulin-dependent redistribution of AS160 in neuronal cells, and how this redistribution correlates with GLUT4 translocation, we examined membrane translocation and possible co-localization of AS160 and GLUT4. Differentiated N2A cells were stimulated with or without insulin, immunostained with anti-GLUT4 and anti-AS160 antibody and were subjected to confocal microscopy (Fig. 6). Immunocytochemical analysis revealed that under basal conditions, GLUT4 was localized inside the cell (Fig. 6I, Panel C, red arrows), and AS160 was distributed just below the membrane (Fig. 6I, Panel D, green arrows), possibly tethering GLUT4 to the GSVs. Co-localization of AS160 and GLUT4 inside the cell was observed (Fig. 6I, Panel E, yellow arrows). The two proteins co-localized with a Pearson's coefficient of 0.53 (Fig. 6II). Post-insulin stimulation, GLUT4 was found to be present on the membrane (Fig. 6I, Panel H, red arrows), considerably more than unstimulated cells (Fig. 6I, Panel C vs Panel H). Alternatively, AS160 was found dispersed inside the cytoplasm (Fig. 6I, Panel I, green arrows) as compared to unstimulated cells (Fig. 6I, Panel D vs Panel I). Co-localization of AS160 and GLUT4 was observed (Fig. 6I, Panel J, yellow arrows) with a Pearson's coefficient of 0.37 (Fig. 6II), however, GLUT4 was seen at the membrane independently as well, thus decreasing the co-localization (Fig. 6I, Panel J, red arrows) by a significant 30% with or without insulin stimulation (Fig. 6II). Data strongly show insulin-dependent redistribution of AS160 in neuronal cells, and how this redistribution correlates with GLUT4 translocation and glucose uptake.

Subcellular translocation of Akt1, Akt2, Akt3, and AS160 in mice whole brain tissue

Having observed in two different neuronal cells, we wished to assess whether the translocation of Akt isoforms is indeed critical, we tested it in High-Fat-Diet (HFD) fed diabetic mice against Normal Diet fed mice (ND) (Kind gift from Dr. Prosenjit Mondal, Indian Institute of Technology—Mandi, Himachal Pradesh, India). Our data show that in cytoplasmic fractions of HFD mice Akt1 expression was down-regulated by 11.07% (Fig. 7A, Panel 1 and 4, lane 1 vs lane 2), Akt2 expression was down-regulated by 13.71% (Fig. 7A, Panel 2 and 4, lane 1 vs lane 2), and Akt3 expression was down-regulated by 13.55% (Fig. 7A, Panel 3 and 4, lane 1 vs lane 2) as compared to respective ND mice controls. In contrast to this, in the membrane fraction of HFD mice, none of the Akt isoforms translocated to the plasma membrane (Fig. 7B, lane 3 vs lane 4). This is an interesting result as this not only corroborates with our results in neuronal cells, but also points to novel role of all three Akt isoforms in neuronal insulin resistance.

Testing expression and phosphorylation of AS160 Thr-642 in the cytoplasm and plasma membrane fractions of ND and HFD mice, as described above (Fig. 7A), phosphorylation of AS160 at Thr-642 decreased in cytoplasmic fraction by 19.96% (Fig. 7B, Panel 1 and 2, lane 1 vs lane 2), and in membrane fraction by 46.70% (Fig. 7B, Panel 1 and 2, lane 3 vs lane 4) in HFD as compared to ND mice. Expression of AS160 decreased in cytoplasm by 29.28% (Fig. 7B, Panel 2 and 3, lane 1 vs lane 2) and plasma membrane by 51.47% (Fig. 7B, Panel 2 and 3, lane 3 vs lane 4) in ND as well as HFD mice.

This is the first study to report differential subcellular translocation of Akt isoforms under ND and HFD condition in mice whole brain tissue. This result prompted us to study the role of Akt isoforms in insulin-resistant neuronal cells.

Expression and activation of Akt1, Akt2, and Akt3 in insulin-resistant neuronal cells

We had previously generated an insulin-resistant diabetic neuronal cell model by differentiating N2A in the chronic presence of insulin (100 nM) in serum-free medium (MFI) [6, 8, 48–50]. This model cellular system was used in the present study to investigate the role of Akt isoforms in insulin-sensitive (MF) and insulin-resistant (MFI) condition. No change was observed in the expression of Akt1, Akt2 or Akt3 post-insulin stimulation in MF and MFI condition (Fig. 8A, B, C). However, phosphorylation of Akt1, Akt2 or Akt3 at Ser-473, Ser-474, and Ser-472, respectively, was decreased differentially post-insulin stimulation in MF and MFI condition. Insulin stimulation led to a decrease in Akt1 phosphorylation by 43.36% (Fig. 8A, lane 2 vs lane 4), in Akt2 phosphorylation by 72.79% (Fig. 8B, lane 2 vs lane 4) and in Akt3 phosphorylation by 52.45% (Fig. 8C, lane 2 vs lane 4). Previous studies in skeletal muscles and adipocytes of diabetic obese patients, Akt2 phosphorylation was reported to be affected [51, 52]. Our data point to differential role of all three Akt isoforms, as phosphorylation of all was affected in neuronal insulin-resistant condition, with Akt2 phosphorylation affected the most, followed by Akt3 and then Akt1.

Effect of silencing of Akt isoforms in insulin-resistant neuronal cells

To determine whether there is any isoform specific role in regulating neuronal glucose uptake under insulin-resistant condition, Akt isoforms were silenced in pair (Akt^{-2-3}, Akt^{-1-3} and Akt^{-1-2}). It was found that, in MF condition, the pattern was similar as observed previously in N2A (Fig. 4B) as well as in HT22 cells (Fig. 4C). Under MF condition, Akt^{-1-3} silenced N2A cells showed 50.70% decrease in insulin stimulated 2-NBDG uptake as compared to scrambled

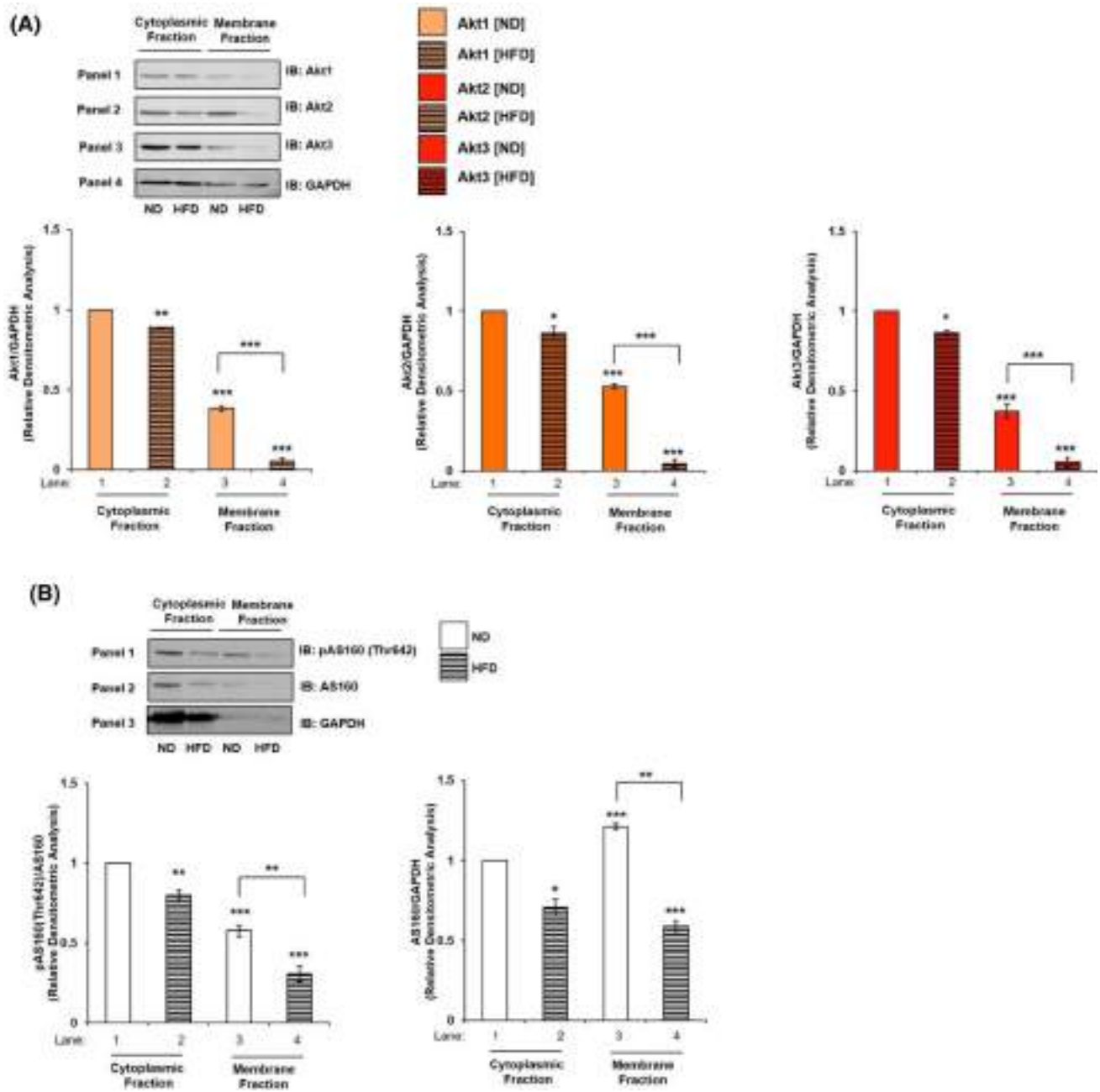

Fig. 7 Mechanism underlying Akt isoforms specificity in mice whole brain tissue. **A** Subcellular translocation of Akt isoforms in mice whole brain tissue. Mice whole brain was lysed, membrane and cytosol fraction were isolated and subjected to western blotting, followed by probing with relevant primary antibodies. Bar represents relative change in Akt1, Akt2 or Akt3 when probed with anti-Akt isoform specific antibody. Experiments were executed with three independent animals and a representative result is shown. **B** Subcellular redistribution of AS160 post-insulin stimulation. Bar represents relative change in AS160 when probed with anti-AS160 antibody. Bar represents relative change in pAS160 (Thr-642) when probed with anti-AS160 antibody. GAPDH has been used as a loading control. Experiments were executed with three independent animals and a representative result is shown. Data expressed are mean ± SE. $^{***}P < 0.001$, $^{**}P < 0.01$, $^{*}P < 0.05$ compared to lane 1 or as indicated. (*ND* Normal Diet; *HFD* High-Fat-Diet). *IB* Immunoblot

siRNA transfected cells (Fig. 8D, lane 2 vs lane 6). Similarly, Akt^{-2-3} and Akt^{-1-2} silenced cells also showed 71.28% and 61.86% decrease, respectively, in insulin stimulated 2-NBDG uptake as compared to scrambled siRNA transfected cells (Fig. 8D, lane 2 vs lane 4; and lane 2 vs lane

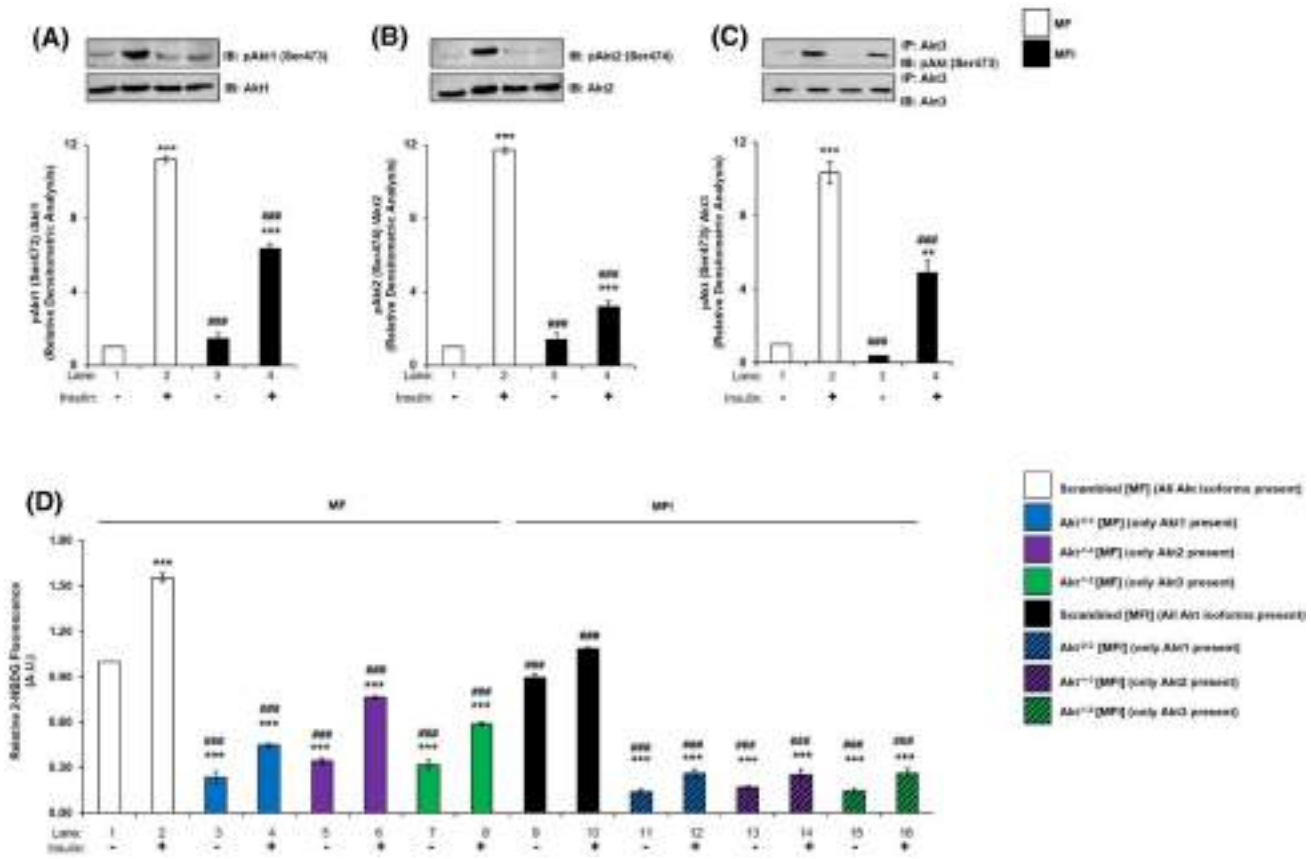

Fig. 8 Expression and activation of Akt1, Akt2, and Akt3, glucose uptake and subcellular translocation under insulin-resistant condition in neuronal cells. (**A**–**C**) N2A cells were differentiated in serum-free medium in the absence of (MF) or chronic presence of 100 nM insulin (MFI) for 3 days. Cells were lysed and subjected to western blotting, followed by probing with relevant primary antibodies. Bar represents relative change when probed with anti-Akt isoform specific antibody. **A** Bar represents relative change in pAkt1 (Ser-473) probed with anti-Akt1 antibody. **B** Bar represents relative change in pAkt2 (Ser-474) probed with anti-Akt2 antibody. **C** Post-insulin stimulation, lysates were subjected to immunoprecipitation using anti-Akt3 antibody. Bar represents relative change in pAkt (Ser-473) probed with anti-Akt3 antibody. **D** Three days post-proliferation, N2A cells were transfected with double (Akt^{-2-3}, Akt^{-1-3} or Akt^{-1-2}) specific siRNA and then differentiated under MF MFI condition for 3 days. Differentiated N2A cells were serum starved for 2 h, followed by 100 nM insulin for 30 min. Uptake of 2-NBDG was then measured. **E** Subcellular translocation of Akt isoforms post-insulin stimulation. N2A cells were differentiated under MF MFI condition for 3 days and stimulated with or without 100 nM insulin for 30 min as indicated. Cells were lysed, and membrane and cytosol fraction were isolated and subjected to western blotting, followed by probing with relevant primary antibodies. Bar represents relative change in Akt1, Akt2 or Akt3 when probed with anti-Akt isoform specific antibody. **F** Subcellular translocation of AS160 post-insulin stimulation. Bar represents relative change in pAS160 (Thr-642) when probed with anti-AS160 antibody. GAPDH has been used as a loading control. Experiments were executed three times and a representative result is shown. Data expressed are mean ± SE. $^{***}P<0.001$, $^{**}P<0.01$, $^{*}P<0.05$ compared to lane 1 or as indicated; $^{###}P<0.001$, $^{##}P<0.01$, $^{#}P<0.05$ compared to lane 2. *IP* Immunoprecipitation; *IB* Immunoblot; *A.U* Arbitrary Units

8, respectively). Akt2 contributes most to glucose uptake, followed by Akt3 and then Akt1 in MF N2A cells. However, interestingly, in MFI condition, Akt^{-2-3}, Akt^{-1-3}, and Akt^{-1-2} silenced N2A cells showed similar decrease in insulin stimulated 2-NBDG uptake, indicating that all Akt isoforms are affected in insulin-resistant neuronal cells. Akt^{-1-3} silenced N2A cells showed 83.64% decrease in insulin stimulated 2-NBDG uptake as compared to scrambled siRNA transfected cells (Fig. 8D, lane 2 vs lane 14). Similarly, Akt^{-2-3} and Akt^{-1-2} silenced cells also showed 83.14% and 82.95% decrease, respectively, in insulin stimulated 2-NBDG uptake as compared to scrambled siRNA transfected cells (Fig. 8D, lane 2 vs lane 12; and lane 2 vs lane 16, respectively). Data consolidate that all Akt isoforms contribute in neuronal glucose uptake in insulin-sensitive as well as insulin-resistant cells.

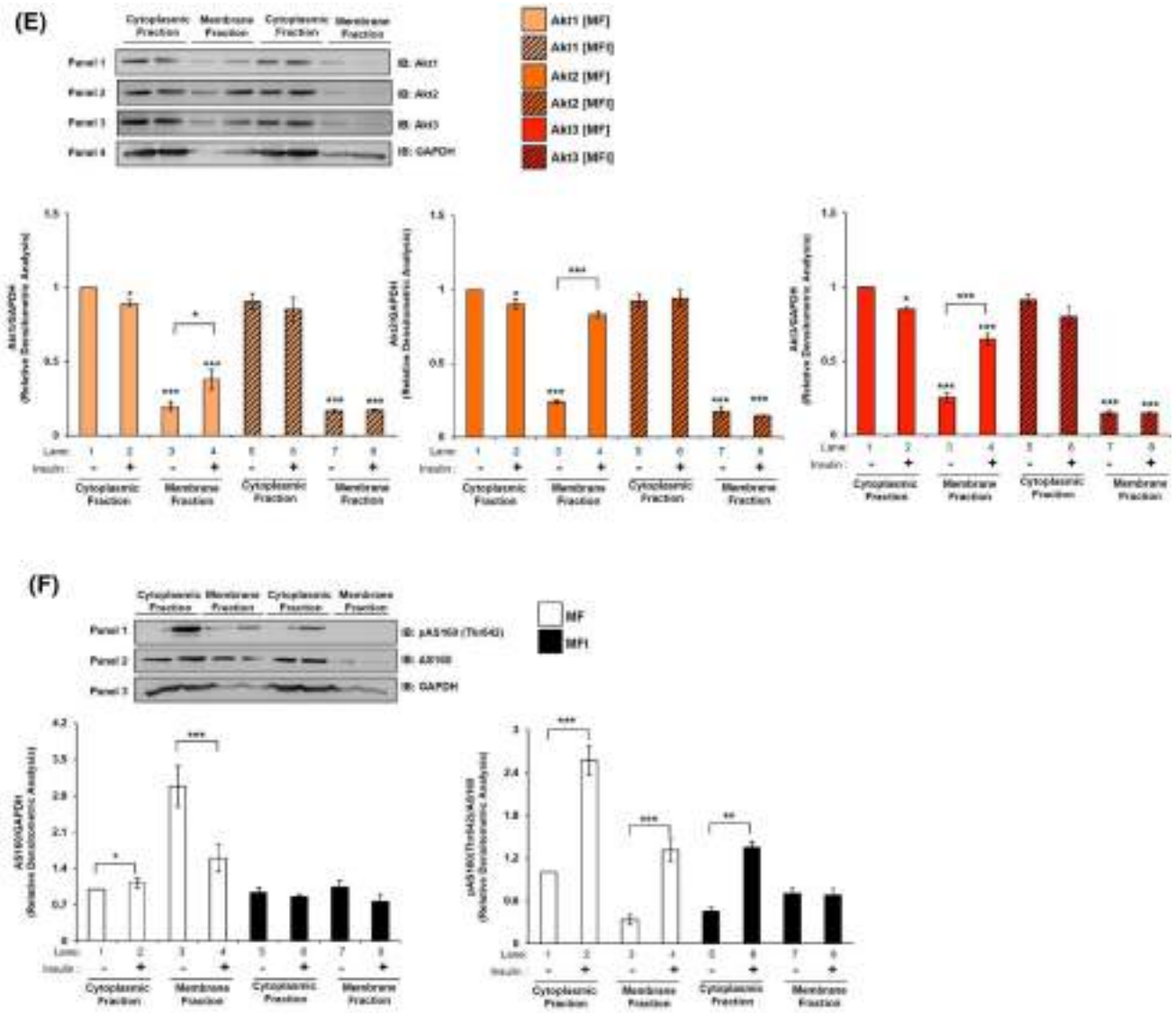

Fig. 8 (continued)

Effect of insulin stimulation on the translocation of Akt isoforms and AS160 in insulin-resistant neuronal cells

Having established the involvement of all Akt isoforms in regulating neuronal insulin-resistance we proceeded to test their subcellular translocation post-insulin stimulation. Our data show that, under MF condition, Akt1, Akt2, and Akt3 maintained a similar trend as in Fig. 5A, that is, Akt2 translocated and accumulated to the plasma membrane the most by 245.47% (Fig. 8E, Panel 2 and 4, lane 3 vs lane 4), with Akt1 and Akt3 by 93.42% (Fig. 8E, Panel 1 and 4, lane 3 vs lane 4) and 155.94% (Fig. 8E, Panel 3 and 4, lane 3 vs lane 4), respectively, as compared to their respective controls without insulin. In contrast to this, none of the Akt isoforms translocated to the plasma membrane post-insulin stimulation under resistant condition (Fig. 8E, lane 7 vs lane 8). This is similar to our data observed in mice whole brain tissue, where translocation of all isoforms were affected in HFD diabetic mice. Data show that, translocation of all isoforms is affected under insulin-resistant condition.

Testing of expression and phosphorylation of AS160 Thr-642 in the cytoplasm and plasma membrane fractions in insulin-sensitive and insulin-resistant cells showed the expression of AS160 increased in cytoplasmic fraction in MF by 21.46% but remained unchanged in MFI condition (Fig. 8F, Panel 2 and 3, lane 1 vs lane 2, and lane 5 vs lane 6, respectively). However, in contrast to MF condition, where expression of AS160 decreased in membrane fraction by 46.39% (Fig. 8F, Panel 2 and 3, lane 3 vs lane 4), there was only a 27.51%

decrease under MFI condition (Fig. 8F, Panel 2 and 3, lane 7 vs lane 8). Thus, insulin-dependent AS160 dissociation from plasma membrane reduces in insulin-resistant condition, possibly due to inefficient upstream Akt phosphorylation under MFI condition. Phosphorylation of AS160 at Thr-642, under MF condition, showed increase in cytoplasmic fraction by 157.03% (Fig. 8F, Panel 1 and 2, lane 1 vs lane 2) and membrane fraction by 291.44% (Fig. 8F, Panel 1 and 2, lane 3 vs lane 4). Under MFI condition, phosphorylation of AS160 in cytoplasmic fraction increased by 193.50% (Fig. 8F, Panel 1 and 2, lane 5 vs lane 6), but this increase was nominal as compared to MF condition which was 47.40% (Fig. 8F, Panel 1 and 2, lane 2 vs lane 6). However, there was no significant change in phosphorylation of AS160 in membrane fraction under MFI condition (Fig. 8F, Panel 1 and 2, lane 7 vs lane 8). Data strongly show that in insulin-resistant condition, improper translocation of Akt isoforms to plasma membrane regulates GLUT4 translocation and thereby reduced glucose uptake.

Effect of Akt1, Akt2 and Akt3 over-expression on expression and activation of AS160 under insulin-resistant condition

Having seen for the first time that all isoforms are differentially affected under insulin-resistant condition, we wished to understand whether over-expression of specific isoforms in resistant condition can cause reversal of resistance. To undertake this experiment, we over-expressed each isoform individually and transfected cells were then subjected to MF and MFI conditions, and the effect of over-expression on specific isoform was tested with or without insulin. As compared to controls (respective empty plasmid backbones), Akt^{+1}, Akt^{+2} or Akt^{+3} over-expression led to a ~ tenfold increase in expression of Akt1 (Fig. 9A), Akt2 (Fig. 9C) or Akt3 (Fig. 9E), respectively. There was no change in expression of AS160 under all the conditions tested (Fig. 9B, D, F). However, under all control conditions (respective empty plasmid backbone), activation of AS160, as determined by phosphorylation at Thr-642, was down-regulated from MF to MFI conditions (Fig. 9B, D, E lane 2 vs lane 4). Due to over-expression of Akt^{+1}, activation of AS160 was up-regulated by insulin stimulation by 30.70% (Fig. 9B, lane 2 vs lane 6), and by 172.15% (Fig. 9B, lane 4 vs lane 8) under MF and MFI conditions, respectively. Similarly, post-Akt^{+2} over-expression activation of AS160 was up-regulated by insulin stimulation by 48.66% (Fig. 9D, lane 2 vs lane 6), and by 331.84% (Fig. 9D, lane 4 vs lane 8) under MF and MFI conditions, respectively. Post-Akt^{+3} over-expression activation of AS160 was up-regulated by insulin stimulation by 31.62% (Fig. 9F, lane 2 vs lane 6), and by 247.55% (Fig. 9F, lane 4 vs lane 8) under MF and MFI conditions, respectively. Activation of AS160 by insulin stimulation under MFI condition was affected most by Akt^{+2} by 38.26% (Fig. 9D, lane 2 vs lane 8), as compared to Akt^{+1} by 0.12% (Fig. 9B, lane 2 vs lane 8) or Akt^{+3} by 11.50% (Fig. 9F, lane 2 vs lane 8). Thus, over-expression of all Akt isoforms was able to up-regulate AS160 phosphorylation in insulin-sensitive (MF) and insulin-resistant (MFI) condition.

Effect of Akt1, Akt2, and Akt3 over-expression on neuronal glucose uptake under insulin-resistant condition

To determine how isoform specific over-expression regulates neuronal glucose uptake in insulin-sensitive and insulin-resistant condition, Akt1, Akt2 or Akt3 were over-expressed and subjected to glucose uptake assay. Under MF condition, Akt^{+2} over-expressed N2A cells showed 75.05% increase in insulin stimulated 2-NBDG uptake as compared to control-transfected cells (Fig. 9H, lane 2 vs lane 6). Similarly, Akt^{+1} or Akt^{+3} over-expressed N2A cells showed 27.50% and 34.06% increase, respectively, in insulin stimulated 2-NBDG uptake as compared to respective control-transfected cells (Fig. 9G, lane 2 vs lane 6; Fig. 9I and lane 2 vs lane 6, respectively). Similarly, in MFI condition, Akt^{+2} over-expressed N2A cells showed 118.85% increase in insulin stimulated 2-NBDG uptake as compared to control-transfected cells (Fig. 9H, lane 4 vs lane 8). Akt^{+1} or Akt^{+3} over-expressed N2A cells showed 44.12% and 58.82% increase, respectively, in insulin stimulated 2-NBDG uptake as compared to respective control-transfected cells (Fig. 9G, lane 4 vs lane 8; Fig. 9I lane 4 vs lane 8, respectively). However, important point to note that only Akt^{+2} over-expression up-regulated neuronal glucose uptake under MFI condition by 47.43% as compared to MF condition (Fig. 9H, lane 2 vs lane 8). Overall, Akt^{+2} over-expression influenced neuronal glucose uptake most, followed by Akt3 or Akt1 in MF as well as MFI condition. Data prove that Akt isoforms over-expression reverses insulin-resistance in neuronal cells. Although Akt isoforms were differentially silenced as presented above, but the functional trend was revalidated through the over-expression data.

Overall, all isoforms participate in reversal, however, the effect is differential between the isoforms.

Discussion

Compensatory role of Akt isoforms in regulating neuronal glucose uptake

In the present study, utilizing two different neuronal cell lines we are reporting for the first time that in neuronal system, all isoforms of Akt contribute to neuronal glucose uptake. It turns out that Akt2 contributes most, followed by Akt3 and then Akt1 (Fig. 4 A–C). However, from single

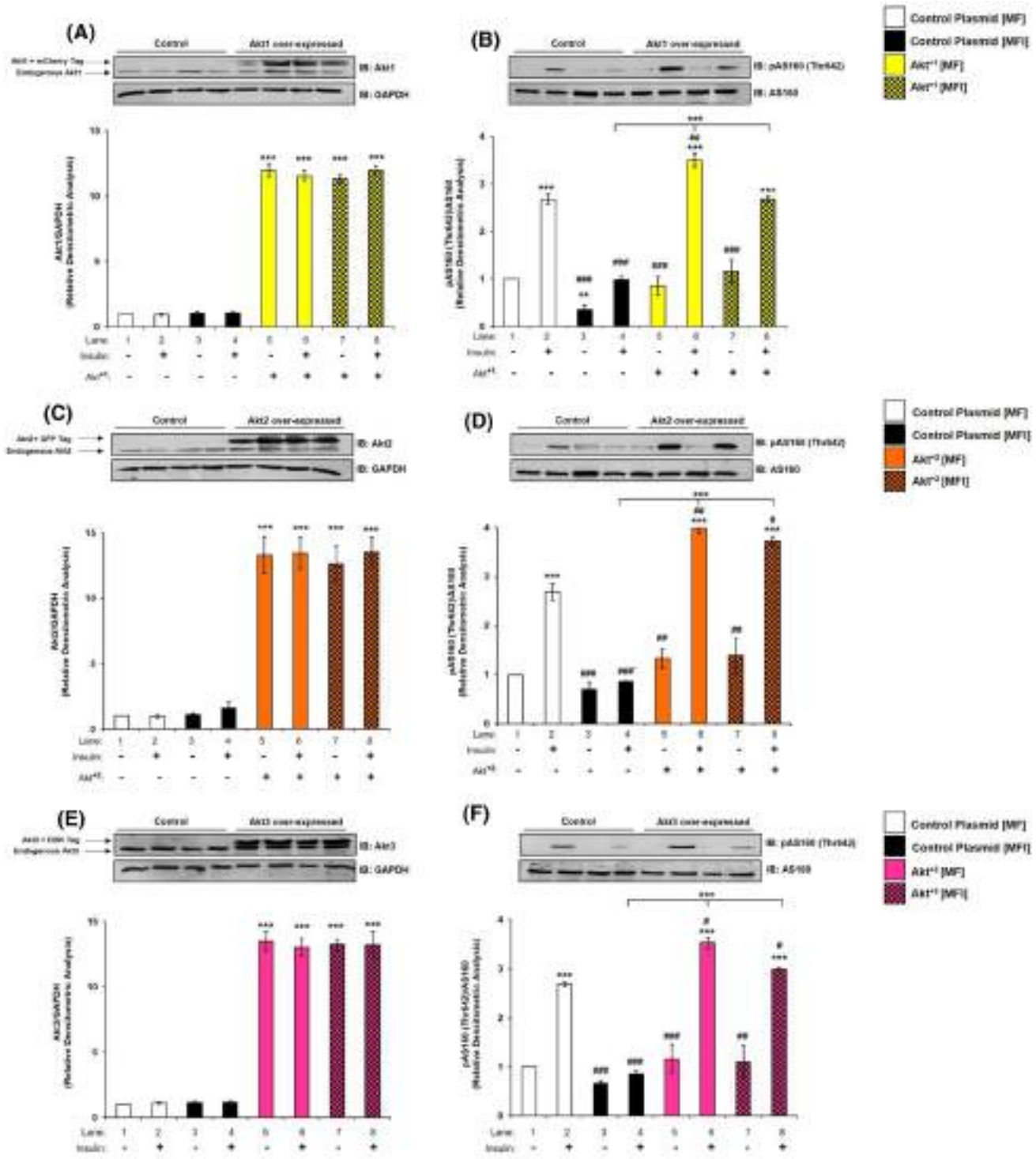

Fig. 9 Effect of Akt1, Akt2, and Akt3 over-expression on expression and activation of AS160, and neuronal glucose uptake under insulin-resistant condition in neuronal cells. **A**–**F** Three days post-proliferation, Akt1, Akt2 or Akt3 were over-expressed using isoform specific plasmids. N2A cells were differentiated in serum-free medium in the absence of (MF) or chronic presence of 100 nM insulin (MFI) for 3 days. Cells were lysed and subjected to western blotting, followed by probing with relevant primary antibodies. Bar represents relative change when probed with anti-Akt isoform specific antibody. **A**, **C**, **E** Bar represents relative change in Akt1/Akt2/Akt3 probed with anti-Akt isoform specific antibody. GAPDH was used as loading control **B**, **D**, **F** Bar represents relative change in pAS160 (Thr-642) when probed with anti-AS160 antibody. **G**–**I** Three days post-proliferation, Akt1, Akt2 or Akt3 were over-expressed using isoform specific plasmids. N2A cells were differentiated in serum-free medium in the absence of (MF) or chronic presence of 100 nM insulin (MFI) for 3 days. N2A cells were serum starved for 2 h, followed by 100 nM insulin for 30 min. Uptake of 2-NBDG was then measured. Experiments were executed three times and a representative result is shown. Data expressed are mean ± SE. $^{***}P<0.001$, $^{**}P<0.01$, $^{*}P<0.05$ compared to lane 1 or as indicated, $^{\#\#\#}P<0.001$, $^{\#\#}P<0.01$, $^{\#}P<0.05$ compared to lane 2. *IB* Immunoblot; *A.U* Arbitrary Units

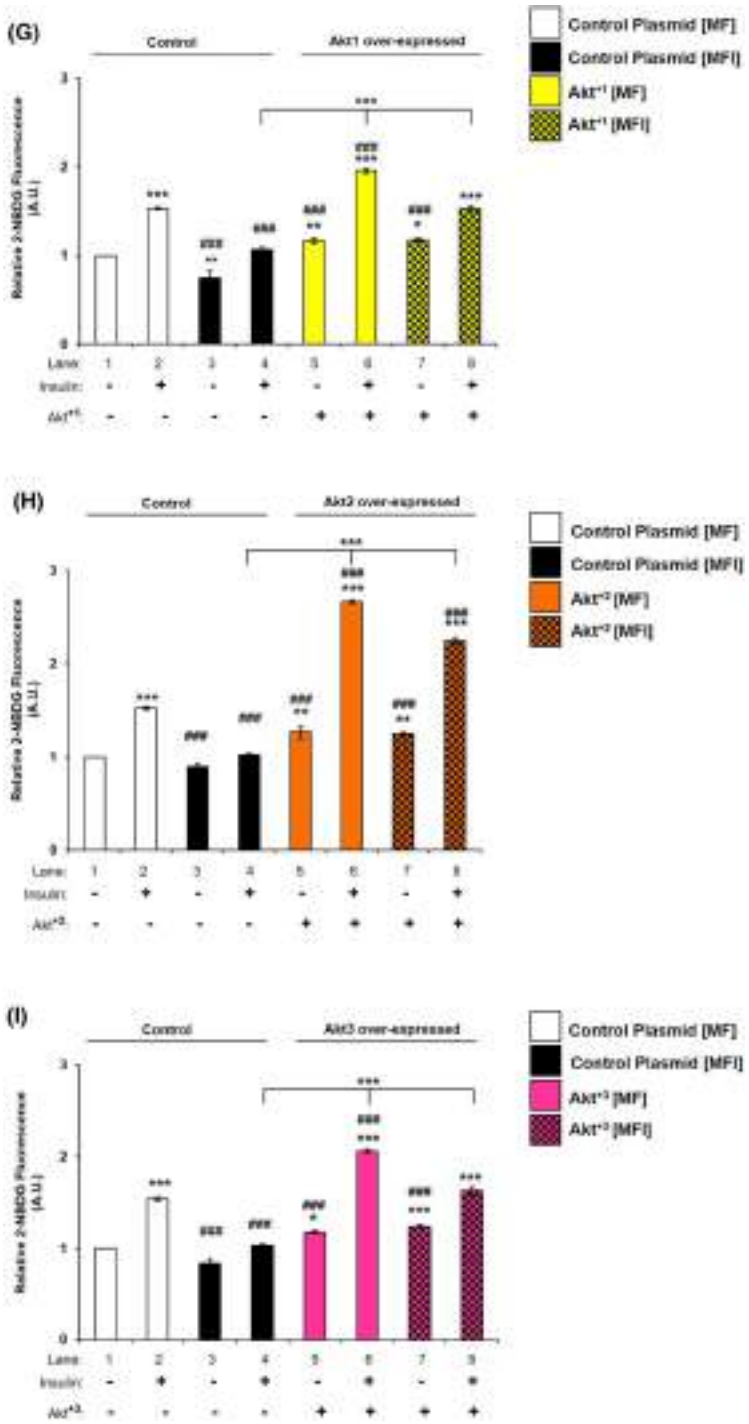

Fig. 9 continued

isoform silenced condition to double, we noticed an additional decrease in glucose uptake, but not additive, although maintaining the trend under both conditions (Table S1). This points to a functional compensatory role of Akt isoforms under double isoform silenced condition. This compensation has previously been reported in neuronal system with requirement of all Akt isoforms in regulating Tau phosphorylation [53]. Interestingly, in insulin-resistant condition, double silencing decreased glucose uptake further (Fig. 8D). However, this decrease was not isoforms specific, pointing to functional compensation yet again. In addition to this, even post-double silencing, the sustained glucose uptake points to additional pathways working in regulating glucose metabolism. These results were further corroborated by isoform specific over-expression studies under insulin-resistant condition. While over-expression of all three isoforms increased neuronal glucose uptake in insulin-sensitive as well as insulin-resistant condition, only Akt2 over-expression increased glucose uptake in insulin-resistant condition to a level comparable to its respective insulin-sensitive condition (Fig. 9H, lane 2 vs lane 8). Our study reports a predominant role of Akt2, novel role of Akt1 and Akt3, and functional compensation by all Akt isoforms in regulating neuronal glucose uptake.

Subcellular translocation determines Akt isoform specificity

In the present study, we examined translocation of Akt isoforms post-insulin stimulation in N2A (Fig. 5A) and HT22 (Fig. 5B) cell lines, and all isoforms translocated to plasma membrane post-insulin stimulation. Interestingly, Akt2 translocated to the plasma membrane the most, followed by Akt3 and Akt1. This has been explained in Fig. 10B. Previous studies by McGraw and Gonzalez (in adipocytes) and Zheng and Cartee (in rat skeletal muscles) have discussed only Akt2 translocates post-insulin stimulation, with very limited translocation of Akt1 [23, 43]. Akt3 has not been studied. We also studied subcellular translocation of Akt isoforms in insulin-resistant diabetic mice whole brain tissue lysate [Normal Diet vs High-Fat-Diet] (Fig. 7A) and in N2A (Fig. 8E). Resistance caused due to high-fat-diet or hyperinsulinemia, caused all Akt isoforms to be affected, such that none of the isoforms translocated to plasma membrane. This has been explained in Fig. 10D. To our knowledge, this is the first report to study isoform specific translocation of all isoforms in neuronal system, more so, in both insulin-sensitive as well as in insulin-resistant condition. Thus, preferential accumulation on plasma membrane is the key determining factor for Akt isoform specific activation, which translates into differential glucose uptake.

We also tested the redistribution of AS160 post-insulin stimulation in N2A (Fig. 5C) and HT22 (Fig. 5D) cells. In the present study, phosphorylation of AS160 was detected in cytoplasm and membrane fraction. It is reported that AS160 gets phosphorylated at the plasma membrane due to a small pool of it being present attached to both the plasma membrane and the GSVs via its second PTB domain [54]. Akt, once phosphorylated and activated at the plasma membrane, in-turn phosphorylates AS160 there. This has been explained in Fig. 10A, B. Thus, phosphorylated AS160 was detected at the membrane. In the cytoplasm, phosphorylated AS160 at Thr-642 acts as binding site for 14-3-3 proteins that mediate AS160's subcellular localization and GLUT4 translocation [44, 54, 55]. We also detected phosphorylated AS160 in the cytoplasm. We observed a sharp decrease in plasma membrane bound AS160 post-insulin stimulation (Fig. 5C, D 7B, 8F). This was also reestablished using confocal microscopy, where we demonstrated decrease in AS160 and GLUT4 co-localization post-insulin stimulation (Fig. 6). This is in coherence with previous study in adipocytes [45] but first time being reported in neuronal system, where insulin stimulation leads to redistribution of AS160 from the GSVs and plasma membrane to cytoplasm. Our data show that post-insulin stimulation AS160 undergoes phosphorylation on the plasma membrane by activated Akt. This leads to redistribution of AS160 from near the membrane to the cytoplasm, allowing GLUT4 translocation. This has been explained in Fig. 10A, B. All these have never been reported before in neuronal cell. Data prove that Akt isoforms interact with downstream insulin signaling molecule, AS160, thereby creating a pathway eventually leading to part of the glucose uptake in neuronal cells. We have observed phosphorylated AS160 in the cytosolic fraction. As insulin stimulated glucose uptake is regulated by a variety of mechanisms running side-by-side, therefore, it is possible that due to insulin stimulation cytosolic interaction(s) between phosphorylated AS160 and 14-3-3 proteins help in the GLUT4 translocation and Akt isoform specific interaction with AS160 dictates total amount of glucose uptake by a neuronal cell. Overall, the data prove that Akt2 despite being lesser in expression as compared to other two isoforms, translocates to the membrane more than the other isoforms, gets phosphorylated and interact with AS160 thereby phosphorylating it, and regulates glucose uptake in neuronal system (Fig. 10A, B).

Akt isoforms differentially regulate activation of AS160

AS160 is a RabGAP (Rab GTPase-activating protein) that provided an early link between Akt and GLUT4 translocation by vesicular traffic [41, 56–58]. It is a negative regulator of insulin signaling as knockdown of AS160 causes increase in GLUT4 translocation in basal state whereas over-expression of its phosphorylation-defective

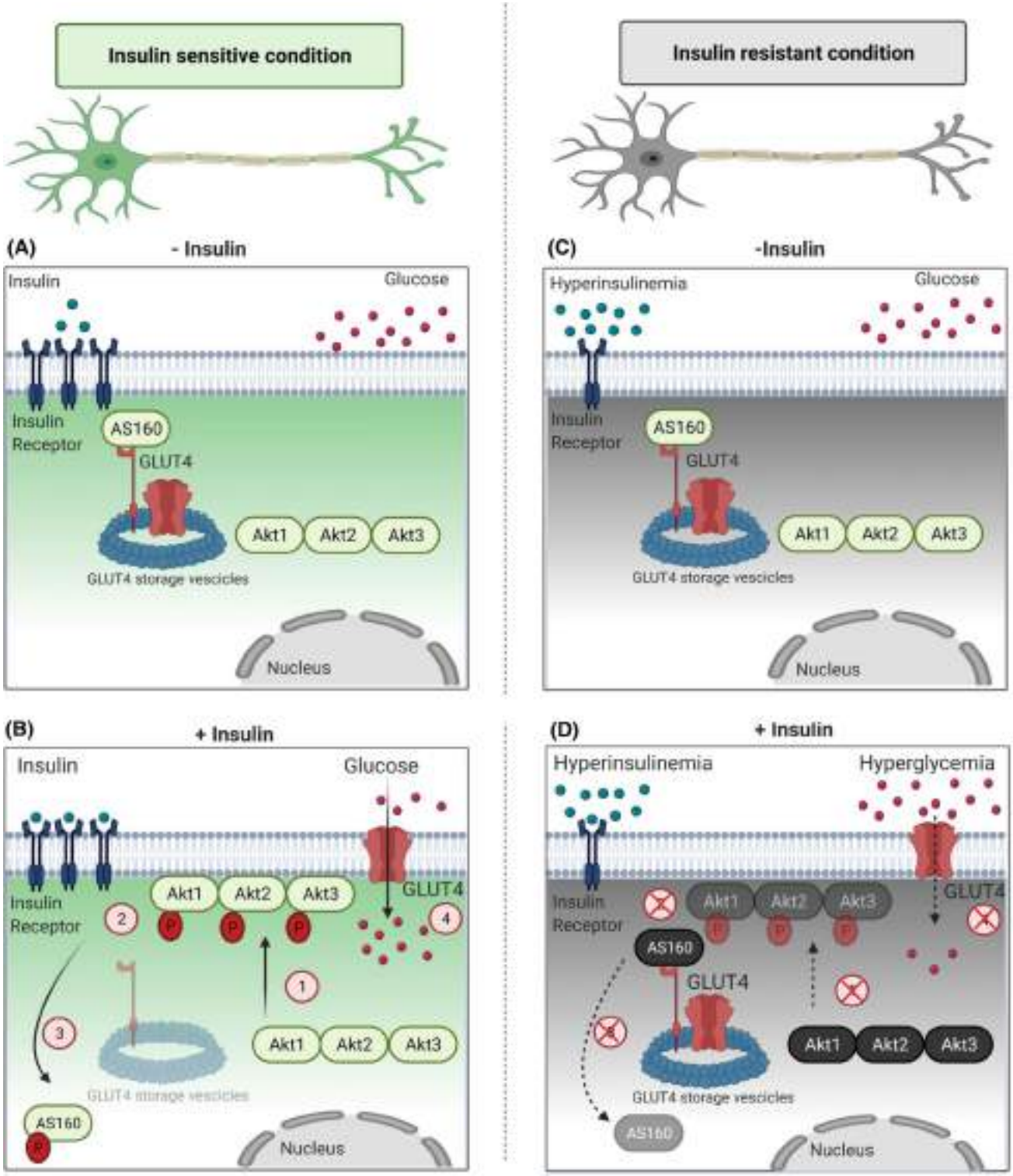

mutant decreases it [44, 59–62]. There is no information about how individual Akt isoforms regulate activation of AS160, more so, in a neuronal system. Here, we studied two AS160 phosphorylation sites, Ser-588 and Thr-642. Activation determined by both showed down-regulation, with Thr-642 getting more severely affected by Akt isoform specific knockdown than Ser-588 (Fig. 3). Previously, a cluster analysis study has showed that the threonine and serine sites on AS160 clustered separately, with threonine site grouped with other Akt substrates [42]. Further analysis also showed that both of these sites are mutually exclusive with Ser-588 phosphorylation also

◂**Fig. 10** Schematic diagram depicting role of Akt isoforms in regulating neuronal insulin signaling. **A** In an insulin-sensitive, under unstimulated condition, Akt (Akt1, Akt2, and Akt3) are present in the cytoplasm. AS160 binds to GSVs (GLUT4 Storage Vesicles) and tethers GLUT4. This does not allow GLUT4 exocytosis under basal conditions. **B** In an insulin-sensitive, insulin stimulated condition, Akt translocates to plasma membrane in an isoform specific insulin-dependent way (1), getting phosphorylated there (2). In neuronal system, all Akt isoforms translocate in the order Akt2 > Akt3 > Akt1. An activated Akt phosphorylates AS160, hence inactivating it. Phosphorylated and thus inactivated AS160 translocated to cytoplasm (3), promoting GLUT4 dissociation from GSVs and allowing glucose uptake (4). **C** In an insulin-resistant, unstimulated condition, hyperinsulinemia occurs due to defects in insulin signaling. **D** In an insulin-resistant, insulin stimulated condition, hyperinsulinemia triggers insulin receptor down-regulation, not allowing Akt isoform specific translocation to the plasma membrane (1). This leads to inadequate phosphorylation (2), leading to Akt's inability to phosphorylate AS160. Unphosphorylated, thus, active AS160 continues tethering GLUT4 to GSVs, not allowing GLUT4 exocytosis, hence affecting neuronal glucose uptake. (Created with BioRender.com)

reported downstream of PKCζ [42]. Other studies have pointed to Thr-642 as better measure of AS160 activation as point mutation of threonine to alanine leads to a significantly major decrease in GLUT4 translocation, followed by Ser mutation leading to further decrease [41]. AS160 Thr-642 phosphorylation also acts as a binding site for 14–3–3 proteins, ultimately affecting GLUT4 translocation [54, 55]. Our data suggested that expression of AS160 did not change post-single/ double silencing (Fig. 3). However, all three Akt isoforms contribute to AS160 regulation, with Akt2 contributing maximum, followed by Akt3 and then Akt1 (Fig. 3). Interestingly, Akt isoforms showed functional compensation in regulating AS160 at both the sites post-silencing. While over-expression of all Akt isoforms up-regulated phosphorylation of AS160 both under insulin-sensitive and insulin-resistant condition, over-expression of Akt2 affected AS160 phosphorylation the most (Fig. 9D). This is explained in Fig. 10. This is the first study reporting regulation of AS160 by all Akt isoforms in neuronal system. McGraw and Gonzalez studied AS160 regulation in adipocytes and reported that Akt2 specifically regulates activation of AS160 [14]. Similar studies have been reported in skeletal muscles [43, 61]. These studies specifically reported no regulation by Akt1. Akt3 was not addressed in either of these studies. This difference may be partly attributed to tissue specific regulation of isoform specific functionality of Akt.

Akt isoform specific role in neuronal insulin-resistance

In the present study, we report differential decrease in phosphorylation of all Akt isoforms in insulin-resistant neuronal cells post-insulin stimulation. Akt2 phosphorylation was affected most, followed by Akt3 and Akt1 (Fig. 8A–C). This is in contrast to peripheral insulin-sensitive tissue systems, where role of Akt isoforms and their interplay has been paradoxical. Gosmanov et al. (2004) reported that in skeletal muscles of obese patients with severe hyperglycemia and atypical diabetes, only Akt2 phosphorylation was affected, with no effect on Akt1 phosphorylation [63]. Akt 3 was not addressed in this study. Brozinick et al. (2003) also reported impaired Akt2 as well as Akt3 phosphorylation in skeletal muscles from lean and obese insulin-resistant humans, without any effect on Akt1 phosphorylation [52]. Similarly, Cozzone et al. (2008) studied primary myotubes from healthy control participants and Type-II diabetic patients and reported decrease in activation of all three isoforms [51]. Kim et al. (2000) reported redundant role of Akt1 and Akt2 in insulin-resistant tissue systems [64]. Addressing in the neuronal system, Gabbouj et al. (2019) reported decrease in Akt2 phosphorylation APP/PS1 Alzheimer mice hippocampus as compared to normal mice post-insulin stimulation, without any effect on Akt1 [35]. Akt3 was not addressed in this study. Previously, involvement of all Akt isoforms has been established with a special emphasis on regulating Tau phosphorylation with reference to Alzheimer's disease and not on insulin signaling or insulin resistance. Wang et al. (2015) reported that only Akt 3 isoform conditional knockout (but not single or double knockouts) in cortical and cerebellar samples in mice brain affected Tau phosphorylation, pointing to requirement of all Akt isoforms and possible compensation in neuronal systems [53]. To the best of our knowledge, our study is the first to have undertaken all Akt isoform in the neural cells in the study and reported role of all Akt isoforms in regulating neuronal insulin signaling and resistance.

Conclusions

Our study is the first to report isoform specific role of all Akt isoforms in regulating neuronal insulin signaling and resistance. We find that in neuronal cells (a) all Akt isoforms regulate AS160 activation and glucose uptake; Akt2 plays a predominant role, with Akt1 and Akt3 playing significant role as well; (b) Activation of all isoforms decreased differentially under insulin-resistance with Akt2 being affected most, followed by Akt3 and Akt1; (c) Insulin-resistance is reversed by over-expression of any isoform of Akt, but predominantly by Akt2; (d) Insulin-dependent translocation on plasma membrane determines isoform specificity with Akt2 translocating the most, followed by Akt3 and then Akt1; (e) Insulin-resistance hampered this insulin-dependent translocation of all Akt isoforms to plasma membrane, irrespective of isoform; (f) Akt3, despite being neuron specific isoform

contributed substantially to AS160 regulation, neuronal glucose uptake, and insulin-resistance. However, Akt2 was still the predominant isoform in regulating all the above functions. This points to a novel, differential yet compensatory interplay of all Akt isoforms in neuronal insulin signaling and resistance. These findings are fundamentally important on their own right for deeper understanding of insulin signaling and resistance in neuronal cells. This may in future help in solving a spectrum of problems associated with a diabetes, diabetes complications and neurodegenerative disorders.

Materials and methods

Materials

Minimum essential media (MEM), Dulbecco's Minimum essential media (DMEM), foetal bovine serum (FBS), trypsin–EDTA, Opti-MEM, 2-(*N*-(7-nitrobenz-2-oxa1,3-diazol-4-yl) amino)-2 deoxy glucose (2-NBDG) (Cat. No. N13195), Lipofectamine 2000 (Cat. No. 11668019) and anti-Akt3 antibody (Cat. No. 41700) were procured from Thermo Fisher Scientific Inc. (USA). MCDB 201 medium, nutrient mixture F-12 Ham, albumin from bovine serum (cell culture grade), anti-GAPDH antibody (Cat. No. 9545), and dimethyl sulfoxide (DMSO) were purchased from Sigma–Aldrich Co. (USA). Anti-phospho-Akt (serine-473) (Cat. No. 4058), anti-Akt antibody (Cat. No. 9272), anti-phospho-Akt1 (Serine-473) (Cat. No. 9018), anti-phospho-Akt2 (Serine-474) (Cat. No. 8599), anti-Akt1 antibody (Cat. No. 2938), anti-Akt2 antibody (Cat. No. 3063), anti-phospho-AS160 (serine-588) (Cat. No. 8730), anti-phospho-AS160 (threonine-642) (Cat. No.8881), anti-AS160 antibody (Cat. No. 2670), IgG conformational (Cat. No. 3678) were purchased from Cell Signalling Technology Inc. (USA). Protein A/G agarose beads (Cat no. sc:2003), anti-GLUT-4 (Cat no. sc:1608) were purchased from Santa Cruz Biotechnology (USA). Anti-Caveolin-1 (Cat no.: 894) was kindly gifted by Dr. Chinmoy Mukhopadhyay, Jawaharlal Nehru University, New Delhi. Recombinant insulin (Cat. No. 407709) was purchased from Calbiochem (Germany).

Cell culture

N2A (mice neuroblastoma cell line) and HT22 (mice hippocampal cell line) cells were proliferated in MEM and DMEM, respectively, supplemented with 10% FBS, and antibiotics-penicillin 100 IU/ml and streptomycin 100 mg/ml, at 37 °C in 5% CO_2. For N2A cells, 3 days post-proliferation, cells were subjected to differentiation in MEM supplemented with 1% FBS and 2% DMSO at 37 °C in 5% CO_2 for 3 days [8]. For HT22, 2 days post-proliferation, cells were subjected to differentiation in neurobasal media containing 2 mmol/L glutamine and 1 × N2 supplement for 2 days [39, 40]. Insulin-resistance in N2A cells was generated as reported earlier from our laboratory [6]. Briefly, cells were kept in an equal mixture of two serum-free media (MCDB 201 medium and nutrient mixture F-12 Ham) in the absence (MF; insulin-sensitive) or in chronic presence of 100 nM insulin for 3 days (MFI; insulin-resistant). Media were replaced after every 12 h. Differentiated neuronal cells were subjected to 30 min insulin stimulation as per standard assay conditions as reported previously from other as well as from our laboratory [8, 48, 49, 65, 66].

Gene silencing by siRNA transfection

Akt isoforms in the cells were silenced as previously reported [39]. To select the specific siRNA among 4 different siRNAs against each isoform provided by the manufacture (Qiagen), specific siRNA for each isoform was chosen based on the one that provided maximum silencing (Fig. S2A, S3A and S4A). Selected isoform specific siRNA sequences were: Akt1:5′ ATGCTGTTCAGAGACATTTA3′; Akt2:5′AAC ATTTCTCTGTAGCAGAA3′; Akt3:5′GATTGATAATAT ATAGGAGGA3′. Selection of specific siRNA was followed by optimization of dose of selected siRNA (Fig. S2B, S3B and S4B). For double silencing, optimized doses as selected above for the single silencing were used additively. Scrambled (non-specific) and Akt isoform specific siRNAs were transfected in Opti-MEM using Lipofectamine 2000. Six hours post-transfection, Opti-MEM was changed to respective proliferation media depending on the cell line used. Twelve hours post-media change, cells were subjected to differentiation as explained above.

Plasmid DNA transfection using Akt isoform specific plasmids

Akt isoform specific constructs were purchased from Addgene [Akt1 (#86631) and Akt2 (#86593)] and Origene [Akt3 (NM_RC221051)]. Specific plasmid constructs were transfected in the cells as previously reported [39]. Briefly, N2A cells were transiently transfected with either Akt isoform specific construct or control (respective empty backbone) constructs in Opti-MEM using Lipofectamine 2000 according to manufacturer's instructions.

Immunoprecipitation

Because a specific phospho-Akt3 antibody was not available to measure phosphorylation levels of Akt3, Akt3 protein was immunoprecipitated using Akt3 specific antibody (Thermo, PA-41700), and probed with Anti-phospho-Akt (serine-473) (CST, Cat. No. 4058). Anti-IgG conformational antibody (CST, Cat No. 3678) was used to mask remaining IgG bands.

Cells were proliferated and differentiated as described above. 500 µg of protein lysate with certain amount of primary antibody (as referred in datasheet of the manufacturer) was added and incubated overnight at 4 °C in a microfuge rotator at 10 rpm (Test tube Rotator, Tarsons, Cat. No.: 3070). Next day, protein A/G beads were added for 4 h, along with lysis buffer and protease inhibitors. After 4 h of incubation, cells were centrifuged at 5000 rpm (Centrifuge, Sigma Cat. No.: 2-16KL) for 5 min. Supernatant was discarded and pellet was washed 3 times with lysis buffer along with protease inhibitors. Pellet was suspended in SDS–PAGE sample buffer and heated at 90 °C. The protein samples were resolved on SDS–PAGE [38].

Cell lysis and immunoblotting

After differentiation, cells were stimulated with or without 100 nM insulin for 30 min as indicated above. Cells were lysed in lysis buffer (50 mM HEPES, 150 mM NaCl, 1.5 mM $MgCl_2$, 1 mM EGTA, 10 mM $Na_4P_2O_7$, 50 mM NaF, 50 mM β-glycerophosphate, 1 mM Na_3VO_4 and 1% triton X-100) as described previously from our laboratory for 30 min at 4 °C [39]. Supernatants were collected and protein was estimated by Bicinchoninic Acid (BCA) method [67]. Lysates were boiled with Laemmli sample buffer (Tris-HCl 62.5 mM, pH 6.7; glycerol 10% (v/v); SDS 2% (w/v); bromophenol blue 0.003% (w/v) containing β-mercaptoethanol 14.3 M) for 5 min, resolved by SDS–PAGE gel electrophoresis and transferred to nitrocellulose membrane. Membranes were blocked with BSA (5%) and incubated with the indicated primary antibodies for 12–16 h, followed by 2 h incubation with HRP-conjugated secondary antibody. The protein bands were visualized with Pierce ECL Plus Western Blotting substrate (Thermo, Cat No. 32132) on Typhoon FLA 9500 (GE Healthcare Bio-Sciences AB). Quantification of all blots was done using Quantity One 1-D Analysis Software (Bio-Rad Laboratories, Inc.). Blots were normalized with the relative expression of the (non-phospho) protein being tested or a housekeeping protein (GAPDH) under the same conditions [39, 48].

Membrane fractionation

N2A/HT22 cells were differentiated in 100 mm tissue culture plates. After respective treatment, cells were lysed in lysis buffer (20 mM Tris, pH 7.5; 250 mM sucrose; 2 mM EDTA; 2 mM EGTA; 1 mM PMSF; 10 µg/ml aprotinin and leupeptin), as reported earlier from our laboratory for 5 min [68]. Lysate was homogenized for 10 min with 30 strokes in Glass homogenizer at 4 °C. Lysates were subjected to ultra-centrifugation, at 200,000×*g* for 1 h. Supernatant was collected and termed as 'Cytosolic fraction' and pellet was re-suspended in lysis buffer with 1% NP-40 (20 mM Tris, pH 7.5; 1% NP-40; 150 mM NaCl; 1 mM EDTA; 1 mM EGTA; 1 mM PMSF; 10 µg/ml aprotinin and leupeptin) at 4 °C for 30 min. Centrifuged supernatant was collected and termed as 'Membrane fraction'. The presence of membrane-specific marker like Caveolin-1 was tested and GAPDH was used as a loading control in all membrane translocation experiments [47].

Mice whole brain tissue lysis and Immunoblotting

Insulin resistance was generated in 16 weeks old high-fat-diet (HFD) fed Swiss Albino male mice in the laboratory of Dr. Prosenjit Mandal, Indian Institute of Technology—Mandi, over 10 weeks, as previously reported [69, 70], and whole brain tissues of those mice, which were kind gifts from Dr. Mandal, Indian Institute of Technology—Mandi, were used for our experiments. Glucose tolerance test and insulin tolerance tests were performed; however, perfusion was not done before brain collection. Mice were divided into two groups: normal diet (ND) and high-fat-diet (HFD), each group containing three animals. Levels of triglyceride, cholesterol, serum glutamic-oxaloacetic transaminase (SGOT), serum glutamic-pyruvic transaminase (SPGT), and fasting blood glucose were elevated by 48%, 29%, 50%, 53%, and 40%, respectively, in HFD mice as compared to ND mice. Mice whole brain were lysed in a homogenizer in lysis buffer (50 mM HEPES pH 7.4, 150 mM NaCl, 1.5 mM $MgCl_2$, 1 mM EGTA, 10 mM sodium pyrophosphate, 50 mM sodium fluoride, 50 mM β-glycerophosphate, 1 mM $Na3VO_4$, 1% Triton X-100 supplemented with 2 mM PMSF, 10 µg/ml each of leupeptin and aprotinin) at 4 °C for 15 min. Mice whole brain tissues were homogenized as described previously [68]. Supernatants were collected and protein was estimated by Bicinchoninic acid test [67]. For plasma membrane fractionation of whole brain lysates, 150 µl of whole brain lysates were ultra-centrifuged as described above in "Membrane fractionation" step. All experiments were performed following the guidelines prescribed by CPCSEA (Committee for the Purpose of Control and Supervision of Experiments on Animals) with the approval of the Internal Animal Ethics Committee, Visva-Bharati (IAEC/VB/2017/01). The legal requirements/guidelines in the country for the care and use of animals have been followed.

Glucose uptake assay

Glucose uptake assays were performed as described previously from our laboratory [38]. Briefly, differentiated N2A and HT22 were washed and subjected to glucose starvation for 2 h. After respective treatment, cells were treated with 50 µM 2-NBDG for 1 h and lysed in buffer containing 20 mM Tris–HCl pH 7.4, 40 mM KCl, 1% sodium deoxycholate and 1% NP-40 for 15 min at 25 °C with gentle shaking.

Cells were then scraped off and centrifuged at 13,000×*g* for 20 min at 4 °C. The fluorescence was then measured using a fluorescence spectrophotometer LS55 (Perkin Elmer, USA) at the excitation and emission wavelengths of 485 nm and 535 nm, respectively.

Confocal-microscopy

Immunofluorescence studies of N2A cells carried out as described previously [66]. Briefly, N2A cells were treated with 100 nM insulin for 30 min at 37 °C. Cells were fixed with 4% paraformaldehyde for 15 min. Cells were permeabilized by incubating with 0.5% Triton X-100 for 5 min, followed by washing with PBS. Cells were washed in PBS and blocked using blocking buffer (BSA 1% in PBS) for 1 h. Cells were incubated with anti-GLUT4 antibody overnight at 4 °C, washed with PBS solution, followed by incubation with anti-AS160 antibody overnight at 4 °C. Cells were washed using PBS and incubated with Donkey anti-Goat Alexa 555 (for GLUT4) and Mice anti-Goat Alexa 488 (for AS160) secondary antibodies for 45 min at room temperature. Cells were washed further with PBS and mounted using ProLong™ Diamond Antifade Mountant with DAPI on to glass slides. Images were taken using Carl Zeiss LSM 880 microscope using 63 X (with oil) confocal objective. For Pearson's coefficient, images were run in triplicates and the calculations are performed on the entire population of pixels, without selecting any specific ROI (Region of Interest), using Zen 2.6 (Blue/Black edition) software. Images were taken at Regional Center for Biotechnology, Faridabad, Haryana. Images were processed using Zen 2.6 (Blue/Black edition) software.

Replicates and statistical analysis

Data presented depict three or more biological replicates and are depicted as mean ± SE, with error bars indicating standard error. One-way (Fig. 1C–H, Fig.S6) or two-way (Figs. 1A, B 2, 3, 4, 5, 7, 8, 9, Figs. S2–S5) analysis of variance (ANOVA) followed by Bonferroni post hoc test was used for multiple comparison. $p < 0.05$ was deemed significant.

Supplementary Information The online version contains supplementary material available at https://doi.org/10.1007/s00018-021-03993-6.

Acknowledgements We are grateful to Indian Institute of Technology-Delhi for their support. We would like to thank Dr. Prosenjit Mondal, Indian Institute of Technology—Mandi, Himachal Pradesh, India, for helping us in providing with normal diet and high-fat-fed diet mice whole brain samples. We would like to thank Dr. Nishi Raj, Jamia Hamdard-Institute of Molecular Medicine (JHIMM), New Delhi, India for providing pCMV6 Empty vector backbone. We would like to thank Dr. Chinmoy Mukhopadhyay, Jawaharalal Nehru University, New Delhi, for providing us with Caveolin-1 antibody. We would like to thank Dr. Pallavi Varshney for her assistance in training some methodologies. We are grateful to Advanced Technology Platform Centre, Regional Centre for Biotechnology, Faridabad, Haryana, India, for Confocal Microscopy.

Author contributions MS performed all the experiments, analyzed the data and wrote the original drafts, approved the final version of the manuscript. CSD conceived the idea, provided resources, acquired the funding, written, reviewed and edited the manuscript and approved the final version of the manuscript.

Funding MS is a recipient of Senior Research Fellowship (09/086 (1256)/2016-EMR-1) from Council of Scientific and Industrial Research (CSIR), Government of India. CSD is supported by a grant from Department of Biotechnology, Government of India, New Delhi, India (PR32795/MED/122/229/2019).

Data availability All the data related to this manuscript are available with the first author and corresponding author.

Code availability Not applicable.

Declarations

Conflict of interest The authors declare no conflicts of interest.

Ethical approval Mice whole brain tissues were kind gift from Dr. Prosenjit Mondal, Indian Institute of Technology—Mandi, HP, India. All experiments were performed following the guidelines prescribed by CPCSEA (Committee for the Purpose of Control and Supervision of Experiments on Animals) with the approval of the Internal Animal Ethics Committee, Visva-Bharati (IAEC/VB/2017/01). The legal requirements/guidelines in the country for the care and use of animals have been followed.

Consent to participate Not applicable.

Consent for publication Not applicable.

References

1. Gonzalez E, McGraw TE (2009) The Akt kinases: isoform specificity in metabolism and cancer. Cell Cycle 8:2502–2508
2. Hay N (2011) Akt isoforms and glucose homeostasis—the leptin connection. Trends Endocrinol Metab 22:66–73
3. Manning BD, Toker A (2017) AKT/PKB signaling: navigating the network. Cell 169:381–405
4. Huang X, Liu G, Guo J, Su Z (2018) The PI3K/AKT pathway in obesity and type 2 diabetes. Int J Biol Sci 14:1483–1496
5. Gupta A, Bisht B, Dey CS (2012) Focal adhesion kinase negatively regulates neuronal insulin resistance. Biochim Biophys Acta 1822:1030–1037
6. Gupta A, Dey CS (2012) PTEN, a widely known negative regulator of insulin/PI3K signaling, positively regulates neuronal insulin resistance. Mol Biol Cell 23:3882–3898
7. de la Monte SM, Wands JR (2008) Alzheimer's disease is type 3 diabetes-evidence reviewed. J Diabetes Sci Technol 2:1101–1113
8. Gupta A, Bisht B, Dey CS (2011) Peripheral insulin-sensitizer drug metformin ameliorates neuronal insulin resistance and Alzheimer's-like changes. Neuropharmacology 60:910–920

9. Humbert S, Bryson EA, Cordelières FP, Connors NC, Datta SR, Finkbeiner S et al (2002) The IGF-1/Akt pathway is neuroprotective in huntington's disease and involves huntingtin phosphorylation by Akt. Dev Cell 2:831–837
10. Chen H-K, Fernandez-Funez P, Acevedo SF, Lam YC, Kaytor MD, Fernandez MH et al (2003) Interaction of Akt-phosphorylated ataxin-1 with 14-3-3 mediates neurodegeneration in spinocerebellar ataxia type 1. Cell 113:457–468
11. Emamian ES, Hall D, Birnbaum MJ, Karayiorgou M, Gogos JA (2004) Convergent evidence for impaired AKT1-GSK3beta signaling in schizophrenia. Nat Genet 36:131–137
12. Furlong RM, Lindsay A, Anderson KE, Hawkins PT, Sullivan AM, O'Neill C (2019) The Parkinson's disease gene PINK1 activates Akt via PINK1 kinase-dependent regulation of the phospholipid PI(3,4,5)P3. J Cell Sci 132:jcs233221
13. Cleasby ME, Reinten TA, Cooney GJ, James DE, Kraegen EW (2007) Functional studies of Akt isoform specificity in skeletal muscle in vivo; maintained insulin sensitivity despite reduced insulin receptor substrate-1 expression. Mol Endocrinol 21:215–228
14. Kajno E, McGraw TE, Gonzalez E (2015) Development of a new model system to dissect isoform specific Akt signalling in adipocytes. Biochem J 468:425–434
15. Lu M, Wan M, Leavens KF, Chu Q, Monks BR, Fernandez S et al (2012) Insulin regulates liver metabolism in vivo in the absence of hepatic Akt and Foxo1. Nat Med 18:388–395
16. Tschopp O, Yang Z-Z, Brodbeck D, Dummler BA, Hemmings-Mieszczak M, Watanabe T et al (2005) Essential role of protein kinase B gamma (PKB gamma/Akt3) in postnatal brain development but not in glucose homeostasis. Development 132:2943–2954
17. Chen WS, Xu P-Z, Gottlob K, Chen M-L, Sokol K, Shiyanova T et al (2001) Growth retardation and increased apoptosis in mice with homozygous disruption of the akt1 gene. Genes Dev 15:2203–2208
18. Cho H, Thorvaldsen JL, Chu Q, Feng F, Birnbaum MJ (2001) Akt1/PKBα is required for normal growth but dispensable for maintenance of glucose homeostasis in mice. J Biol Chem 276:38349–38352
19. Cho H, Mu J, Kim JK, Thorvaldsen JL, Chu Q, Crenshaw EB et al (2001) Insulin resistance and a diabetes mellitus-like syndrome in mice lacking the protein kinase Akt2 (PKB beta). Science 292:1728–1731
20. Garofalo RS, Orena SJ, Rafidi K, Torchia AJ, Stock JL, Hildebrandt AL et al (2003) Severe diabetes, age-dependent loss of adipose tissue, and mild growth deficiency in mice lacking Akt2/PKB beta. J Clin Invest 112:197–208
21. Easton RM, Cho H, Roovers K, Shineman DW, Mizrahi M, Forman MS et al (2005) Role for Akt3/protein kinase bγ in attainment of normal brain size. Mol Cell Biol 25:1869–1878
22. Lee RS, House CM, Cristiano BE, Hannan RD, Pearson RB, Hannan KM (2011) Relative expression levels rather than specific activity plays the major role in determining in vivo AKT isoform substrate specificity. Enzyme Res 2011:720985
23. Gonzalez E, McGraw TE (2009) Insulin-modulated Akt subcellular localization determines Akt isoform-specific signaling PNAS. Nat Acad Sci 106:7004–7009
24. Ding J, Du K (2009) ClipR-59 interacts with Akt and regulates Akt cellular compartmentalization. Mol Cell Biol 29:1459–1471
25. Alessi DR, Andjelkovic M, Caudwell B, Cron P, Morrice N, Cohen P et al (1996) Mechanism of activation of protein kinase B by insulin and IGF-1. EMBO J 15:6541–6551
26. Sharma M, Dey CS (2021) AKT ISOFORMS-AS160-GLUT4: the defining axis of insulin resistance. Rev Endocr Metab Disord. https://doi.org/10.1007/s11154-021-09652-2 (**Epub ahead of print. PMID: 33928491**)
27. Bae SS, Cho H, Mu J, Birnbaum MJ (2003) Isoform-specific regulation of insulin-dependent glucose uptake by Akt/protein kinase B. J Biol Chem 278:49530–49536
28. Dummler B, Tschopp O, Hynx D, Yang Z-Z, Dirnhofer S, Hemmings BA (2006) Life with a single isoform of Akt: mice lacking Akt2 and Akt3 are viable but display impaired glucose homeostasis and growth deficiencies. Mol Cell Biol 26:8042–8051
29. George S, Rochford JJ, Wolfrum C, Gray SL, Schinner S, Wilson JC et al (2004) A family with severe insulin resistance and diabetes due to a mutation in AKT2. Science 304:1325–1328
30. Noda S, Kishi K, Yuasa T, Hayashi H, Ohnishi T, Miyata I et al (2000) Overexpression of wild-type Akt1 promoted insulin-stimulated p70S6 kinase (p70S6K) activity and affected GSK3 beta regulation, but did not promote insulin-stimulated GLUT4 translocation or glucose transport in L6 myotubes. J Med Invest 47:47–55
31. Chen WS, Peng X-D, Wang Y, Xu P-Z, Chen M-L, Luo Y et al (2009) Leptin deficiency and beta-cell dysfunction underlie type 2 diabetes in compound Akt knockout mice. Mol Cell Biol 29:3151–3162
32. Jiang ZY, Zhou QL, Coleman KA, Chouinard M, Boese Q, Czech MP (2003) Insulin signaling through Akt/protein kinase B analyzed by small interfering RNA-mediated gene silencing. Proc Natl Acad Sci USA 100:7569–7574
33. Hajduch E, Alessi DR, Hemmings BA, Hundal HS (1998) Constitutive activation of protein kinase B alpha by membrane targeting promotes glucose and system A amino acid transport, protein synthesis, and inactivation of glycogen synthase kinase 3 in L6 muscle cells. Diabetes 47:1006–1013
34. Levenga J, Wong H, Milstead RA, Keller BN, LaPlante LE, Hoeffer CA (2017) AKT isoforms have distinct hippocampal expression and roles in synaptic plasticity. Elife. https://doi.org/10.7554/eLife.30640
35. Gabbouj S, Natunen T, Koivisto H, Jokivarsi K, Takalo M, Marttinen M et al (2019) Intranasal insulin activates Akt2 signaling pathway in the hippocampus of wild-type but not in APP/PS1 Alzheimer model mice. Neurobiol Aging 75:98–108
36. Diez H, Garrido JJ, Wandosell F (2012) Specific Roles of Akt iso Forms in Apoptosis and Axon Growth Regulation in Neurons. PLoS ONE 7:e32715
37. Schrötter S, Leondaritis G, Eickholt BJ (2016) Capillary isoelectric focusing of Akt isoforms identifies highly dynamic phosphorylation in neuronal cells and brain tissue. J Biol Chem 291:10239–10251
38. Arora A, Dey CS (2014) SIRT2 negatively regulates insulin resistance in C2C12 skeletal muscle cells. Biochim Biophys Acta 1842:1372–1378
39. Varshney P, Dey CS (2016) P21-activated kinase 2 (PAK2) regulates glucose uptake and insulin sensitivity in neuronal cells. Mol Cell Endocrinol 429:50–61
40. Liu J, Li L, Suo WZ (2009) HT22 hippocampal neuronal cell line possesses functional cholinergic properties. Life Sci 84:267–271
41. Sano H, Kane S, Sano E, Mîinea CP, Asara JM, Lane WS et al (2003) Insulin-stimulated phosphorylation of a Rab GTPase-activating protein regulates GLUT4 translocation. J Biol Chem 278:14599–14602
42. Ng Y, Ramm G, Burchfield JG, Coster ACF, Stöckli J, James DE (2010) Cluster analysis of insulin action in adipocytes reveals a key role for Akt at the plasma membrane. J Biol Chem 285:2245–2257
43. Zheng X, Cartee GD (2016) Insulin-induced effects on the subcellular localization of AKT1, AKT2 and AS160 in rat skeletal muscle. Sci Rep 6:39230
44. Larance M, Ramm G, Stöckli J, van Dam EM, Winata S, Wasinger V et al (2005) Characterization of the role of the Rab

GTPase-activating protein AS160 in insulin-regulated GLUT4 trafficking. J Biol Chem 280:37803–37813
45. Stöckli J, Davey JR, Hohnen-Behrens C, Xu A, James DE, Ramm G (2008) Regulation of glucose transporter 4 translocation by the Rab guanosine triphosphatase-activating protein AS160/TBC1D4: role of phosphorylation and membrane association. Mol Endocrinol 22:2703–2715
46. Williams TM, Lisanti MP (2004) The caveolin proteins. Genome Biol 5:214
47. Sirover MA (2012) Subcellular dynamics of multifunctional protein regulation: mechanisms of GAPDH intracellular translocation. J Cell Biochem 113:2193–2200
48. Arora A, Dey CS (2016) SIRT2 regulates insulin sensitivity in insulin resistant neuronal cells. Biochem Biophys Res Commun 474:747–752
49. Mishra D, Dey CS (2019) Protein kinase C attenuates insulin signalling cascade in insulin-sensitive and insulin-resistant neuro-2a cells. J Mol Neurosci 69:470–477
50. Varshney P, Dey CS (2017) Resveratrol regulates neuronal glucose uptake and insulin sensitivity via P21-activated kinase 2 (PAK2). Biochem Biophys Res Commun 485:372–378
51. Cozzone D, Fröjdö S, Disse E, Debard C, Laville M, Pirola L et al (2008) Isoform-specific defects of insulin stimulation of Akt/protein kinase B (PKB) in skeletal muscle cells from type 2 diabetic patients. Diabetologia 51:512–521
52. Brozinick JT, Roberts BR, Dohm GL (2003) Defective signaling through Akt-2 and -3 But Not Akt-1 in insulin-resistant human skeletal muscle: potential role in insulin resistance. Diabetes Am Diabetes Assoc 52:935–941
53. Wang L, Cheng S, Yin Z, Xu C, Lu S, Hou J et al (2015) Conditional inactivation of Akt three isoforms causes tau hyperphosphorylation in the brain. Mol Neurodegener 10:33
54. Tan S-X, Ng Y, Burchfield JG, Ramm G, Lambright DG, Stöckli J et al (2012) The Rab GTPase-activating protein TBC1D4/AS160 contains an atypical phosphotyrosine-binding domain that interacts with plasma membrane phospholipids to facilitate GLUT4 trafficking in adipocytes. Mol Cell Biol 32:4946–4959
55. Ramm G, Larance M, Guilhaus M, James DE (2006) A role for 14-3-3 in insulin-stimulated GLUT4 translocation through its interaction with the RabGAP AS160. J Biol Chem 281:29174–29180
56. Bruss MD, Arias EB, Lienhard GE, Cartee GD (2005) Increased phosphorylation of Akt substrate of 160 kDa (AS160) in rat skeletal muscle in response to insulin or contractile activity. Diabetes 54:41–50
57. Kane S, Sano H, Liu SCH, Asara JM, Lane WS, Garner CC et al (2002) A method to identify serine kinase substrates. Akt phosphorylates a novel adipocyte protein with a Rab GTPase-activating protein (GAP) domain. J Biol Chem 277:22115–22118
58. Zeigerer A, McBrayer MK, McGraw TE (2004) Insulin stimulation of GLUT4 exocytosis, but not its inhibition of endocytosis, is dependent on RabGAP AS160. Mol Biol Cell 15:4406–4415
59. Brewer PD, Romenskaia I, Kanow MA, Mastick CC (2011) Loss of AS160 Akt substrate causes Glut4 protein to accumulate in compartments that are primed for fusion in basal adipocytes. J Biol Chem 286:26287–26297
60. Eguez L, Lee A, Chavez JA, Miinea CP, Kane S, Lienhard GE et al (2005) Full intracellular retention of GLUT4 requires AS160 Rab GTPase activating protein. Cell Metab 2:263–272
61. Kramer HF, Witczak CA, Fujii N, Jessen N, Taylor EB, Arnolds DE et al (2006) Distinct signals regulate AS160 phosphorylation in response to insulin, AICAR, and contraction in mouse skeletal muscle. Diabetes 55:2067–2076
62. Lansey MN, Walker NN, Hargett SR, Stevens JR, Keller SR (2012) Deletion of Rab GAP AS160 modifies glucose uptake and GLUT4 translocation in primary skeletal muscles and adipocytes and impairs glucose homeostasis. Am J Physiol Endocrinol Metab 303:E1273–E1286
63. Gosmanov AR, Umpierrez GE, Karabell AH, Cuervo R, Thomason DB (2004) Impaired expression and insulin-stimulated phosphorylation of Akt-2 in muscle of obese patients with atypical diabetes. Am J Physiol Endocrinol Metab 287:E8-15
64. Kim YB, Peroni OD, Franke TF, Kahn BB (2000) Divergent regulation of Akt1 and Akt2 isoforms in insulin target tissues of obese Zucker rats. Diabetes 49:847–856
65. Heide LPVD, Hoekman MF, Biessels GJ, Gispen WH (2003) Insulin inhibits extracellular regulated kinase 1/2 phosphorylation in a phosphatidylinositol 3-kinase (PI3) kinase-dependent manner in Neuro2a cells. J Neurochem 86:86–91
66. Bisht B, Dey CS (2008) Focal Adhesion Kinase contributes to insulin-induced actin reorganization into a mesh harboring Glucose transporter-4 in insulin resistant skeletal muscle cells. BMC Cell Biol 9:48
67. Smith PK, Krohn RI, Hermanson GT, Mallia AK, Gartner FH, Provenzano MD et al (1985) Measurement of protein using bicinchoninic acid. Anal Biochem 150:76–85
68. Goel HL, Dey CS (2002) Insulin stimulates spreading of skeletal muscle cells involving the activation of focal adhesion kinase, phosphatidylinositol 3-kinase and extracellular signal regulated kinases. J Cell Physiol 193:187–198
69. Silva G, Ferraresi C, de Almeida RT, Motta ML, Paixão T, Ottone VO et al (2020) Insulin resistance is improved in high-fat fed mice by photobiomodulation therapy at 630 nm. J Biophotonics 13:e201960140
70. Mujawdiya PK, Sharma P, Sharad S, Kapur S (2020) Reversal of increase in intestinal permeability by mangifera indica seed kernel extract in high-fat diet-induced obese mice. Pharmaceuticals (Basel). https://doi.org/10.3390/ph13080190

Yadav *et al.*
Cell Communication and Signaling (2023) 21:82
https://doi.org/10.1186/s12964-023-01071-x

Cell Communication and Signaling

RESEARCH

Open Access

PP1γ regulates neuronal insulin signaling and aggravates insulin resistance leading to AD-like phenotypes

Yamini Yadav, Medha Sharma and Chinmoy Sankar Dey*

Abstract

Background PP1γ is one of the isoforms of catalytic subunit of a Ser/Thr phosphatase PP1. The role of PP1γ in cellular regulation is largely unknown. The present study investigated the role of PP1γ in regulating neuronal insulin signaling and insulin resistance in neuronal cells. PP1 was inhibited in mouse neuroblastoma cells (N2a) and human neuroblastoma cells (SH-SY5Y). The expression of PP1α and PP1γ was determined in insulin resistant N2a, SH-SY5Y cells and in high-fat-diet-fed-diabetic mice whole-brain-lysates. PP1α and PP1γ were silenced by siRNA in N2a and SH-SY5Y cells and effect was tested on AKT isoforms, AS160 and GSK3 isoforms using western immunoblot, GLUT4 translocation by confocal microscopy and glucose uptake by fluorescence-based assay.

Results Results showed that, in one hand PP1γ, and not PP1α, regulates neuronal insulin signaling and insulin resistance by regulating phosphorylation of AKT2 via AKT2-AS160-GLUT4 axis. On the other hand, PP1γ regulates phosphorylation of GSK3β via AKT2 while phosphorylation of GSK3α via MLK3. Imbalance in this regulation results into AD-like phenotype.

Conclusion PP1γ acts as a linker, regulating two pathophysiological conditions, neuronal insulin resistance and AD.

Keywords PP1γ, AKT isoforms, MLK3, Neuronal insulin signaling, Insulin resistance, Alzheimer disease

Introduction

Neuronal insulin signaling regulates myriads of processes like neuronal survival, neurotransmission, and cognitive performance [1]. Any impairment in insulin signaling leads to insulin resistance, which has been linked to various neurodegenerative disorders like Alzheimer's disease (AD) [2], Parkinson's disease (PD) [3] Huntington's disease (HD) [4] etc. In contrast to peripheral tissues like skeletal muscle, liver and adipocytes where insulin signaling and effect of insulin resistance has been studied extensively, the regulation of neuronal insulin signaling is not explored as much. Phosphorylation/dephosphorylation of important proteins in insulin signaling cascade is one of the key regulatory events. To fully understand regulation of neuronal insulin signaling, unraveling the processes regulated through complementary and countervailing actions of protein kinases and phosphatases are extremely crucial. So far, the contributions of kinases like AKT [5], CDK5 [6], PKC [7] and PAK2 [8] have been studied addressing insulin signaling and insulin resistance in neuronal system. Conversely, studies reporting the role of phosphatases is anyway very limited, with an even lesser number of studies in the neuronal system.

One such phosphatase is Protein Phosphatase 1 (PP1). PP1 belongs to Ser/Thr phosphatase, a heteromeric protein composed of three isoforms of catalytic subunits naming PP1α, PP1β/δ and PP1γ interacting with > 200 regulatory subunits. The ability of PP1 to recognize

*Correspondence:
Chinmoy Sankar Dey
csdey@bioschool.iitd.ac.in
Kusuma School of Biological Sciences, Indian Institute of Technology, Delhi, New Delhi 110016, India

different substrates lies in the combination of binding of different isoforms of catalytic subunit(s) with different regulatory subunit(s). Previously, some studies have reported the role of PP1 in insulin signaling. Corvera et al. [9] and Rondinone et al. [10] suggested the participation of a phosphatase responsible for GLUT4 transport in response to insulin in adipocyte. A small number of studies demonstrate specific role of catalytic and regulatory subunits of PP1, acting on different molecules of insulin signaling cascade. Geetha et al. [11] observed that in skeletal muscle, catalytic subunit PP1δ combines with PP1 regulatory subunit PP1R12A, and acts on IRS-1, regulating inulin signaling cascade. Sharma et al. [12] demonstrated that PP1α catalytic subunit acts directly on AS160, dephosphorylate it and regulate insulin signaling in skeletal muscle.

PP1 and isoforms of catalytic subunit are abundantly expressed in mammalian brain. Among three isoforms of catalytic subunits of PP1, PP1α and PP1γ, are reported to be highly expressed in brain [13]. However, role of PP1 and isoforms of PP1 catalytic subunits is not yet studied in neuronal insulin signaling and resistance. Innumerable reports connected neuronal insulin resistance to AD [14–17]. PP1 has been linked to AD pathogenesis [18]. However, possible role of PP1 isoforms in regulating both pathological disorders, if any, has not been reported.

In our current study, we for the first time determined regulatory role of PP1, and more precisely PP1γ, in neuronal insulin signaling and insulin resistance. We also found that PP1γ is involved in precipitating AD-like phenotypes. PP1γ acts, possibly, like a linker in the progression of insulin resistance and AD-like pathogenesis. Widespread studies in future are required for in depth understanding to recognize the role of PP1γ in the development of AD pathogenesis in diabetic conditions.

Results

Effect of PP1 inhibition on neuronal insulin signaling

To understand the role of PP1, if any, in neuronal insulin signaling, we inhibited PP1 by Okadaic Acid (OA) [19] and tested the effect of inhibition on activation of AKT (as determined by phosphorylation at Ser473 and Thr308). Differentiated N2a cells were treated with or without 4 μM OA for 120 min followed by 100 nM insulin for 30 min [19]. Treated cells were lysed and protein lysates were subjected to western immunoblotting and probed with specific antibodies. Cells treated with OA showed 49 ± 0.06% and 34 ± 0.10% increase in phosphorylation of AKT at Ser473 and Thr308 respectively (Fig. 1A and B, Lane 4 vs. Lane 2, $^{***}p < 0.001$) in insulin stimulated N2a cells. This provided us with the first evidence that PP1 is involved in neuronal insulin signaling. Since PP1 inhibition affected the activation of AKT, we next tested the effect of PP1 inhibition on activation of immediate downstream target of AKT i.e., AS160. AS160 is a Rab-GTPase that regulates translocation of GLUT4 from the cytoplasm to the plasma membrane in response to insulin, leading to glucose uptake. Post insulin stimulation, activation of AS160 (as determined by phosphorylation at Ser588 and Thr642) was found to be increased by 37 ± 0.03% and 46 ± 0.02% respectively post PP1 inhibition (Fig. 1C and D, Lane 4 vs. Lane 2, $^{***}p < 0.001$). Having observed PP1 inhibition regulated the activities of AKT and AS160, we next tested the effect of PP1 inhibition on neuronal glucose uptake. Cells treated with 4 μM OA for 120 min followed by 100 nM insulin for 30 min were subjected to 2-NBDG uptake [6, 7, 5–22], displayed 22 ± 0.01% increase in neuronal glucose uptake as compared to control (Fig. 1E, Lane 4 vs. Lane 2, $^{***}p < 0.001$).

We next tested the effect of PP1 inhibition on activation of another AKT downstream substrate, GSK3. GSK3 has two isoforms, GSK3α and GSK3β, which when undergoes phosphorylation at Ser21 and Ser9 residues respectively, gets inactivated. We observed that post PP1 inhibition, phosphorylation of GSK3α at Ser21 was decreased by 51 ± 0.02% (Fig. 1F, Lane 4 vs. Lane 2, $^{***}p < 0.001$). On the contrary, phosphorylation of GSK3β was increased by 57 ± 0.01% (Fig. 1G, Lane 4 vs. Lane 2, $^{***}p < 0.001$) in response to insulin.

To determine whether the above-mentioned effects were not cell and species specific, we tested the effect of PP1 inhibition on the activations of AKT, AS160, GSK3 and uptake of glucose in differentiated human neuroblastoma SH-SY5Y cells. We observed results similar to N2a cells, that is, as a function of PP1 inhibition, phosphorylation of AKT and AS160, neuronal glucose uptake was increased post insulin stimulation and phosphorylations of GSK3 isoforms were affected oppositely (Additional

(See figure on next page.)

Fig. 1 Effect of PP1 inhibition on neuronal insulin signaling in N2a cells: Differentiated N2a cells were treated with or without 4 μM OA for 120 min, followed by 100 nM insulin for 30 min. Treated cells were lysed and subjected to western immunoblotting followed by probing with relevant primary antibodies. Bar represents relative change in **A** pAKT (Ser473) **B** pAKT (Thr308) **C** pAS160 (Ser588) **D** pAS160 (Thr642) **F** pGSK3α (Ser21) **G** pGSK3β (Ser9). For glucose uptake assay differentiated N2a cells were serum-starved for 2 h and then treated with or without 4 μM OA for 120 min, followed by 100 nM insulin for 30 min. Uptake of 2-NBDG was then measured. Bar represents (**E**) relative change in the uptake of 2-NBDG. Experiments were executed three times and a representative western blot is shown. Data expressed are mean ± SE $^{***}p < 0.001$ compared to Lane 2. (**A** and **B**) AKT was used as a loading control (**C** and **D**) AS160 was used as a loading control (**F**) pGSK3α was used as a loading control (**G**) pGSK3β was used as a loading control. *A.U.* Arbitrary Units. *IB* Immunoblot, *OA* Okadaic Acid

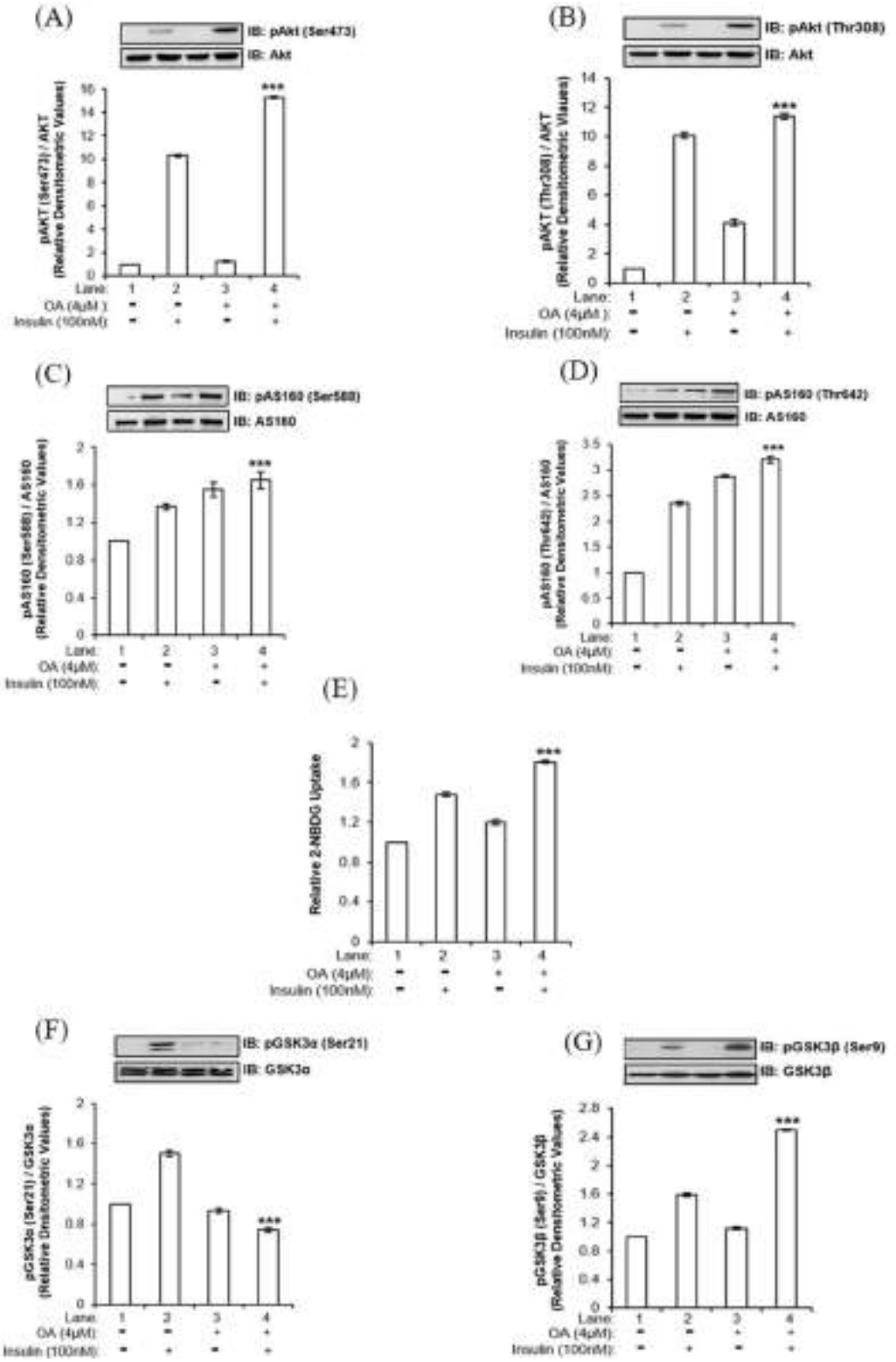

Fig. 1 (See legend on previous page.)

file 1: Fig. S1). Data suggests that PP1 participates in neuronal insulin signaling by dephosphorylating AKT and regulating the phosphorylations of two GSK3 isoforms.

Effect of insulin stimulation on expression of PP1α and PP1γ in insulin sensitive and insulin resistant neuronal cells

Among the three isoforms, namely PP1α, PP1β/δ and PP1γ, PP1α and PP1γ are reported to be predominantly expressed in mammalian brain [13]. Therefore, in order to figure out which isoform(s) is/are participate in the neuronal insulin signaling, we first tested the expression of PP1α and PP1γ in neuronal insulin sensitive and insulin resistant N2a and SH-SY5Y cells. To generate insulin resistant neuronal cells, we have subjected the cells in hyperinsulinemic condition, as reported previously from our laboratory [6, 7, 5–22]. As described in "materials and methods" section, we differentiated N2a and SH-SY5Y cells in a serum free insulin sensitive (MF) condition and an insulin resistant (MFI) condition in the chronic presence of 100 nM insulin for three days and then the cells were stimulated with or without 100 nM insulin for 30 min, subjected to western immunoblotting, probed with PP1α and PP1γ specific antibodies. We observed that both PP1α and PP1γ isoforms are expressed in N2a and SH-SY5Y cells under insulin sensitive and resistant conditions and insulin did not alter the expression of neither of the isoforms under any conditions tested (Fig. 2A–H). We also tested the expression of PP1α and PP1γ in whole mice brain lysates of High-fat-diet (HFD) fed insulin resistant mice and Normal-diet (ND) fed mice. No change in expression of PP1α and PP1γ was observed in HFD mice whole brain lysates when compared to ND (Fig. 2I and J). Data shows expression of PP1α and PP1γ in insulin sensitive and insulin resistant neuronal cells.

Effect of PP1α and PP1γ silencing on AKT isoforms and AS160 in insulin sensitive and insulin resistant neuronal cells

Having observed the expression of both PP1α and PP1γ in insulin sensitive and insulin resistant neuronal cells we proceeded to further investigate the role of each isoform of PP1 catalytic subunits in regulating downstream substrates. To test the effect, isoforms were individually silenced and the effect on expression and activation were tested on the downstream substrates, with or without insulin stimulation. Silencing was optimized at 100 nM of siRNA for PP1α (Additional file 1: Fig S2A) and PP1γ, each (Additional file 1: Fig S2B). Cells were transfected with 100 nM of either PP1α or PP1γ siRNA and then subjected to differentiation under MF or MFI condition, with or without insulin stimulation. Lysates were subjected to western immunoblotting probed with relevant antibodies as and when mentioned with reference to the relevant experiment.

PP1α silencing did not affect the expression or phosphorylation of any isoform of AKT both under insulin sensitive (MF) and insulin resistant (MFI) condition when compared to respective control (Fig. 3A–C, Lane 4 vs. Lane 2 and Lane 8 vs. Lane 6). However, PP1γ silencing affected the phosphorylation of only AKT2 (Fig. 3E), while phosphorylation of AKT1 (Fig. 3D) and AKT3 (Fig. 3F) remained unaffected. PP1γ silenced cells under insulin sensitive condition showed 36 ± 0.1% increase in phosphorylation of AKT2 and 64 ± 0.15% increase in phosphorylation of AKT2 under insulin resistant condition as compared to control (Fig. 3E, Lane 4 vs. Lane 2, $^{\#\#\#}p < 0.001$ and Lane 8 vs. Lane 6 respectively, $^{\delta\delta}p < 0.01$). When phosphorylation of downstream target of AKT i.e., was tested, the phosphorylation of AS160 was unaffected both at Ser588 and Thr642 residues post PP1α silencing under insulin sensitive and insulin resistant condition when compared to control (Fig. 3G and H). However, cells transfected with PP1γ siRNA showed 39 ± 0.02% (Fig. 3I, Lane 4 vs. Lane 2, $^{\#\#\#}p < 0.001$) and 16 ± 0.02% (Fig. 3I, Lane 6 vs. Lane 4, $^{\delta\delta\delta}p < 0.001$) increase in phosphorylation of AS160 at Ser588 under insulin sensitive and insulin resistant condition, respectively, when compared to cells transfected with scrambled siRNA. Phosphorylation of AS160 at Thr642 was also found to be increased by 27 ± 0.05% (Fig. 3J, Lane 4 vs. Lane 2, $^{\#\#\#}p < 0.001$) and 77 ± 0.04% (Fig. 3J, Lane 8 vs. Lane 6, $^{\delta\delta\delta}p < 0.001$) under insulin sensitive and insulin resistant condition, respectively, when compared to control. Data shows that PP1α does not regulate any of the three AKT isoforms in neuronal insulin signaling and insulin resistance. In contrast, PP1γ regulates phosphorylation of AKT2 only, without affecting the phosphorylation of AKT1 or AKT3, in turn affecting the phosphorylation of AS160. Data strongly suggest that PP1γ isoform of PP1 serine-threonine phosphatase, and not PP1α, participates in the pathway of regulation of insulin signaling and insulin resistance in neuronal cell.

Effect of PP1α and PP1γ silencing on GLUT4 translocation and glucose uptake in insulin sensitive and insulin resistant neuronal cells

Looking at the participation in the insulin signaling pathway, we next tested the effect of PP1α and PP1γ silencing on neuronal GLUT4 translocation and glucose uptake. For glucose uptake assay, PP1α and PP1α silenced N2a cells were stimulated with or without 100 nM insulin for 30 min and subjected to 2 NBDG uptake [6, 7, 5, 20, 8–21]. PP1α silenced N2a cells did not show any change in uptake of glucose under insulin sensitive and insulin

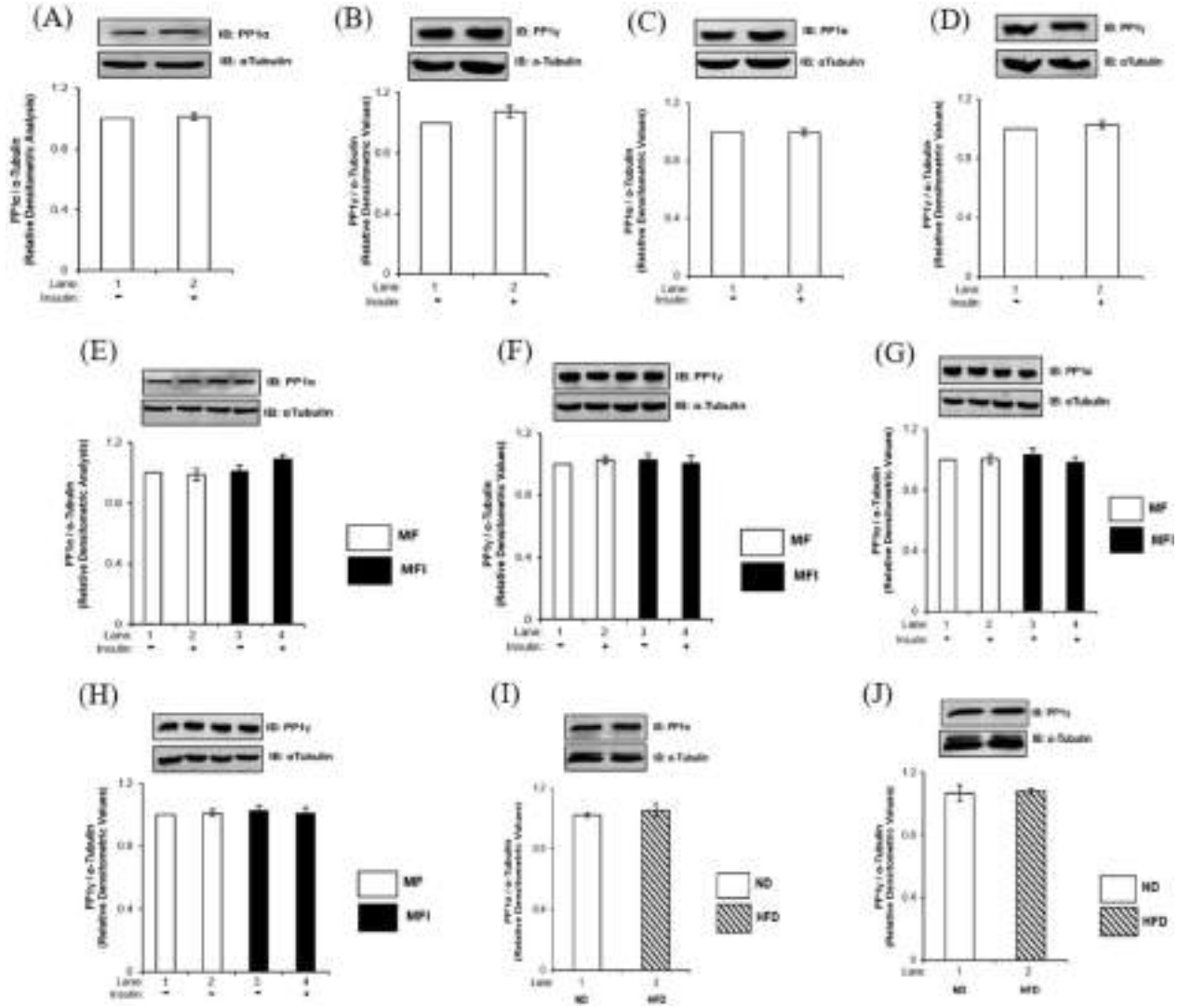

Fig. 2 Effect of insulin stimulation on expression of PP1α and PP1γ in insulin sensitive and insulin resistant condition: Differentiated **A** and **B** N2a cells **C** and **D** SH-SY5Y cells were treated with or without 100 nM insulin for 30 min and lysed **E** and **F** ND and HFD mice brains were lysed **G** and **H** N2a cells were differentiated in insulin sensitive (MF) or in insulin resistant (MFI) conditions for 3 days and treated with or without 100 nM insulin for 30 min and were lysed, **I** and **J** SH-SY5Y cells were differentiated in insulin sensitive (MF) or in insulin resistant (MFI) conditions for 4 days and were treated with or without 100 nM insulin for 30 min and lysed. Resulting lysates were subjected to western immunoblotting and probed with relevant antibodies Bar represents relative change in expression of PP1α (**A**, **C**, **E**, **G** and I) and PP1γ (**B**, **D**, **F**, **H** and **J**). Experiments were executed three times and representative western blot is shown. Data expressed are mean ± SE. Open bars: MF, filled bars: MFI, *IB* Immunoblot, *ND* Normal diet, *HFD* High-fat-fed-diet. α-Tubulin was used as loading control

resistance (Fig. 4A). However, PP1γ silenced cells showed increase in insulin stimulated neuronal glucose uptake by 35 ± 0.03% (Fig. 4B, Lane 4 vs. Lane 2, $^{\#\#\#}p < 0.001$) under insulin sensitive condition and 34 ± 0.17% under insulin resistant condition when compared to control (Fig. 4B, Lane 8 vs. Lane 6, $^{\delta\delta}p < 0.001$). PP1α and PP1γ were also silenced in SH-SY5Y cells and stimulated with or without 100 nM insulin for 30 min and subjected to 2 NBDG uptake and we observed the similar trend (Additional file 1: Fig. S3). Data confirms that PP1γ isoform of PP1 serine-threonine phosphatase regulate neuronal insulin signaling and insulin resistance.

To validate and further confirm our observations, we tested GLUT4 translocation from inside the cell to the plasma membrane in PP1α and PP1γ gamma silenced N2a cells under insulin sensitive and insulin resistant condition, through confocal microscopy (Fig. 4C). In MF and MFI, under control (scrambled siRNA transfected) conditions, in absence of insulin, GLUT4 was localized at perinuclear region as well as dispersed in the cytoplasm

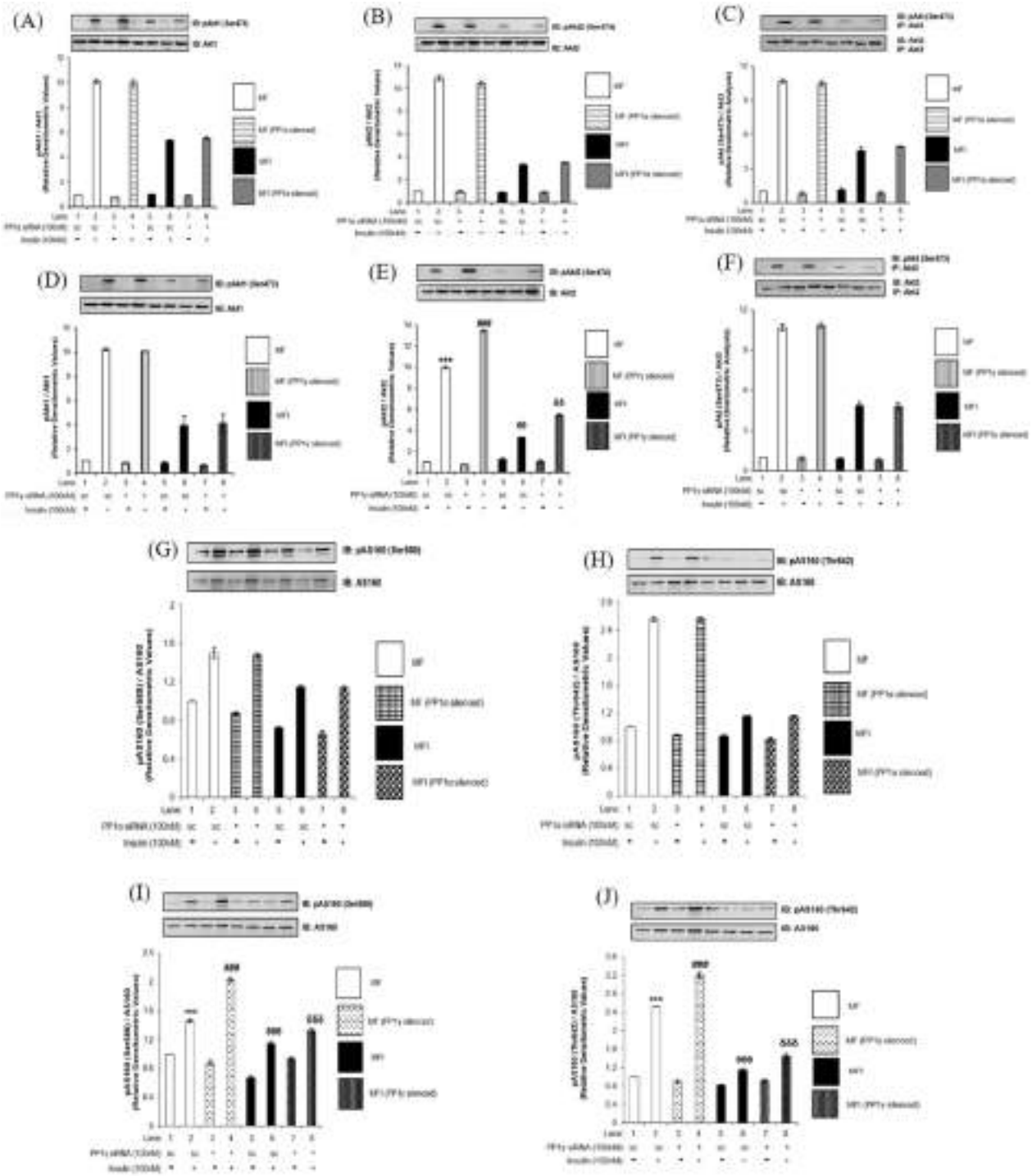

Fig. 3 Effect of PP1α and PP1γ silencing on AKT isoforms and AS160 in insulin sensitive and insulin resistant condition: Proliferated N2a cells were transfected with non-specific (scrambled) and PP1α and PP1γ specific siRNA. Post transfection cells were differentiated in the absence (MF; insulin sensitive) or chronic presence of 100 nM insulin (MFI; insulin resistant) for 3 days. Transfected N2a cells were treated with or without 100 nM insulin for 30 min, lysed and probed with relevant primary antibodies for immunoblotting. **C** and **F** Post insulin stimulation, lysates were subjected to immunoprecipitation using anti-Akt3 antibody. Bar represents relative change in **A** and **D** pAKT1 (Ser473) **B** and **E** pAKT2 (Ser474) **C** and **F** pAKT (Ser473) **G** and **H** pAS160 (Ser588) **I** and **J** pAS160 (Thr672). Experiments were executed three times and a representative western blot is shown. Data expressed are mean ± SE. $^{***}p < 0.001$ compared to Lane 1, $^{\#\#\#}p < 0.001$ compared to Lane 2, $^{\theta\theta\theta}p < 0.001$ compared to lane 4 and $^{\delta\delta\delta}p < 0.001$ compared to Lane 6. (**A** and **D**) AKT1, (**B** and **E**) AKT2, (**C** and **F**) AKT3, (**G**–**J**) AS160 was used as a loading control. Open bars: MF, filled bars: MFI, *IP* Immunoprecipitation *IB* Immunoblot, *SC* Scrambled

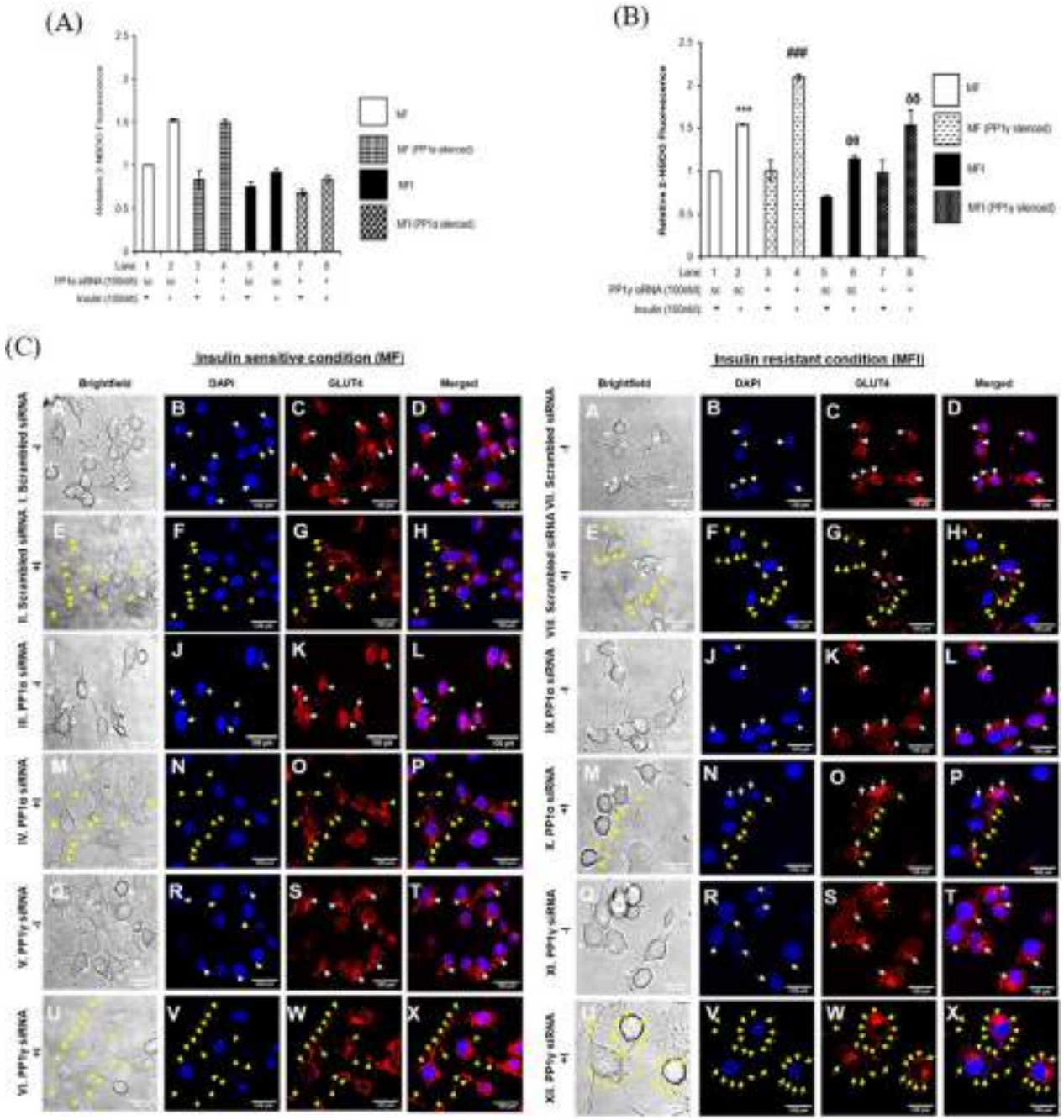

Fig. 4 Effect of PP1α and PP1γ silencing on Glucose uptake and GLUT4 translocation in insulin sensitive and insulin resistant condition: Proliferated N2a cells were transfected with non-specific (scrambled) and PP1α and PP1γ specific siRNA. Post transfection cells were differentiated in the absence (MF; insulin sensitive) or chronic presence of 100 nM insulin (MFI; insulin resistant) for 3 days. **A** and **B** For glucose uptake assay, transfected N2a cells were serum-starved for 2 h and treated with 100 nM insulin for 30 min. Treated cells were lysed and uptake of 2-NBDG was then measured. Bar represents relative change in the uptake of 2-NBDG. Data expressed are mean ± SE. $^{***}p < 0.001$ compared to Lane 1, $^{\#\#\#}p < 0.001$ compared to Lane 2, $^{\theta\theta}p < 0.01$ compared to Lane 4 and $^{\delta\delta}p < 0.001$ compared to Lane 6. Open bars: MF, filled bars: MFI, *A.U.* Arbitrary Units, *SC* Scrambled **C** For GLUT4 translocation, post transfection, MF MFI differentiated N2a cells were treated with or without 100 nM insulin for 30 min followed by fixation and permeabilization. Cells were subjected to immunofluorescence microscopy by using anti-goat Alexa 555 secondary antibody. Images were captured from different fields and a representative image of three images is presented. Scale Bar: 100 µm. White arrow: GLUT4 redistribution around the nucleus; Yellow arrows: GLUT4 redistribution/translocation on the plasma membrane

(Fig. 4C, I and VII, Panel C, white arrows). In MF under control condition post insulin stimulation, GLUT4 was found to be present on the membrane (Fig. 4C, II, Panel G, yellow arrows). However, in MFI, under control condition post insulin stimulation, GLUT4 was found to be present on the membrane (Fig. 4C, VIII, Panel G, yellow arrows) (with a limited occurrence at the perinuclear region as well) (Fig. 4C, VIII, Panel G, white arrows). In MF and MFI under PP1α silenced condition in absence of insulin, GLUT4 was localized as similar to respective controls (Fig. 4C, III, IX, Panel K, white arrows). In MF, under PP1α silenced condition post insulin stimulation, GLUT4 was found onto the membrane (Fig. 4C, IV, Panel O, yellow arrows) similar to the respective control (Fig. 4C, II, Panel G vs. IV, Panel O). Similarly, in MFI, under PP1α silenced condition post insulin stimulation, GLUT4 was found on the membrane (Fig. 4C, X, Panel O, yellow arrows) similar to the respective control (Fig. 4C, VII, Panel G vs. X, Panel O). In MF, under PP1γ silenced condition post insulin stimulation, GLUT4 was found onto the membrane (Fig. 4C, VI, Panel W, yellow arrows) considerably more than the respective control (Fig. 4C, II, Panel G vs. VI, Panel W). In MFI, under PP1γ silenced condition post insulin stimulation, GLUT4 was found on the membrane (Fig. 4C, XII, Panel W, yellow arrows) considerably more than the respective control (Fig. 4C, VII, Panel G vs. XII, Panel W). This GLUT4 translocation (Fig. 4C) is in coherence with the glucose uptake (Fig. 4A and B), wherein only PP1γ silencing increases GLUT4 translocation and glucose uptake in neuronal cells but not PP1α silencing. Data revalidates and confirms that PP1γ regulates the neuronal insulin signaling and insulin resistance by dephosphorylating AKT2 via AKT-AS160-GLUT4 axis.

Effect of silencing of AKT isoforms, PP1α and PP1γ on GSK3 isoforms in insulin sensitive and insulin resistant condition

Post PP1 inhibition, we observed increase in phosphorylation of GSK3β, while decrease in phosphorylation of GSK3α (Fig. 1G and H). We also observed PP1γ mediated specific dephosphorylation of AKT2 (Fig. 3E) and reduced neuronal glucose uptake (Fig. 4B). Therefore, we tested whether this decrease in phosphorylation of GSK3α could be the effect of differential regulation by AKT isoforms. We have previously reported isoform specific effect of AKT in regulating phosphorylation of AS160 by AKT isoform specific silencing [5]. In the current study we used the same strategy and methodologies to study AKT isoform specific role in regulating phosphorylation of GSK3α. Post AKT isoform specific silencing, differentiated N2A cells with or without insulin stimulation (100 nM, 30 min), were subjected to western immunoblotting probed with anti-phospho GSK3α, anti-phospho GSK3β, anti- GSK3α and anti-GSK3β antibodies.

The phosphorylation of GSK3α (Ser21) was decreased by 32.54 ± 0.06% (Fig. 5B, Lane 4 vs. Lane 2, $^{***}p < 0.001$) post AKT2 silencing. However, there was no effect on phosphorylation of GSK3α (Ser21) post AKT1 and AKT3 silencing when compared to respective control (Fig. 5A and C). On the other hand, the phosphorylation of GSK3β at Ser9 was decreased by 35 ± 0.1% (Fig. 5D, Lane 4 vs. Lane 2, $^{**}p < 0.01$) post AKT1 silencing, by 32 ± 0.05% (Fig. 5E Lane 4 vs. Lane 2, $^{**}p < 0.01$) post AKT2 silencing and by 44 ± 0.01% (Fig. 5F, Lane 4 vs. Lane 2, $^{***}p < 0.001$) post AKT3 silencing when compared with their respective controls. Thus, AKT isoform specific silencing demonstrates that while all AKT isoforms regulate phosphorylation of GSK3β, only AKT2 regulates phosphorylation of GSK3α. Although this reports AKT isoform specific regulation of GSK3 isoforms in neuronal insulin signaling and resistance for the first time, this still does not answer the increase in phosphorylation of GSK3α post PP1 inhibition.

To determine whether PP1 isoforms regulate the phosphorylation of GSK3α, we tested the effect of PP1α and PP1γ silencing on phosphorylation of GSK3α at Ser21 and GSK3β at Ser9 in insulin sensitive and insulin resistant neuronal cells. PP1α silencing did not cause any change in phosphorylation of GSK3α at Ser21 (Fig. 5G) and GSK3β at Ser9 (Fig. 5H) in insulin sensitive and insulin resistant cells as compared to respective controls. However, PP1γ silencing showed 30 ± 0.07% increase in phosphorylation of GSK3β at Ser9 under insulin sensitive condition when compared to respective control (Fig. 5I, Lane 4 vs. Lane 2,$^{**}p < 0.01$). Under insulin resistant condition, PP1γ silencing caused further 42 ± 0.09% increase in phosphorylation of GSK3β at Ser9 when compared to respective control (Fig. 5I, Lane 8 vs. Lane 6, $^{\theta\theta}p < 0.01$). On the contrary, PP1γ silencing caused 25 ± 0.01% decrease in phosphorylation of GSK3α at Ser21 under insulin sensitive condition (Fig. 5J, Lane 4 vs. Lane 2, $^{*}p < 0.05$) and further decrease by 38 ± 0.07% under insulin resistant condition (Fig. 5J, Lane 8 vs. Lane 6, $^{\theta\theta}p < 0.01$) when compared to their respective controls.

Thus, PP1γ silencing (but not PP1α) increased phosphorylation of GSK3β and decreased phosphorylation of GSK3α in insulin sensitive and insulin resistant neuronal cells. This data corroborates with our PP1 inhibition data. Interestingly, what we observed here is that inhibition or silencing of a phosphatase resulted into decrease in phosphorylation of GSK3α. Further studies were required to address this issue.

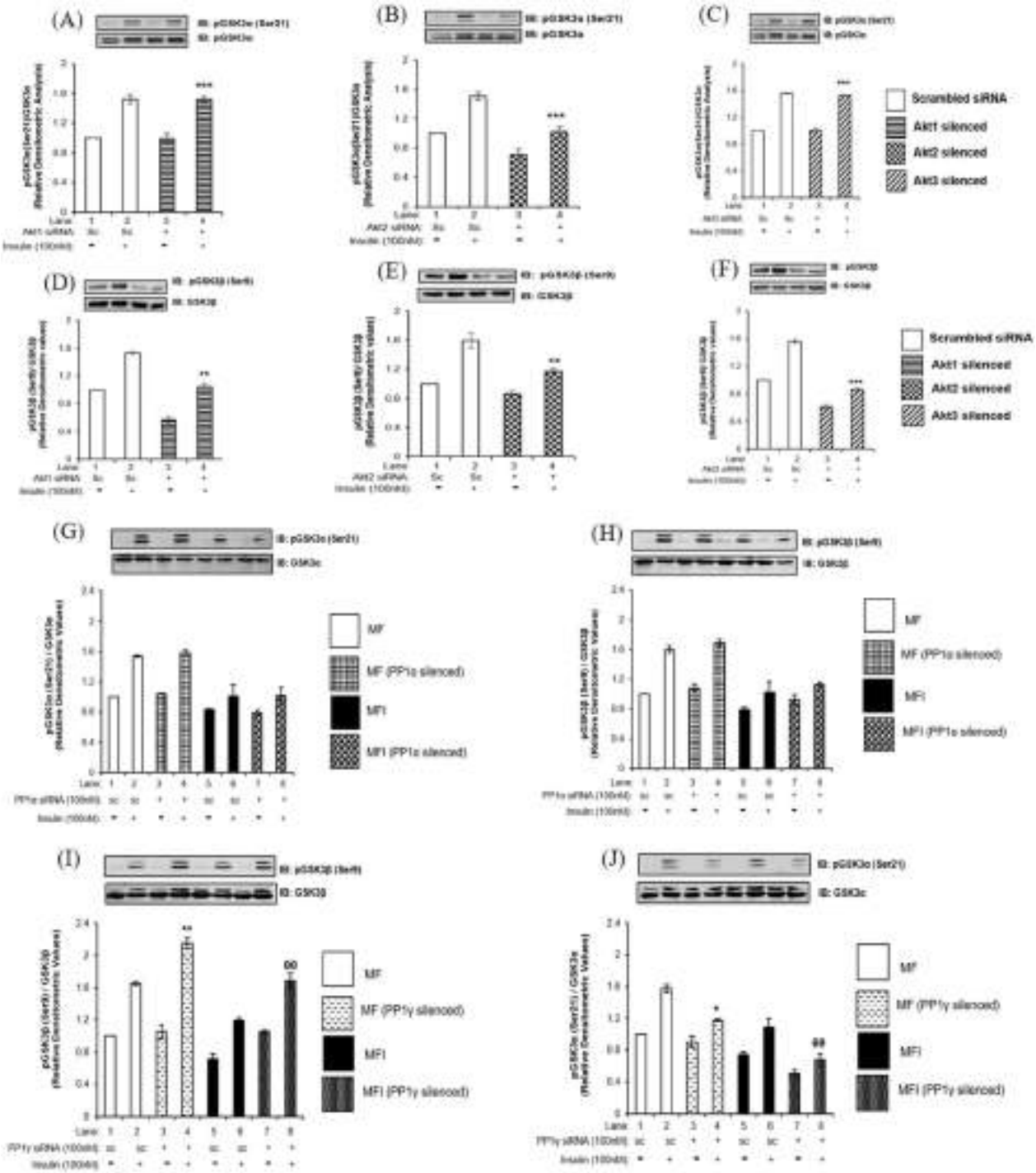

Fig. 5 Effect of silencing of AKT isoforms, PP1α and PP1γ on GSK3 isoforms in insulin sensitive and insulin resistant condition: Three days post-proliferation, N2A cells were transfected with **A–F** AKT1, AKT2, and AKT3) specific siRNA and then differentiated in 2% DMSO for 3 days. Cells were stimulated with or without 100 nM insulin for 30 min prior to cell lysis. **G**–**J** Proliferated N2a cells were transfected with non-specific (scrambled) and PP1α and PP1γ specific siRNA. Post transfection cells were differentiated in the absence (MF; insulin sensitive) or chronic presence of 100 nM insulin (MFI; insulin resistant) for 3 days. Transfected N2a cells were treated with or without 100 nM insulin for 30 min. Lysates was subjected to western blotting, followed by probing with relevant primary antibodies. Bar represents relative change in **A**–**C**, **G** and **J** pGSK3α (Ser 21) when probed with anti-GSK3α antibody. **D**–**F**, **H** and **I** Bar represents relative change in pGSK3β (Ser9) when probed with anti-GSK3β antibody. Experiments were executed three times and a representative result is shown. Data expressed are mean ± SE. $^{***}p < 0.001$ as compared to Lane 1; $^{\#\#\#}p < 0.001$, $^{\#\#}p < 0.01$ as compared to Lane 2, $^{\Theta\Theta}p < 0.01$ as compared to Lane 4. *IB* Immunoblot. Open bars: MF, filled bars: MFI, *IP* Immunoprecipitation *IB* Immunoblot, *SC* Scrambled

Effect of PP1α and PP1γ silencing on MLK3 and IKK in insulin sensitive and insulin resistant condition

To further investigate this issue, we ventured into possible intermediate proteins between the pathway of PP1 and GSK3α. Since GSK3α phosphorylation was getting affected, one of the possibilities was of a kinase, modulated under certain circumstances relaying PP1 specific effects downstream.

Previously, two kinases, namely AKT2 and IKK, have been reported to specifically regulate phosphorylation of GSK3α in 3T3-L1 adipocytes and 293-IL-1R, respectively [23, 24]. However, in our study, we found that decrease in phosphorylation of GSK3α was not due to differential effect of AKT isoforms. This prompted us to investigate the possible role of IKK in regulating the phosphorylation of GSK3α. We tested the effect of PP1α and PP1γ silencing on the activity of IKK (as determined by phosphorylation at Ser179/180) under insulin sensitive and insulin resistant neuronal cells. PP1α silencing did not affect phosphorylation of IKK at Ser179/180 under both insulin sensitive and insulin resistant conditions (Fig. 6A). However, PP1γ silencing decreased phosphorylation of IKK by 48 ± 0.04% under insulin sensitive condition (Fig. 6B, Lane 4 vs. Lane 2, $^{\#\#\#}p < 0.01$) and 60 ± 0.01% decrease under insulin resistant condition when compared to respective control (Fig. 6B, Lane 8 vs. Lane 4,$^{\theta\theta\theta}p < 0.01$). Thus, PP1γ specific effects in regulating GSK3α could be mediated by upstream kinase IKK and not AKT2 (as depicted in Fig. 6E). Since, decrease in IKK phosphorylation was observed post PP1γ silencing, this prompted us to look further upstream in the signaling cascade. Previously, MLK3 is one such kinase reported to negatively regulate IKK in NIH3T3 fibroblasts [25]. To test if PP1 regulates MLK3 and if this regulation extends to IKK and GSK3α, we tested the effect of PP1α and PP1γ silencing on phosphorylation of MLK3 at Ser674 post insulin stimulation under insulin sensitive and insulin resistant conditions. Under insulin sensitive control condition (scrambled siRNA transfected), post insulin stimulation the phosphorylation of MLK3 at Ser674 was decreased by 55 ± 0.009% (Fig. 6C and D, Lane 2 vs. Lane 1, $^{***}p < 0.001$). However, post insulin stimulation, PP1γ silencing led to 55 ± 0.05% (Fig. 6D, Lane 4 vs. Lane 2, $^{\#\#\#}p < 0.001$) increase in phosphorylation of MLK3 under insulin sensitive condition, and 170 ± 0.04% % (Fig. 6D, Lane 8 vs. Lane 4, $^{\theta\theta\theta}p < 0.001$) increase under insulin resistant condition, as compared to their respective controls. Interestingly, silencing of PP1α did not affect phosphorylation of MLK3 under all conditions tested.

Thus, under insulin sensitive and insulin resistant condition, PP1γ, and not PP1α, dephosphorylates and activates MLK3. Activated MLK3 phosphorylates its downstream kinase IKK which in turn phosphorylates GSK3α (as depicted in Fig. 6E (ii)). When PP1γ was silenced, it could not dephosphorylate MLK3, causing its inactivation (as depicted in Fig. 6E (iii)). Inactivated MLK3 could not phosphorylate and activate IKK leading to decreased GSK3α phosphorylation (as depicted in Fig. 6E (iii). Thus, GSK3α phosphorylation is mediated by PP1γ via ML3-IKK and not via AKT2 in neuronal cells (as depicted in Fig. 6E).

Effect of MLK3 inhibition on activities of IKK and GSK3α

To confirm that indeed PP1γ mediated dephosphorylation of MLK3 regulates the activity of GSK3α through IKK, we inhibited MLK3 by its specific inhibitor, URMC099 [26], and tested the effect of inhibition on the activity of IKK and GSK3α. We treated N2a cells with different concentrations of URMC and tested the effect on the phosphorylation of MLK3 at Ser674. Dose-dependent inactivation of MLK3 was observed with a maximum inhibition at 10 μM concentration of URMC (Additional file 1: Fig. S4). We therefore treated N2a cells with 10 μM URMC and tested the effect of inhibition on the activations of IKK and GSK3α. Both under insulin sensitive and insulin resistant conditions, the inhibition of MLK3 reduced the activation of IKK by 45 ± 0.03% and 55 ± 0.03% (Fig. 7A, Lane 4 vs. Lane 2 and Lane 8 vs. Lane 6, $^{***}p < 0.01$, $^{\theta\theta\theta}p < 0.01$) and GSK3α by 17 ± 0.01%

(See figure on next page.)

Fig. 6 Effect of PP1α and PP1γ silencing on MLK3 and IKK in insulin sensitive and insulin resistant condition: **A**–**D** Proliferated N2a cells were transfected with non-specific (scrambled) and PP1α and PP1γ specific siRNA. Post transfection cells were differentiated in the absence (MF; insulin sensitive) or chronic presence of 100 nM insulin (MFI; insulin resistant) for 3 days. Transfected N2a cells were treated with or without 100 nM insulin for 30 min, lysed and probed with relevant primary antibodies for immunoblotting. Bar represents relative change in **A** and **B** pIKKα/β (Ser179/180) **C** and **D** pMLK3 (Ser674). Experiments were executed three times and a representative western blot is shown. Data expressed are mean ± SE. $^{**}p < 0.01$, compared to Lane 1, $^{\#\#\#}p < 0.001$ compared to Lane 2, $^{\theta\theta\theta}p < 0.001$ compared to lane 4. **A** and **B** IKKα, **C** and **D** MLK3 was used as a loading control. Open bars: MF, filled bars: MFI, *IB* Immunoblot, *SC* Scrambled. (E) (i) Under basal condition, when PP1γ is present and insulin is not present, MLK3 is phosphorylated at its inhibitory site leading to its inactivation. Inactivated MLK3 cannot phosphorylate and activate IKK which in turn leads to the activation of GSK3α. (ii) Under insulin stimulated condition, when PP1γ is present it removes inhibitory phosphorylation of MLK3 and activating it. Activated MLK3 phosphorylates and activates IKK causing GSK3α phosphorylation and inactivation. (iii) When PP1γ was downregulated, it cannot dephosphorylate MLK3 causing its inactivation. Inactivated MLK3 in turn cannot phosphorylate and activate IKK leading to activation of GSK3α. Created with BioRender.com

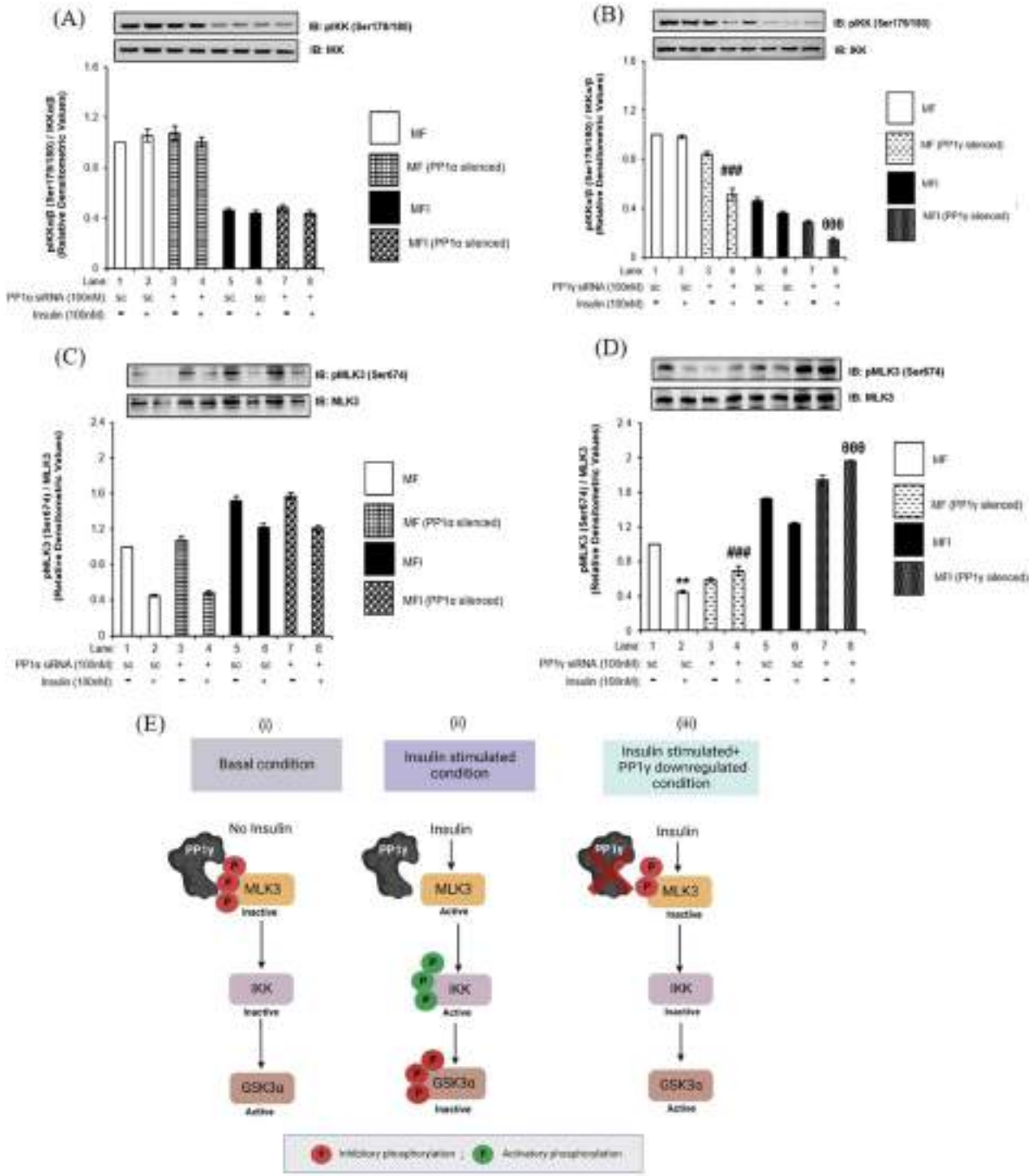

Fig. 6 (See legend on previous page.)

and 48 ± 0.03% (Fig. 7B, Lane 4 vs. Lane 2 and Lane 6 vs. Lane 8, $^{***}p < 0.001$, $^{\theta\theta\theta}p < 0.001$) respectively, confirming the activation of GSK3α being regulated via MLK3-IKK arm.

Effect of PP1α and PP1γ silencing on AD-like phenotypes

Previous studies have already established connection between defective insulin signaling and involvement of GSK3 isoforms in the development of pathological condition, like AD [14–28]. Studies also established insulin

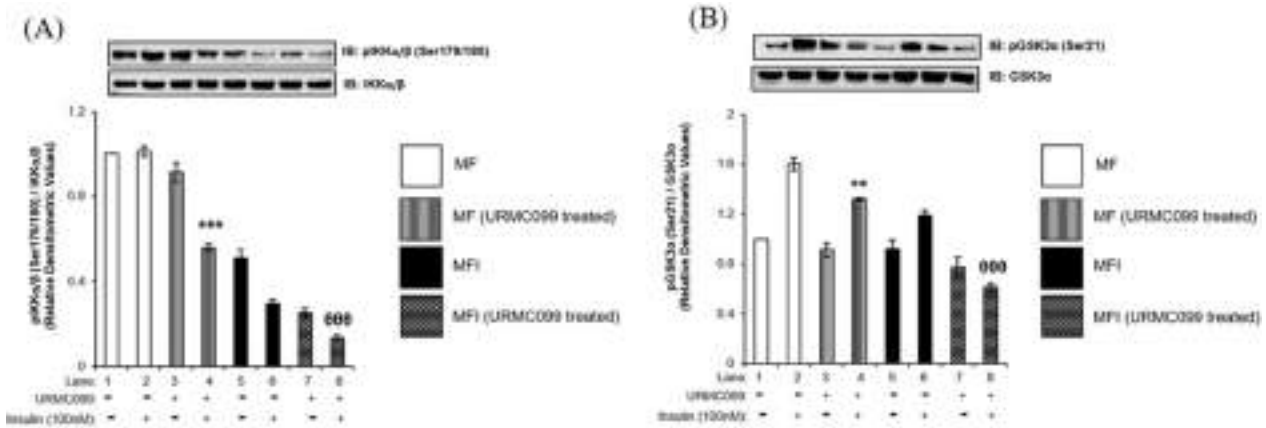

Fig. 7 Effect of MLK3 inhibition on activities of IKK and GSK3α: N2a cells were differentiated in the absence (MF; insulin sensitive) or chronic presence of 100 nM insulin (MFI; insulin resistant) for 3 days and treated with or without 10 μM URMC099 for 2 h followed by 100 nM insulin for 30 min. Treated cells were lysed and subjected to western immunoblotting followed by probing with relevant primary antibodies. Bar represents relative change in **A** pIKKα/β (Ser179/180), **B** pGSK3α (Ser21). Experiments were executed three times and a representative western blot is shown. Data expressed are mean ± SE. $^{***}p < 0.001$ compared to Lane 2, $^{\theta\theta\theta}p < 0.001$ compared to lane 4. **A** IKKα, **B** GSK3α was used as a loading control. Open bars: MF, filled bars: MFI, *IB* Immunoblot

resistance leading to AD [15, 14, 29, 30]. Our laboratory has previously reported role of a phosphatase, PTEN, in regulating neuronal insulin resistance and AD [31]. Therefore, in order to address the same, we wished to determine whether insulin resistance, further aggravated by PP1γ, caused AD-like phenomena. To achieve this, we tested the effect of PP1α and PP1γ silencing on molecules like BACE and Tau, very well-known proteins to be involved in progression of AD pathogenesis. We also tested the effect of PP1α and PP1γ downregulation on the formation of Aβ plaques and neurofibrillary tangles (NFTs), two pathological hallmarks of AD. We found that both under insulin sensitive and insulin resistant conditions, PP1α downregulation did not affect expression and phosphorylation of Tau at Ser396 when compared to the respective control (Fig. 8A). Post PP1γ silencing, Ser 396 phosphorylation of Tau displayed decrease by 20 ± 0.04% (Fig. 8B, Lane 4 vs. Lane 8, $^{\theta}p < 0.001$) under insulin resistant condition when compared to the sensitive. PP1α downregulation did not affect formation of NFTs (Fig. 8C, II and V, Panel D and J), however, PP1γ downregulation reduced the formation of NFTs both in insulin sensitive and insulin resistant cells (Fig. 8C, III and VI, Panel F and L). On the contrary, upon PP1α downregulation while the expression of BACE remained unaffected both under insulin sensitive and insulin resistant conditions (Fig. 8D), PP1γ downregulation caused 130 ± 0.07% increase in expression of BACE under insulin sensitive condition (Fig. 8E, Lane 4 vs. Lane 2, $^{***}p < 0.001$) and 86 ± 0.04% increase under insulin resistance when compared to control (Fig. 8E, Lane 8 vs. Lane 6, $^{\delta\delta\delta}p < 0.001$). Downstream to BACE, we observed that PP1α downregulation did not affect formation of Aβ plaques (Fig. 8F) whereas PP1γ downregulation increased Aβ plaque formation by 48% (Fig. 8G, Lane 2 vs. Lane 1) under insulin sensitive condition and 23% (Fig. 8G, Lane 4 vs. Lane 3) under insulin resistance when compared to control. We tested the same in insulin sensitive (MF) and insulin resistant (MFI) SH-SY5Y cells. Data obtained post silencing was similar to what was

(See figure on next page.)

Fig. 8 Effect of PP1α and PP1γ silencing on AD markers: (**A**, **B** and **D**, **E**) Proliferated N2a cells were transfected with non-specific (scrambled) and PP1α and PP1γ specific siRNA. Post transfection cells were differentiated in the absence (MF; insulin sensitive) or chronic presence of 100 nM insulin (MFI; insulin resistant) for 3 days. Transfected N2a cells were treated with or without 100 nM insulin for 30 min, lysed and probed with relevant primary antibodies for immunoblotting. Bar represents relative change in **A** and **B** pTau (Ser396), **C** and **D** BACE. Experiments were executed three times and a representative western blot is shown. Data expressed are mean ± SE. $^{***}p < 0.001$ compared to Lane 2, $^{\theta}p < 0.05$ compared to lane 4, $^{\delta\delta\delta}p < 0.001$ compared to Lane 6. **C** For thioflavin S staining proliferated N2a cells were transfected with non-specific (scrambled) and PP1α and PP1γ specific siRNA. Post transfection cells were differentiated in the absence (MF; insulin sensitive) or chronic presence of 100 nM insulin (MFI; insulin resistant) for 3 days. Transfected N2a cells were fixed, permeabilized, stained using ThS stain and visualized under an immunofluorescence microscope. Experiments were executed twice and representative images are shown. Scale bar: 100 μm. **F** and **G** For Amyloid-β measurement PP1α and PP1γ was silenced and conditioned media was collected, concentrated 2 times using speed vacuum and secreted amyloid-β (1–42) levels were measured using Beta-amyloid (1–42) colorimetric ELISA kit. Experiments were executed twice and average is shown. **A** and **B** Tau, **D** and **E** GAPDH was used as a loading control. Open bars: MF, filled bars: MFI, *IB* Immunoblot, *SC* Scrambled

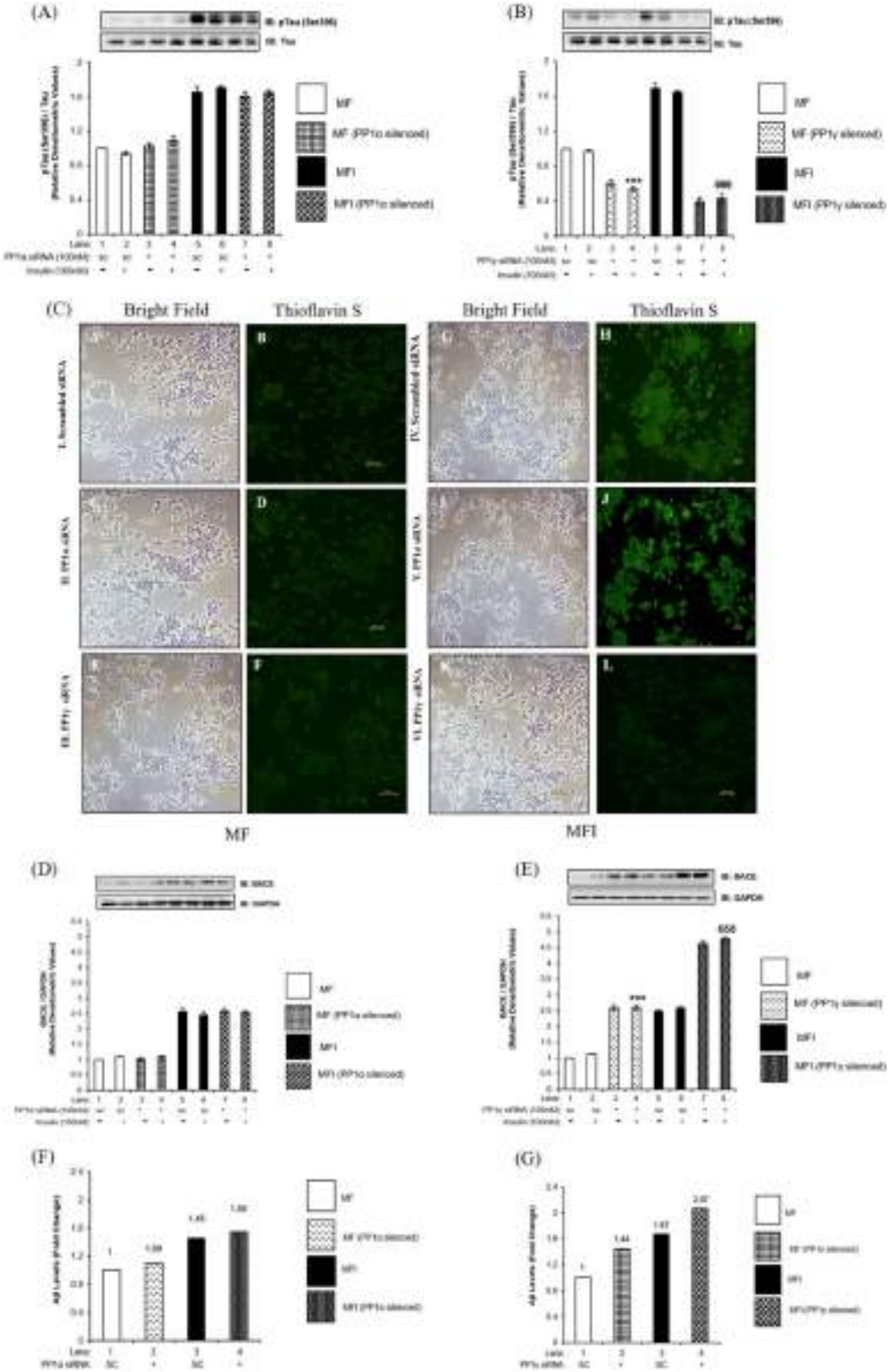

Fig. 8 (See legend on previous page.)

observed in N2a cells (Fig. 9). The results demonstrate insulin resistance, further aggravated by PP1γ, caused AD-like phenotype however, through a phenomenon of oppositely regulating phosphorylation of GSK3α and GSK3β isoforms wherein one promotes AD-like phenotypes while the other prevent it. Data shows that PP1γ, on

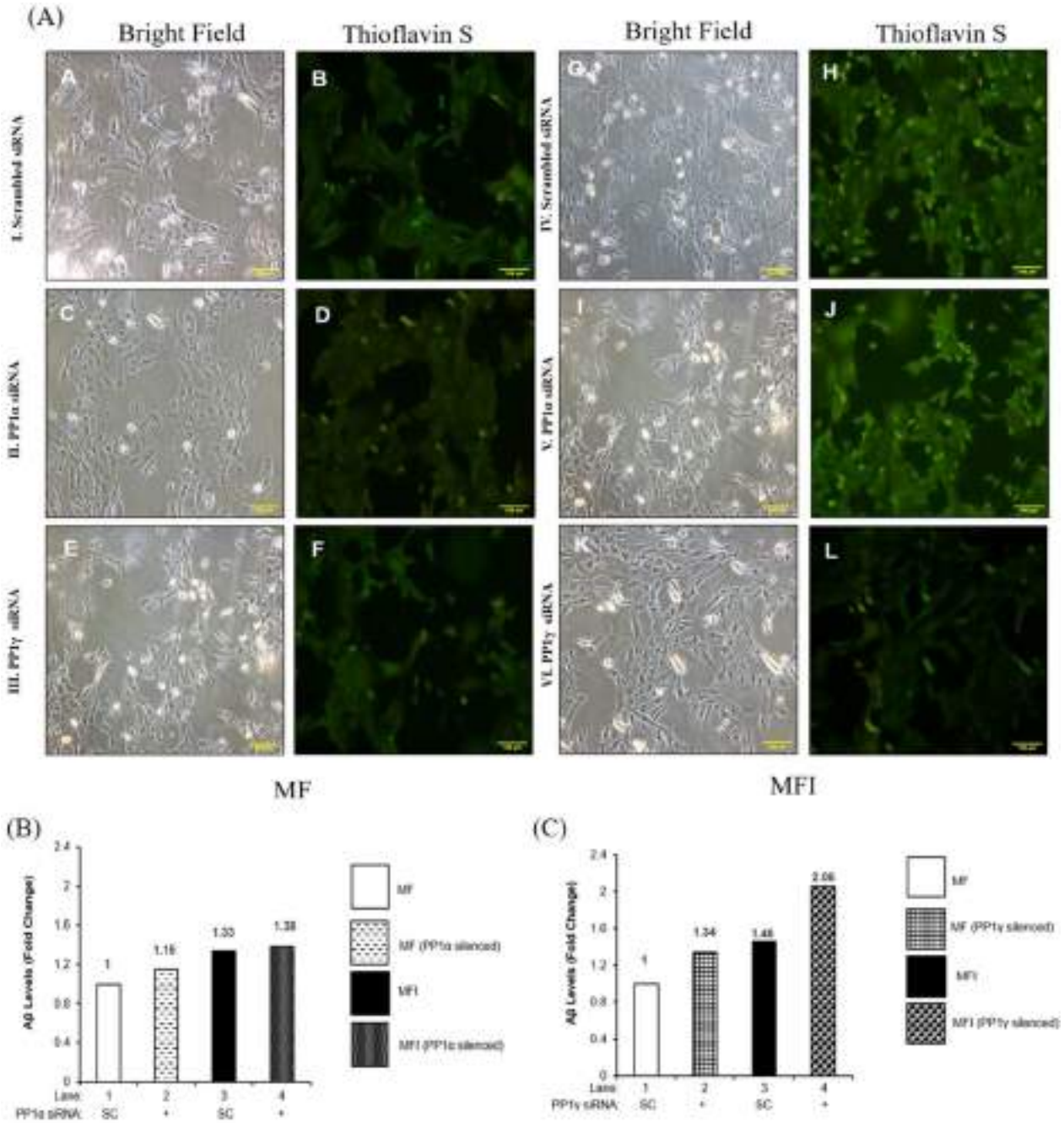

Fig. 9 Effect of PP1α and PP1γ silencing on AD markers in SH-SY5Y cells: Proliferated N2a cells were transfected with non-specific (scrambled) and PP1α and PP1γ specific siRNA. Post transfection cells were differentiated in the absence (MF; insulin sensitive) or chronic presence of 100 nM insulin (MFI; insulin resistant) for 4 days. **A** For thioflavin S staining differentiated SH-SY5Y cells were fixed, permeabilized, stained using ThS stain and visualized under an immunofluorescence microscope. Experiments were executed twice and representative images are shown. Scale bar: 100 µm. **B** and **C** For Amyloid-β measurement PP1α and PP1γ was silenced and conditioned media was collected, concentrated 2 times using speed vacuum and secreted amyloid-β (1–42) levels were measured using Beta-amyloid (1–42) colorimetric ELISA kit. Experiments were executed twice and average is shown

one hand, regulates neuronal insulin signaling and insulin resistance via AKT2-AS160-GLUT4-glucose uptake arm and AD-like phenomena via AKT2-GSK3β-Tau-NFT arm. On the other hand, PP1γ regulates AD markers via MLK3-IKK-GSK3α-BACE-Aβ plaques formation arm. Therefore, PP1γ act like a possible linker between two disorders, insulin resistant diabetes and AD through AKT2 and MLK3, generating a possibility leading to Type-3 diabetes.

Discussion

PP1 and its isoforms in neuronal insulin signaling and insulin resistance

The activity of PP1 relies on its interaction with catalytic and regulatory subunits which determines its substrate specificity. Both catalytic and regulatory subunits have various isoforms. Isoforms of catalytic subunits were reported to be differentially expressed in different tissues. Silva et al. [13] in mice extracts of various tissues like brain, liver, skeletal muscle, kidney, small intestine, heart, lung, spleen, thymus, and testis determined the expression of different isoforms of PP1 catalytic subunits. These studies found that different isoforms have different expression level in different tissues. The expression of catalytic subunit α and δ was found in all the abovementioned tissues with a limited expression in skeletal muscle. However, PP1γ expression level was the highest in brain tissue. These tissue specific differential expression of these isoforms suggests the significance of different isoforms of catalytic subunit of PP1 and possible tissue specific complexity in functions. Whatever little is known, the role(s) of each isoform of catalytic subunit in insulin signaling has been inconclusive. Corvera et al. [32] and Rondinone et al. [9] suggested the participation of a phosphatase responsible for GLUT4 transport in response to insulin in rat and human adipose tissue respectively. Although both of these studies had reported possible role of a phosphatases in insulin signaling, they were neither phosphatase nor catalytic subunit specific studies. Sharma et al. [12] reported α catalytic subunit of PP1 as a regulator of AS160 dephosphorylation in skeletal muscle, without affecting AKT. Geetah et al. [11] reported the combination of PP1δ catalytic subunit with regulatory subunit 12A as a new member in regulating skeletal muscle insulin signaling pathway. There is no study yet that defined the involvement specifically of PP1 in regulating insulin mediated GLUT4 transport neither in peripheral tissues (skeletal muscle, hepatocytes, cardiomyocytes etc.) nor in neurons and none of these studies are on insulin resistance. In the current study, we report with regard to expression and regulatory activity of PP1 catalytic subunits in normal as well as hyperinsulinemia mediated insulin resistant mouse (N2a), human (SH-SY5Y) neuroblastoma cell lines and High-fat-diet-fed mice whole brain lysates. The expression of PP1α and PP1γ did not change post insulin stimulation or under insulin resistant condition in neuronal cells; however, their functionality, did.

PP1γ regulates neuronal glucose uptake through AKT2-AS160 axis

Several studies have reported PP1 to regulate dephosphorylation of pan-AKT in signaling cascades other than insulin signaling [33–35]. Jiang et al. [36] reported that liposomal C6 ceramide activated PP1, which in-turn dephosphorylated AKT1 in human melanoma cell lines. This is the only study so far which discussed the specific role of PP1 in regulating AKT2, in contrast to previous studies those reported pan-AKT findings. Our study determines isoform specific interactions between these two proteins in insulin signaling in any cellular system. We observe PP1γ but not PP1α regulating AKT2 specifically, without affecting AKT1 and AKT3. This isoform specific effect gets translated to the downstream target AS160, which in turn affects the translocation of GLUT4 from cytoplasm to plasma membrane leading to the uptake of glucose inside the cell. We, therefore, for the first time report the role of catalytic subunit PP1γ in regulating neuronal insulin signaling and insulin resistance through one of the isoforms of AKT.

PP1γ regulates GSK3 isoforms via AKT2 and MLK3-PP1γ regulates GSK3 isoforms via AKT2 and MLK3

Our data on PP1 inhibition (Sect. "Effect of PP1 inhibition on neuronal insulin signaling") surprisingly demonstrated different regulation of phosphorylation of two GSK3 isoforms. Previous evidences reported that the phosphorylation of GSK3α and GSK3β have been regulated through different kinases [24, 40]. Gulen *et. al* [37] reported IKK to phosphorylate GSK3α and not GSK3β. Our study, interestingly, reports that PP1γ regulates the phosphorylation of GSK3β through AKT2 but of GSK3α through IKK. Additionally, post PP1γ silencing we also observed a decrease in phosphorylation of IKK, that pointed to a possibility of presence of an upstream kinase relaying PP1γ specific IKK regulation. Previously Cole et al. [25] demonstrated MLK3 negatively regulates the activity of IKK that in human ovarian cancer epithelial cells and murine NIH-3T3 fibroblast cells. Our results demonstrated that PP1γ dephosphorylates and activates MLK3 leading to the activation of IKK, which in turn phosphorylates GSK3α (as depicted in Fig. 6E). So, we here show that PP1γ regulates phosphorylation of two GSK3 isoforms through two different axes; phosphorylation of GSK3β regulated by AKT2-GSK3β axis

and phosphorylation of GSK3α regulated by MLK3-IKK-GSK3α axis.

PP1γ regulates AD markers

As mentioned earlier, previous studies have established connection between aberrant insulin signaling and engagement of GSK3 isoforms in the development of AD [14–28]. Prediabetic conditions and insulin resistance has been confirmed to lead to AD [14, 15, 29, 30, 27, 38]. PTEN, a phosphatase, has previously been reported from our laboratory to participate in AD under the predisposition of insulin resistance [31].

It has been well established that GSK3 plays important role in regulating pathophysiology of AD. Amongst the pathological hallmarks of AD, the most prominent are deposition of Aβ plaques and formation of neurofibrillary tangles (NFTs). Aβ is generated by the sequential cleavage of β- amyloid precursor protein (APP) by β-site APP-cleaving enzyme 1 (BACE1) [39]. Formation of NFTs is the result of Tau hyperphosphorylation [40]. Both the hallmarks of AD are under the control of two isoforms of GSK3. While GSK3α regulates expression of BACE1, ultimately controlling Aβ plaque formation GSK3 regulates Tau hyperphosphorylation, ultimately controlling formation of NFTs. Previously, some phosphatases have been implicated in AD, regulating either the hallmarks of AD directly or by regulating GSK3 isoforms [18]. Silva et al. [41] first reported the role of PP1 in Aβ secretion in COS-1 cells. Subsequently, Sun et al. [42] and Liv et al. [43] reported the role of PP1 in Tau hyperphosphorylation in rat hippocampus and human brain respectively. However, Bennecib et al. [44] reported that PP1 regulates Tau phosphorylation via GSK3β in rat forebrain brain slices. Menendez et al. [45] also corroborated that PP1/GSK3β imbalance regulates AD progression. In our study we see PP1γ mediated opposite phosphorylation/dephosphorylation of two isoforms of GSK3 regulating the hallmarks of AD in neuronal cells.

Rebelo et al. [46] reported that PP1γ specifically binds to, and regulates Aβ aggregation in COS-7 cells, rat hippocampal and cortical primary neurons, and in adult rat hippocampus and cortex. Most recently, Combs et al. (2021) reported that both wildtype and mutant pathological Tau bind to PP1α and PP1γ, but only PP1γ silencing rescued mutant Tau effects in primary hippocampal neurons [47]. In the present study we determined how GSK3 isoforms relay PP1γ specific effects in AD progression. In the current study, PP1γ fine tunes AD-like phenotype in neuronal system, where on one hand the silencing of PP1γ increased the formation of Aβ plaques while on the other hand silencing of PP1γ decreased the formation of NFTs. These opposite effects in a cell may be attributed to PP1γ specific effects on GSK3 isoforms wherein PP1γ silencing increased the phosphorylation of GSK3β, inactivated it, and hence reduced Tau phosphorylation. This reduction in Tau phosphorylation resulted in lesser formation of NFTs. Oppositely, in the absence of PP1γ, GSK3α phosphorylation was regulated by MLK3 followed by IKK. Inactivation of IKK by MLK3 post PP1γ silencing further reduced the phosphorylation of GSK3α causing its activation. This GSK3α activation enhanced the expression of BACE which ultimately increased the deposition of Aβ plaques inside the cell. Overall, it seems that PP1γ is involved in the progression of insulin resistance and also regulates AD markers. This is the first evidence so far associating PP1γ with AD-like pathogenesis. In depth research is required to fully establish the role of PP1γ in the progression of AD pathogenesis under diabetic condition.

In summary, the study determined that PP1γ regulates neuronal insulin signaling and insulin resistance by dephosphorylating AKT2 and is also involved in regulating AD-like phenotypes through GSK3. The study primarily utilizes two different cell lines and partially utilizes animal models. In depth animal studies are needed to corroborate the finding. But the results obtained so far provided the first ever evidence of involvement of PP1γ in neuronal insulin resistance and AD-like phenotypes.

Experimental procedures

Materials

Minimum Essential Media (MEM), Dulbecco's Modified Eagle Medium (DMEM), Fetal Bovine Serum (FBS) were purchased from Gibco., MCDB 201 medium (Cat No. M6770-1L), nutrient mixture F-12 Ham (Cat No. N3520-1L), dimethyl sulfoxide (DMSO), triton X-100 (Cat No. X100-100ML), retinoic acid (Cat No. R2625-50MG), Okadaic Acid (Cat No. 78111-17-8), anti GAPDH antibody (Cat No. 9545), thioflavin S stain (Cat. No. T1892-25G) were purchased from Sigma-Aldrich Co. (St. Louis, MO, USA). Anti Tau antibody (Cat No. 32274), anti α-tubulin antibody (Cat No. 32293), anti-rabbit HRP antibody (Cat No. SC-2357) was purchased from Santa Cruz Biotechnology Inc. Anti phospho-AKT (Ser473) antibody (Cat No. 9271), anti phospho-AKT (Thr308) antibody (Cat No. 9275), anti AKT antibody (Cat No. 9272), anti phospho-AKT1 (Ser473) antibody (Cat No. 9018), anti AKT1 antibody (Cat No. 2938), anti phospho-AKT2 (Ser474) antibody (Cat No. 8599), anti AKT2 antibody (Cat No. 3063), anti phospho-AS160 (Ser588) antibody (Cat No. 8730), anti phospho-AS160 (Thr642) antibody (Cat No. 8881), anti AS160 antibody (Cat No. 2447), anti phospho-GSK3α (Ser21) antibody (Cat No. 9316), anti GSK3α/β antibody (Cat No. 5676), anti phospho-GSK3β (Ser9) antibody (Cat No. 9336), anti GSK3β antibody (Cat No. 9315), anti PP1α antibody (Cat

No. 2582), anti phospho-IKKα/β (Ser179/180) antibody (Cat No. 2796), anti IKKα antibody (Cat No. 2682), anti MLK3 antibody (Cat No. 2817), anti BACE antibody (Cat No. 5606), anti-mouse HRP antibody (Cat No. 7076) were purchased from Cell Signaling Technology. URMC099 (Cat No. S7343) was purchased from Selleckchem, FK506 (Cat No. 342500-5MG) was purchased from Calbiochem. Anti AKT3 antibody (Cat No. PA-41700), anti phosho-MLK3 (Ser674) antibody (Cat No. PA5-40303), anti phospho-Tau (Ser396) antibody (Cat No. 44-752G), anti PP1γ antibody (Cat No. PA1-12382), Trypsin EDTA (Cat No. 25200056), 2-(*N*-[7-nitrobenz-2-oxa-1, 3-diazol-4-yl] amino)-2 deoxy glucose (2-NBDG) (Cat No. N13195), mouse beta-amyloid [1–42] colorimetric ELISA kit (Cat No. KMB3441) and human beta-amyloid [1–42] colorimetric ELISA kit (Cat No. KHB3441) were purchased from Thermo Fisher Scientific. Mouse PP1α (5′UAGCGACUAAACACAUCAAUU3′) and PP1γ (5′GCGGUGAAGUUGAGGCUUAUU3′) specific siRNA, human PP1α (5′UGGAUUGAUUGUACAGGAAUU3′) and PP1γ (5′GCGGUGAAGUUGAGGCUUAUU3′) specific siRNAs were designed and synthesized by Qiagen, Germany.

Cell culture

Mouse neuroblastoma cells (N2a) were cultured in MEM media supplemented with 10% FBS and human neuroblastoma cells (SH-SY5Y) were cultured in DMEM and Ham's F12 media supplemented with 10% FBS containing antibiotics-penicillin 100 IU/ml and streptomycin 100 mg/ml, at 37 °C in 5% CO_2. Post proliferation, N2a cells were differentiated in MEM supplemented with 1% FBS and 2% DMSO at 37 °C in 5% CO_2 for 3 days. SH-SY5Y cells were differentiated in DMEM supplemented with 1% FBS and 10 μM retinoic acid for 4 days. Insulin resistance was generated as described previously in our laboratory [6, 7, 5–22]. Briefly, for creating insulin resistance in N2a cells, post proliferation, cells were subjected to equal mixture of serum free media (MCDB 201 medium and nutrient mixture F-12 Ham) and 2% DMSO in the absence (MF; insulin-sensitive) or in chronic presence of 100 nM insulin for 3 days (MFI; insulin-resistant). The media was replaced after every 12 h. For creating insulin resistance in SH-SY5Y cells, post proliferation cells were differentiated in equal mixture of serum free media (MCDB 201 medium and nutrient mixture F-12 Ham) and 10 μM retinoic acid for 4 days. The media was replaced after every 12 h. Differentiated N2a and SH-SY5Y cells were treated with 100 nM insulin for 30 min as reported previously in our laboratory [6, 7, 5–22].

Preparation of mice brain lysates

Insulin resistance was generated in sixteen weeks old high-fat-diet (HFD) fed Swiss Albino male mice in the laboratory of Dr. Prosenjit Mondal, Indian Institute of Technology-Mandi, over ten weeks, and brain tissues of those mice, which were kind gifts from Dr. Mondal, Indian Institute of Technology-Mandi, were used for our experiments. Glucose tolerance test and insulin tolerance tests were performed; however, perfusion was not done before brain collection. Mice were divided into two groups: normal diet (ND) and high-fat-diet (HFD), each group containing three animals. Levels of triglyceride, cholesterol, serum glutamicoxaloacetic transaminase (SGOT), serum glutamic-pyruvic transaminase (SPGT), and fasting blood glucose were elevated by 48%, 29%, 50%, 53%, 40%, respectively in HFD mice as compared to ND mice. All experiments were performed following the guidelines prescribed by CPCSEA with the approval of the Internal Animal Ethics Committee, Visva-Bharati (IAEC/VB/2017/01). Mice brain were lysed in a homogenizer in lysis buffer (50 mM HEPES pH 7.4, 150 mM NaCl, 1.5 mM MgCl 2, 1 mM EGTA, 10 mM sodium pyrophosphate, 50 mM sodium fluoride, 50 mM β-glycerophosphate, 1 mM Na 3VO 4, 1% Triton X-100 supplemented with 2 mM PMSF, 10 μg/ml each of leupeptin and aprotinin) at 4 °C for 15 min. Brain tissues were homogenized as described previously [5]. Supernatants were collected and protein was estimated by Bicinchoninic Acid (BCA) method. An equal amount of protein was loaded and resolved on SDS-PAGE, followed by western immunoblotting.

Inhibitor treatment

For inhibiting PP1, differentiated N2a and SH-SY5Y cells were treated with 4 μM okadaic acid for 120 min [19], followed by 100 nM insulin for 30 min at 37°C in 5% CO_2. For inhibiting MLK3, differentiated N2a cells were treated with or without different concentrations of URMC099 (0.1, 5 and 10 μM) for 2 h, followed by 100 nM insulin at 37 °C in 5% CO_2.

Gene silencing by siRNA transfection

For silencing AKT1:5′ ATGCTGTTCAGAGACATTTA3′; AKT2:5′AACATTTCTCTGTAGCAGAA3′ and AKT3:5′GATTGATAATATATAGGAGGA3′ mouse specific siRNA was used as described previously [5]. For silencing PP1α and PP1γ in N2a cells, mouse specific PP1α (5′UAGCGACUAAACACAUCAAUU3′) and PP1γ (5′GCGGUGAAGUUGAGGCUUAUU3′) siRNA respectively [48, 49] was designed and synthesized by Qiagen, Germany. Proliferated N2a cells were subjected to transient transfection with PP1α and PP1γ specific or non-specific scrambled siRNA using lipofectamine 2000 in Opti-MEM media. Transfected cells were incubated in Opti-MEM media for 6 h at 37°C in 5% CO_2, after completion of 6 h, media was changed and cells

were incubated in MEM media supplemented with 10% FBS overnight. Post 12 h, N2a cells were differentiated as described in "cell culture" section. For silencing PP1α and PP1γ in SH-SY5Y cells, human specific PP1α (5′UGG AUUGAUUGUACAGGAAUU3′) and PP1γ (5′ GCG GUGAAGUUGAGGCUUAUU3′) siRNA respectively [50] was designed and synthesized by Qiagen, Germany. Transfection in SH-SY5Y cells was performed similar to N2a cells.

Immunoprecipitation

Because a specific phospho-Akt3 antibody was not available to measure 508 phosphorylation levels of Akt3, Akt3 protein was immunoprecipitated using Akt3 specific 509 antibody (Thermo, PA-41700), and probed with Anti-phospho-Akt (serine-473) (CST, Cat. No. 510 4058). Anti-IgG conformational antibody (CST, Cat No. 3678) was used to mask remaining IgG 511 bands. Cells were proliferated and differentiated as described above. 500 µg of protein lysate with 512 certain amount of primary antibody (as referred in datasheet of the manufacturer) was added and 513 incubated overnight at 4 °C in a microfuge rotator at 10rpm (Test tube Rotator, Tarsons, Cat. No. 514 3070). Next day, protein A/G beads were added for 4hrs, along with lysis buffer and protease 515 inhibitors. After 4 h of incubation, cells were centrifuged at 5000 rpm (Centrifuge, Sigma Cat. No.: 2-16KL) for 5 min. Supernatant was discarded and pellet was washed 3 times with lysis buffer along with protease inhibitors. Pellet was suspended in SDS-PAGE sample buffer and heated at 90 °C. The protein samples were resolved on SDS-PAGE.

Cell lysis and immunoblotting

Treated N2a and SH-SY5Y cells were stimulated with or without 100 nM insulin for 30 min at 37°C in 5% CO_2. Cells were then lysed in lysis buffer (50 mM HEPES, 150 mM NaCl, 1.5 mM $MgCl_2$, 1 mM EGTA, 10 mM $Na_4P_2O_7$, 50 mM NaF, 50 mM β-glycerophosphate, 1 mM Na_3VO_4 and 1% triton X-100) as described previously from our laboratory for 30 min at 4 °C [6, 7, 5–22]. Cells were scraped and homogenates were centrifuged at 16,000 x g for 15 min at 4 °C. Supernatant containing protein was collected was estimated by Bicinchoninic Acid (BCA) method [51]. An equal amount of protein was loaded and resolved on SDS-PAGE and western immunoblotting was performed using specific antibodies. Immunoblots were quantified by Quantity One 1-D analysis software (Bio-Rad Laboratories, Inc).

Glucose uptake assay

Glucose uptake was performed as described previously from our laboratory [6, 7, 5–22]. Briefly, differentiated N2A and SH-SY5Y cells were washed and subjected to glucose starvation for 2 h. Treated cells were subjected to 50 µM 2-NBDG for 1 h and lysed in lysis buffer (20 mM Tris–HCl pH 7.4, 40 mM KCl, 1% sodium deoxycholate and 1% NP-40) for 15 min at 25 °C. Cells were then scraped and homogenates were centrifuged at 13,000×*g* for 20 min at 4 °C. Supernatants were collected and fluorescence was measured using a fluorescence spectrophotometer LS55 (Perkin Elmer, USA) at the excitation and emission wavelengths of 485 nm and 535 nm, respectively.

Confocal microscopy

Confocal microscopy of N2A cells was performed as described previously (Sharma and Dey in Cell Mol Life Sci 78:7873–7898, 2021;Bisht and Dey in BMC Cell Biol 9:48, 2008;). Briefly, proliferated N2a were transfected with scrambled and PP1α and PP1γ specific siRNA. Post transfection cells were differentiated in MF MFI medium followed by treatment with 100 nM insulin for 30 min. Treated cells were fixed with 4% paraformaldehyde for 15 min. Cells were permeabilized by incubating with 0.5% Triton X-100 for 5 min, followed by washing with 1X PBS. Cells were blocked in blocking buffer (BSA 1% in PBS) for 1 hour. Cells were incubated overnight with anti-GLUT4 antibody at 4 °C. Cells were washed using 1X PBS and incubated with Donkey anti-Goat Alexa 555 secondary antibody for 45 min at room temperature. Cells were washed further with 1X PBS and mounted using ProLong™ Diamond Antifade Mountant with DAPI on to glass slides. Images were taken using Leica TCS SP8 microscope using 63 X (with oil) confocal objective. Images were taken at Central Research Facility, Sonipat Campus, Indian Institute of Technology-Delhi, Haryana. Images were processed using Leica Application Suite X software.

Thioflavin S staining

Thioflavin S staining was performed as described previously from our laboratory [53]. Briefly, N2a cells were grown on the coverslip and proliferated cells were transfected with PP2Cα specific siRNA as described above. Post transfection cells were differentiated in insulin-sensitive (MF) and insulin-resistant (MFI) conditions for 3 days as described above. On third day of differentiation coverslips was washed with 1X PBS and fixed with 3% paraformaldehyde for 15 min at room temperature (RT). Cells were permeabilized with 0.02% Triton X-100 for 10 min and treated with 0.01% Thioflavin-S (ThS) for 5 min at RT in dark. Excess stain was removed by washing cells with 70% ethanol and washed cells were kept in high phosphate buffer (mM: NaCl 411, KCl 8.1, Na_2HPO_4 30, KH_2PO_4 5.2, pH 7.2) for 30 min on ice. Cells were

visualized under Nikon Eclipse Ti-S immunofluorescence microscope.

Amyloid-β (1–42) measurement

Amyloid-β measurement was performed using Beta-amyloid (1–42) colorimetric ELISA kit (Invitrogen Corp., Camarillo, CA) as per manufacturer's instructions [53]. Briefly, PP2Cα was silenced in N2a cells and subjected to differentiation and on the third day of differentiation conditioned media was collected and 1 mM 4-benzenesulfonyl fluoride hydrochloride (AEBSF) was added at RT. Collected media was then concentrated 4 times using Speed-vacuum and 100 µl of concentrated media was used for the assay.

Statistical analysis

The data expressed as mean±SE. All the experiments were executed three times and a representative result was shown. All the data were analyzed using a two-tailed unpaired *t*-test. $p<0.05$ was considered statistically significant.

Supplementary Information

The online version contains supplementary material available at https://doi.org/10.1186/s12964-023-01071-x.

Additional file 1. Fig S1 Effect of PP1 inhibition on neuronal insulin signaling in SH-SY5Y cells: Differentiated SH-SY5Y cells were treated with or without 4 µM OA for 120 min, followed by 100 nM insulin for 30 min. Treated cells were lysed and subjected to western immunoblotting followed by probing with relevant primary antibodies. Bar represents relative change in (A) pAKT (Ser473) (B) pAKT (Thr308) (C) pAS160 (Ser588) (D) pAS160 (Thr642) (F) pGSK3α (Ser21) (G) pGSK3β (Ser9). For glucose uptake assay differentiated N2a cells were serum-starved for 2 h and then treated with or without 4 µM OA for 120 min, followed by 100 nM insulin for 30 min. Uptake of 2-NBDG was then measured. Bar represents (E) relative change in the uptake of 2-NBDG. Experiments were executed three times and a representative western blot is shown. Data expressed are mean ± SE ***p < 0.001 compared to Lane 1. (A and B) AKT was used as a loading control (C and D) AS160 was used as a loading control (F) pGSK3α was used as a loading control (G) pGSK3β was used as a loading control. A.U.: Arbitrary Units. IB: Immunoblot, OA: Okadaic Acid. **Fig S2 Dose course of PP1α and PP1γ silencing in N2a cells:** Proliferated N2a cells were transfected with non-specific (scrambled) and different concentrations of PP1α and PP1γ specific siRNA. Post transfection cells were differentiated for 3 days, lysed and probed with relevant primary antibodies for immunoblotting. Bar represents relative change in expression of (A) PP1α and (B) PP1γ. Experiments were executed two times and a representative western blot is shown. Data expressed are average. α-Tubulin was used as a loading control. IB: Immunoblot, SC: Scrambled. **Fig S3 Effect of PP1α and PP1γ silencing on Glucose uptake in SH-SY5Y cells:** Proliferated SH-SY5Y cells were transfected with non-specific (scrambled) and PP1α and PP1γ specific siRNA. Post transfection cells were differentiated in the absence (MF; insulin sensitive) or chronic presence of 100 nM insulin (MFI; insulin resistant) for 4 days. (A and B) For glucose uptake assay, transfected SHSY5Y cells were serum-starved for 2 h and treated with 100 nM insulin for 30 min. Treated cells were lysed and uptake of 2-NBDG was then measured. Bar represents relative change in the uptake of 2-NBDG. Data expressed are mean ± SE. ***p < 0.001 compared to Lane 1, $^{\#\#\#}$p < 0.001 compared to Lane 2, $^{\theta\theta\theta}$p < 0.01 compared to Lane 4 and $^{\delta\delta\delta}$p < 0.001 compared to Lane 6. Open bars: MF, filled bars: MFI, A.U.: Arbitrary Units, SC: Scrambled. **Fig S4 Dose course of URMC099 for MLK3 inhibition in N2a cells:** Differentiated N2a cells were treated with or without different concentrations of URMC099 for 2 h, followed by 100 nM insulin for 30 min. Treated cells were lysed and subjected to western immunoblotting followed by probing with pMLK3 (Ser674) and MLK3 antibodies. Bar represents relative change in pMLK3 (Ser473). Experiments were executed two times and a representative western blot is shown. Data expressed are average. MLK3 was used as a loading control. IB: Immunoblot.

Acknowledgements

We thank Indian Institute of Technology-Delhi for its support. We are thankful to Dr. Prosenjit Mondal, Indian Institute of Technology-Mandi, Himachal Pradesh, India, for providing us with normal diet (ND) and high fat fed diet (HFD) mouse brain samples. We are grateful to Central Research Facility, Sonipat Campus, Indian Institute of Technology-Delhi, Haryana, India for Confocal Microscopy.

Author contributions

All authors contributed to the study conception and design. CSD conceived the idea; provided resources; wrote, reviewed and edited the manuscript; and acquired the funding. Material preparation, data collection and analysis were performed by YY, MS. The first draft of the manuscript was written by YY, MS and all authors commented on previous versions of the manuscript. All authors read and approved the final manuscript.

Funding

Y.Y is a recipient of Senior Research Fellowship from DST-INSPIRE, Government of India (IF16013). M.S is a recipient of Senior Research Fellowship (09/086(1256)/2016-EMR-1) from Council of Scientific and Industrial Research (CSIR), Government of India. C.S.D is supported by a Grant from the Council of Scientific and Industrial Research, Government of India, New Delhi, India [27(0346)/19-EMR-ii].

Availability of data and materials

All data generated or analyzed during this study are included in this published article (and its supplementary information files).

Declarations

Ethics approval and consent to participate

All experiments were performed following the guidelines prescribed by CPCSEA with the approval of the Internal Animal Ethics Committee, Visva-Bharati (IAEC/VB/2017/01).

Consent for publication

Not applicable.

Competing interests

The authors have no relevant financial or non-financial interests to disclose.

Received: 10 October 2022 Accepted: 8 February 2023
Published online 2 April 2023

References

1. Blázquez E, Velázquez E, Hurtado-Carneiro V, Ruiz-Albusac JM. Insulin in the brain: its pathophysiological implications for states related with central insulin resistance, type 2 diabetes and Alzheimer's disease. Front Endocrinol. 2014;5:161.
2. Kim B, Feldman EL. Insulin resistance in the nervous system. Trends Endocrinol Metab. 2012;23:133–41.
3. Aviles-Olmos I, Limousin P, Lees A, Foltynie T. Parkinson's disease, insulin resistance and novel agents of neuroprotection. Brain. 2013;136:374–84.
4. Lalić NM, Marić J, Svetel M, Jotić A, Stefanova E, Lalić K, Dragasević N, Milicić T, Lukić L, Kostić VS. Glucose homeostasis in Huntington disease: abnormalities in insulin sensitivity and early-phase insulin secretion. Arch Neurol. 2008;65:476–80.

5. Sharma M, Dey CS. Role of Akt isoforms in neuronal insulin signaling and resistance. Cell Mol Life Sci. 2021;78:7873–98.
6. Manglani K, Dey CS. CDK5 inhibition improves glucose uptake in insulin-resistant neuronal cells via ERK1/2 pathway. Cell Biol Int. 2022;46:488–97.
7. Mishra D, Dey CS. Protein kinase C attenuates insulin signalling cascade in insulin-sensitive and insulin-resistant neuro-2a cells. J Mol Neurosci. 2019;69:470–7.
8. Varshney P, Dey CS. P21-activated kinase 2 (PAK2) regulates glucose uptake and insulin sensitivity in neuronal cells. Mol Cell Endocrinol. 2016;429:50–61.
9. Corvera S, Jaspers S, Pasceri M. Acute inhibition of insulin-stimulated glucose transport by the phosphatase inhibitor, okadaic acid. J Biol Chem. 1991;266:9271–5.
10. Rondinone CM, Smith U. Okadaic acid exerts a full insulin-like effect on glucose transport and glucose transporter 4 translocation in human adipocytes: evidence for a phosphatidylinositol 3-kinase-independent pathway. J Biol Chem. 1996;271:18148–53.
11. Geetha T, Langlais P, Caruso M, Yi Z. Protein phosphatase 1 regulatory subunit 12A and catalytic subunit δ, new members in the phosphatidylinositide 3 kinase insulin-signaling pathway. J Endocrinol. 2012;214:437–43.
12. Sharma P, Arias EB, Cartee GD. Protein phosphatase 1-α regulates AS160 Ser588 and Thr642 dephosphorylation in skeletal muscle. Diabetes. 2016;65:2606–17.
13. e Silva ED, Fox CA, Ouimet CC, Gustafson E, Watson SJ, Greengard P. Differential expression of protein phosphatase 1 isoforms in mammalian brain. J Neurosci. 1995;15(5):3375–89.
14. Gabbouj S, Ryhänen S, Marttinen M, Wittrahm R, Takalo M, Kemppainen S, Martiskainen H, Tanila H, Haapasalo A, Hiltunen M, Natunen T. Altered insulin signaling in alzheimer's disease brain—special emphasis on PI3K-Akt pathway. Front Neurosci. 2019;13:629.
15. Moloney AM, Griffin RJ, Timmons S, O'Connor R, Ravid R, O'Neill C. Defects in IGF-1 receptor, insulin receptor and IRS-1/2 in Alzheimer's disease indicate possible resistance to IGF-1 and insulin signalling. Neurobiol Aging. 2010;31:224–43.
16. Carvalho CR, Brenelli SL, Silva AC, Nunes AL, Velloso LA, Saad MJ. Effect of aging on insulin receptor, insulin receptor substrate-1, and phosphatidylinositol 3-kinase in liver and muscle of rats. Endocrinol. 1996;137:151–9.
17. Kleinridders A, Cai W, Cappellucci L, Ghazarian A, Collins WR, Vienberg SG, Pothos EN, Kahn CR. Insulin resistance in brain alters dopamine turnover and causes behavioral disorders. Proc Natl Acad Sci U S A. 2015;112:3463–8.
18. Liu F, Grundke-Iqbal I, Iqbal K, Gong C-X. Contributions of protein phosphatases PP1, PP2A, PP2B and PP5 to the regulation of tau phosphorylation. Eur J Neurosci. 2005;22:1942–50.
19. Peirce MJ, Warner JA, Munday MR, Peachell PT. Regulation of human basophil function by phosphatase inhibitors. Br J Pharmacol. 1996;119:446–53.
20. Manglani K, Dey CS. Tankyrase inhibition augments neuronal insulin sensitivity and glucose uptake via AMPK-AS160 mediated pathway. Neurochem Int. 2020;141:104854.
21. Gupta A, Dey CS. PTEN, a widely known negative regulator of insulin/PI3K signaling, positively regulates neuronal insulin resistance. Mol Biol Cell. 2012;23:3882–98.
22. Arora A, Dey CS. SIRT2 regulates insulin sensitivity in insulin resistant neuronal cells. Biochem Biophys Res Commun. 2016;474:747–52.
23. Jiang ZY, Zhou QL, Coleman KA, Chouinard M, Boese Q, Czech MP. Insulin signaling through Akt/protein kinase B analyzed by small interfering RNA-mediated gene silencing. Proc Natl Acad Sci U S A. 2003;24:7569–74.
24. Cross DA, Alessi DR, Cohen P, Andjelkovich M, Hemmings BA. Inhibition of glycogen synthase kinase-3 by insulin mediated by protein kinase B. Nature. 1995;378:785–9.
25. Cole ET, Zhan Y, Abi Saab WF, Korchnak AC, Ashburner BP, Chadee DN. Mixed lineage kinase 3 negatively regulates IKK activity and enhances etoposide-induced cell death. Biochim Biophys Acta. 2009;1793:1811–8.
26. Rhoo KH, Granger M, Sur J, Feng C, Gelbard HA, Dewhurst S, Polesskaya O. Pharmacologic inhibition of MLK3 kinase activity blocks the in vitro migratory capacity of breast cancer cells but has no effect on breast cancer brain metastasis in a mouse xenograft model. PLoS ONE. 2014;9:e108487.
27. Stanley M, Macauley SL, Holtzman DM. Changes in insulin and insulin signaling in Alzheimer's disease: cause or consequence? J Exp Med. 2016;213:1375–85.
28. Hölscher C. Diabetes as a risk factor for Alzheimer's disease: insulin signalling impairment in the brain as an alternative model of Alzheimer's disease. Biochem Soc Trans. 2011;39:891–7.
29. Arnold SE, Arvanitakis Z, Macauley-Rambach SL, Koenig AM, Wang H-Y, Ahima RS, Craft S, Gandy S, Buettner C, Stoeckel LE, Holtzman DM, Nathan DM. Brain insulin resistance in type 2 diabetes and Alzheimer disease: concepts and conundrums. Nat Rev Neurol. 2018;14:168–81.
30. Zhang Y, Huang N, Yan F, Jin H, Zhou S, Shi J, Jin F. Diabetes mellitus and Alzheimer's disease: GSK-3β as a potential link. Behav Brain Res. 2018;339:57–65.
31. Gupta A, Dey CS. PTEN and SHIP2 regulates PI3K/Akt pathway through focal adhesion kinase. Mol Cell Endocrinol. 2009;309:55–62.
32. Rondinone CM, Smith U. Okadaic acid exerts a full insulin-like effect on glucose transport and glucose transporter 4 translocation in human adipocytes. Evidence for a phosphatidylinositol 3-kinase-independent pathway. J Biol Chem. 1996;271:18148–53.
33. Xu W, Yuan X, Jung YJ, Yang Y, Basso A, Rosen N, Chung EJ, Trepel J, Neckers L. The heat shock protein 90 inhibitor geldanamycin and the ErbB inhibitor ZD1839 promote rapid PP1 phosphatase-dependent inactivation of AKT in ErbB2 overexpressing breast cancer cells. Cancer Res. 2003;63:7777–84.
34. Li L, Ren CH, Tahir SA, Ren C, Thompson TC. Caveolin-1 maintains activated Akt in prostate cancer cells through scaffolding domain binding site interactions with and inhibition of serine/threonine protein phosphatases PP1 and PP2A. Mol Cell Biol. 2003;23:9389–404.
35. Thayyullathil F, Chathoth S, Shahin A, Kizhakkayil J, Hago A, Patel M, Galadari S. Protein phosphatase 1-dependent dephosphorylation of Akt is the prime signaling event in sphingosine-induced apoptosis in Jurkat cells. J Cell Biochem. 2011;112:1138–53.
36. Jiang F, Jin K, Huang S, Bao Q, Shao Z, Hu X, Ye J. Liposomal C6 ceramide activates protein phosphatase 1 to inhibit melanoma cells. PLoS ONE. 2016;11:e0159849.
37. Gulen MF, Bulek K, Xiao H, Yu M, Gao J, Sun L, Beurel E, Kaidanovich-Beilin O, Fox PL, DiCorleto PE, Wang J, Qin J, Wald DN, Woodgett JR, Jope RS, Carman J, Dongre A, Li X. Inactivation of the enzyme GSK3α by the kinase IKKi promotes AKT-mTOR signaling pathway that mediates interleukin-1-induced TH17 cell maintenance. Immunity. 2012;37:800–12.
38. Mullins RJ, Diehl TC, Chia CW, Kapogiannis D. Insulin resistance as a link between amyloid-beta and tau pathologies in Alzheimer's disease. Front Aging Neurosci. 2017;9:118.
39. Zhang X, Song W. The role of APP and BACE1 trafficking in APP processing and amyloid-β generation. Alzheimer's Res Therapy. 2013;5:46.
40. Brion JP, Anderton BH, Authelet M, Dayanandan R, Leroy K, Lovestone S, Octave JN, Pradier L, Touchet N, Tremp G. Neurofibrillary tangles and tau phosphorylation. Biochem Soc Symp. 2001;67:81–8.
41. da Cruz e Silva EF, da Cruz e Silva OA, Zaia CT, Greengard P. Inhibition of protein phosphatase 1 stimulates secretion of Alzheimer amyloid precursor protein. Mol Med. 1995;1:535–41.
42. Sun L, Liu SY, Zhou XW, Wang XC, Liu R, Wang Q, Wang JZ. Inhibition of protein phosphatase 2A- and protein phosphatase 1-induced tau hyperphosphorylation and impairment of spatial memory retention in rats. Neuroscience. 2003;118:1175–82.
43. Toth C, Brussee V, Martinez JA, McDonald D, Cunningham FA, Zochodne DW. Rescue and regeneration of injured peripheral nerve axons by intrathecal insulin. Neuroscience. 2006;139:429–49.
44. Bennecib M, Gong CX, Grundke-Iqbal I, Iqbal K. Role of protein phosphatase-2A and -1 in the regulation of GSK-3, cdk5 and cdc2 and the phosphorylation of tau in rat forebrain. FEBS Lett. 2000;485:87–93.
45. López-Menéndez C, Gamir-Morralla A, Jurado-Arjona J, Higuero AM, Campanero MR, Ferrer I, Hernández F, Ávila J, Díaz-Guerra M, Iglesias T. Kidins220 accumulates with tau in human Alzheimer's disease and related models: modulation of its calpain-processing by GSK3β/PP1 imbalance. Hum Mol Genet. 2013;22:466–82.
46. Rebelo S, Domingues SC, Santos M, Fardilha M, Esteves SL, Vieira SI, Vintem AP, Wu W, da Cruz e Silva EF, da Cruz e Silva OA. Identification of a novel complex AβPP: Fe65: PP1 that regulates aβpp thr 668 phosphorylation levels. J Alzheimer's Dis. 2013;35(4):761–75.

47. Combs B, Christensen KR, Richards C, Kneynsberg A, Mueller RL, Morris SL, Morfini GA, Brady ST, Kanaan NM. Frontotemporal lobar dementia mutant tau impairs axonal transport through a protein phosphatase 1γ-dependent mechanism. J Neurosci. 2021;41:9431–51.
48. Peters M, Bletsch M, Catapano R, Zhang X, Tully T, Bourtchouladze R. RNA interference in hippocampus demonstrates opposing roles for CREB and PP1alpha in contextual and temporal long-term memory. Genes Brain Behav. 2009;8:320–9.
49. Shioda N, Sawai M, Ishizuka Y, Shirao T, Fukunaga K. Nuclear translocation of calcium/calmodulin-dependent protein kinase IIδ3 promoted by protein phosphatase-1 enhances brain-derived neurotrophic factor expression in dopaminergic neurons. J Biol Chem. 2015;290:21663–75.
50. Bancroft J, Holder J, Geraghty Z, Alfonso-Pérez T, Murphy D, Barr FA, Gruneberg U. PP1 promotes cyclin B destruction and the metaphase-anaphase transition by dephosphorylating CDC20. Mol Biol Cell. 2020;31:2315–30.
51. Smith PK, Krohn RI, Hermanson GT, Mallia AK, Gartner FH, Provenzano MD, Fujimoto EK, Goeke NM, Olson BJ, Klenk DC. Measurement of protein using bicinchoninic acid. Anal Biochem. 1985;150:76–85.
52. Bisht B, Dey CS. Focal Adhesion Kinase contributes to insulin-induced actin reorganization into a mesh harboring Glucose transporter-4 in insulin resistant skeletal muscle cells. BMC Cell Biol. 2008;9:48.
53. Gupta A, Bisht B, Dey CS. Peripheral insulin-sensitizer drug metformin ameliorates neuronal insulin resistance and Alzheimer's-like changes. Neuropharmacol. 2011;60:910–20.

Publisher's Note